Aconitase as Iron–Sulfur Protein, Enzyme, and Iron-Regulatory Protein

Helmut Beinert,*,† Mary Claire Kennedy,‡ and C. David Stout§

Institute for Enzyme Research, Graduate School, and Department of Biochemistry, College of Agricultural and Life Sciences, University of Wisconsin, Madison, Wisconsin 53705, Department of Biochemistry, Medical College of Wisconsin, Milwaukee, Wisconsin 53226, and Department of Molecular Biology, The Scripps Research Institute, La Jolla, California 92037

Received February 21, 1996 (Revised Manuscript Received May 20, 1996)

Contents

I. Introduction 2335
II. Early Research on Aconitase (1950–1978) 2337
III. Research Since 1978 2338
A. Biochemical–Analytical Investigations 2338
B. Spectroscopy (Exploratory Phase) 2339
1. The 3Fe Cluster, EPR Spectroscopy 2339
2. The 3Fe Cluster, Mössbauer (MB) Spectroscopy 2340
C. Protein–Chemical Studies on Aconitase 2341
1. Purity, Molecular Weight, Fe and S^{2-} Stoichiometries 2341
2. Cysteinyl Peptides and Cluster Ligands of Aconitase 2342
3. The Linear 3Fe Cluster 2343
4. "Engineering" of Protein-Bound Fe-S Clusters 2344
D. Spectroscopy on Specifically Isotope-Labeled Samples 2344
1. MB of the $[4Fe\text{-}4S]^{2+}$ State 2344
2. The $[4Fe\text{-}4S]^{1+}$ State 2346
3. Spectroscopy of Se Analogs 2349
4. Resonance Raman (RR) Spectroscopy 2350
IV. Crystal Structures 2352
A. Crystallization 2352
B. Structure Determination 2352
C. Activated Aconitase and Enzyme Complexes 2353
1. Protein Fold 2353
2. Active Site 2354
3. Series of Structures 2354
V. Enzyme Mechanism 2360
VI. Mutational Studies 2363
VII. Inhibition of Aconitase by Fluorocitrate 2364
VIII. The Relationship of Aconitase to the Iron-Regulatory Protein (IRP) 2365
A. Iron Homeostasis, Iron-Responsive Elements (IRE), and IRP 2366
B. Sequence Homology of IRP and m- or c-Aconitase 2366
C. Residues Involved in Aconitase- and RNA-Binding Functions 2367
D. Interconversion of IRP and c-Aconitase 2368
E. Synthesis of Other Proteins Controlled by IRP, Phosphorylation of IRP1, and IRP2 2369
IX. Unanswered Questions and Outlook 2369
X. Acknowledgments 2371
XI. Abbreviations 2371

* Corresponding author.
† University of Wisconsin.
‡ Medical College of Wisconsin.
§ The Scripps Research Institute.

I. Introduction

Sixty years ago Carl Martius (1906−1993), then "Wissenschaftlicher Assistent" to Franz Knoop at the Biochemical Institute of the University of Tübingen, did an experiment, crucial in the development of the concept of the tricarboxylic acid (Krebs) cycle.[1] He incubated 200 mL of an extract from beef liver acetone powder, enriched in isocitrate dehydrogenase activity, with 1.75 g of aconitic acid at pH 6.9 (K^+) in a stoppered flask under vacuum for 7 h at 37 °C. In a parallel experiment he incubated the same amount of extract aerobically with 2 g of trisodium citrate in the presence of methylene blue for 6 h at 37 °C. After deproteinization with tungstate he found that 65% of the aconitate had been converted to citrate in the first aliquot and from the second aliquot 200 mg of α-ketoglutarate dinitrophenylhydrazone was recovered after addition of dinitrophenylhydrazine. This was the most convincing demonstration yet that the isomerization of the tricarboxylic acids—citrate, *cis*-aconitate, and isocitrate—was catalyzed by an enzyme different from that which carried out the oxidative decarboxylation of isocitrate to α-ketoglutarate. The name aconitase was proposed[2] and generally accepted for this enzyme (citrate (isocitrate) hydro-lyase, EC 4.2.1.3). The reactions catalyzed by aconitase are shown in Scheme 1. From then on our knowledge of aconitase has developed in phase with the elaboration and introduction of concepts, approaches, and techniques in biochemistry and its border fields.

Scheme 1

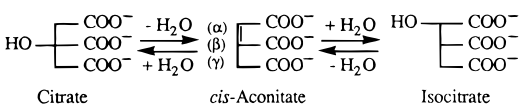

Since that time, the enormous progress in biochemistry that has come about through the influence of developments in molecular genetics and biology and in spectroscopic techniques has widened the scope of almost any problem, which originally lay in the realm of biochemistry, to an unforeseen extent. We will, therefore select a limited number of aspects and will, in the presentation of the material, largely be guided by the historical path taken, as our knowledge of the enzyme and approaches for dealing with it developed.

S0009-2665(95)00040-9 CCC: $25.00

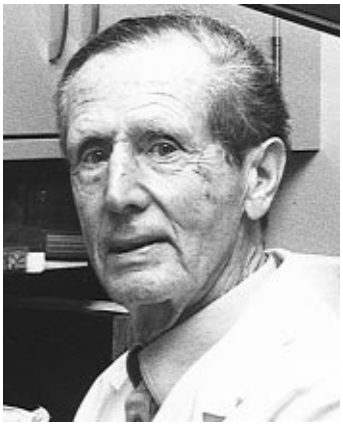

Helmut Beinert, born in 1913 in Southwestern Germany, studied chemistry at the Universities of Heidelberg and Leipzig. In 1943, he received a Dr. of Natural Sciences from the University of Leipzig for thesis work done at the Kaiser-Wilhelm (now Max Planck)-Institute (KWI) for Medical Research at Heidelberg with Richard Kuhn. He continued as postdoctoral associate at the KWI thereafter. In 1950, Beinert joined the Institute for Enzyme Research at the University of Wisconsin, Madison, as postdoctoral fellow with David E. Green. He became Assistant Professor at the Institute in 1952, Associate Professor in 1958, Professor in 1962, and Professor Emeritus in 1984. In 1984/85 he spent a year as Humboldt Senior Scientist at the University of Konstanz and then joined the Medical College of Wisconsin in Milwaukee as Distinguished Scholar in Residence and Professor in the Biochemistry Department and Biophysics Research Institute. In 1994, he returned to the Institute for Enzyme Research in Madison. Beinert contributed to the field of flavoproteins through his work on the various flavoproteins involved in the β-oxidation of fatty acids as well as his revival of interest in flavin semiquinones and the finding of enzyme-substrate charge transfer complexes. This work led him to the use of EPR spectroscopy; in 1959–1960, collaborating with the physicist Richard H. Sands, he was among the first to explore the use of EPR in enzyme chemistry. They discovered, and eventually identified, the Fe-S proteins of the mitochondrial respiratory chain and from there carried on work in the field of Fe-S proteins, to which Beinert has made contributions up to this date.

Mary Claire Kennedy was born in Erie, PA, and is a graduate of Villa Maria College, Erie, PA (B.S., 1950) and Duquesne University, Pittsburgh, PA (M.S., 1955 and Ph.D., 1972). In 1955 she joined the staff of Saint Vincent Health Center where she served as clinical chemist and taught in the Schools of Medical Technology and Nursing. Following teaching assignments at Villa Maria Academy and Villa Maria College (1964), she returned to Duquesne in 1969 where she studied with the late Dr. Oscar Gawron for her Ph.D. It was at that time that she began working with aconitase. Following several years of teaching at Villa Maria College, she spent a sabbatical year (1980) in the laboratories of Dr. Helmut Beinert at the Institute for Enzyme Research in Madison, WI, where she returned in 1982 for two years as a Visiting Associate Professor. After spending a year as a Visiting Scholar at the Universität Konstanz, Germany, where she worked with Dr. Peter M. H. Kroneck, she moved to the Medical College of Wisconsin, Milwaukee (1985) where she has remained since as a Research Associate Professor of Biochemistry. In 1994 she returned to Konstanz for two months as a guest professor. Kennedy is a member of the Sisters of Saint Joseph of Northwestern Pennsylvania, Erie, PA.

Charles David Stout was born in Syracuse and is a graduate of the University of California, Riverside (B.A., 1969) and University of Wisconsin (Ph.D., 1976). He was in the Department of Crystallography at the University of Pittsburgh and since 1985 has been in the Department of Molecular Biology at The Scripps Research Institute as an Associate Member. His research entails macromolecular crystallography with emphasis on the structure and function of Fe-S proteins and enzymes, metalloproteins, and proteins and enzymes involved in fertilization and nucleic acid metabolism.

We prefer doing this over simply stating the present state of knowledge, because, not only does it convey some of the excitement that attended the stepwise progress, but it also seems the more logical approach, as it allows the reader to see more clearly how the various approaches taken depended on each other: preparative biochemistry on analytical or physical chemistry; spectroscopy on preparative and isotope chemistry; crystallography on spectroscopy or protein chemistry, etc. As a consequence, for example, certain spectroscopic approaches were either not feasible or not even thought of, before some problems had been encountered and solved by biochemistry, or vice versa. In this manner of presentation we found it necessary to have two separate sections on spectroscopy—one more exploratory and one more definitive—interspersed by separate sections on biochemical and analytical advances, again one more exploratory and the other more clearly focused in its aims.

There have been a number of recent review articles on the subject, most of them, on request, rather succinct. Historical aspects have been emphasized in articles of 1988[3] and 1993,[4] and structure and mechanism, in 1989[5] and particularly in 1992.[6] We will, following somewhat the pattern of the last-mentioned article, start with a description of the nature of aconitase as an Fe-S protein and its interaction with its substrates and analogues as gleaned from analytical and spectroscopic work; then we will proceed to the structure of the protein, the active site with its Fe-S cluster and details of the mode of binding of substrates and analogues, as derived from X-ray diffraction. All this information has been collected in the last 10–15 years on mitochondrial aconitase. From these data and from earlier stereochemical and kinetic, and recent mutational studies, we will draw conclusions as to the mechanism of the enzymatic reaction. Finally, we will discuss the relationship of cytoplasmic aconitase to mitochondrial aconitase and to IRP, the iron-

regulatory protein, that is involved in intracellular iron homeostasis.

II. Early Research on Aconitase (1950–1978)

The development of our knowledge of aconitase can be cleanly divided into two phases, with the logical hiatus being provided by the discovery of an EPR signal for the enzyme in 1978.[7] From this point on, the application of highly discriminating spectroscopic tools, such as Mössbauer (MB), electron−nuclear double resonance (ENDOR), and low-temperature magnetic circular dichroism (MCD), led to rapid progress in the 10 years until our picture of aconitase once more expanded with the determination of the crystal structure[8,9] and the amino acid (AA) sequence[10] of the protein. Before discussing the more recent contributions, we will briefly summarize what steps seem to us the most important in progress during the early phase following the classical experiments by Martius.

One fundamental aspect about the role of citrate as a key intermediate of metabolism must be mentioned at the outset. At the beginning of the early period referred to above the concept of the citric acid cycle as a central metabolic process was not generally accepted. One of the principal reasons was, that the carbons of citrate were not scrambled in the first steps of the Krebs cycle down to α-ketoglutarate, but retained their identity, i.e, the CO_2 being liberated originated from oxaloacetate (which is represented in the α- and *β*-carbons and their carboxyls in Scheme 1), while the two-carbon fragment containing the carbons of acetyl-CoA (*γ*-) was recovered in α-ketoglutarate.[11] As citrate is a symmetrical molecule, it was argued that, if it were an intermediate, this should have led to scrambling of its carbons. It was the contribution of Alexander Ogston[12] to solve this dilemma by pointing out that even a symmetrical molecule of the structure of citrate could react as though it were chiral, when bound to an active site of an enzyme, which can be expected to be asymmetric; i.e., citrate is, what we call today, a prochiral molecule.

The apparent instability of the enzyme had been a discouraging aspect of all work on aconitase, until it was found in 1951 that most of the lost activity could be readily recovered by the addition of ferrous iron and a reducing agent.[13] It was also suggested at that time that chelation of iron by substrate and groups on the enzyme might play a role in the enzymatic reaction. In the early 1960s the stereochemistry of the dehydration−hydration reaction (Scheme 2) was established as occurring *trans* to the double bond; this was accomplished by the stereospecific synthesis of *threo*-D_S-isocitrate, the natural substrate of the enzyme,[14,15] and was confirmed by isotope studies that provided a link to the stereochemistry of the fumarase reaction, i.e. the interconversion of malate and fumarate.[16] The insights so gained made it feasible to conceive of a plausible overall mechanism for the interconversion of the tricarboxylic acids. As shown in the scheme, it was proposed that in the active site cavity, a 180° rotation of *cis*-aconitate around an axis perpendicular to the double bond which is referred to as "flip", would place the site on the molecule, from

Scheme 2

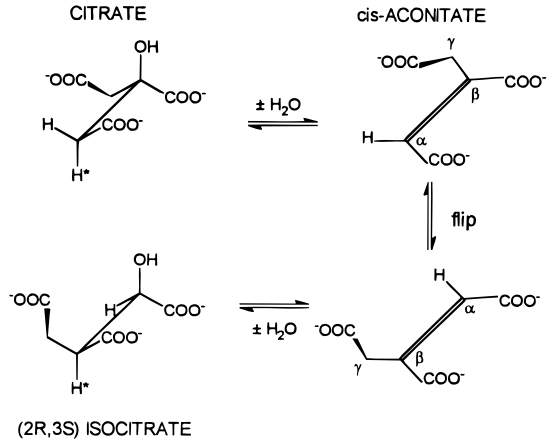

which H^+ had been abstracted, in the same position, where H^+ now had to be added to form the product.[17] The finding in 1967 that the H^+ abstracted in the dehydration reaction does not readily equilibrate with H^+ of the solvent and may be added back to substrate in the rehydration phase (i.e., is a "sticky proton"), lent support to this picture.[18]

It was in the same time span that numerous studies explored the kinetics of the interesting three-substrate reaction catalyzed by the enzyme, even though no details about the active site were then available. The data gathered have remained as valuable guideposts for any kinetic work on the enzyme.[19−22] In 1971 it was demonstrated that iron is not only required for the enzymatic reaction, but is in fact tightly bound to the protein;[23] only one iron per molecule was reported at that time, however. It was clearly established in the same year, as had been suggested from earlier observations, that there are two different aconitases present in tissues, a mitochondrial (m-) and a cytoplasmic (c-) enzyme.[24] The enzymes differ in M_r and AA residues, 82 754 and 754 amino acid residues for m-, and 98 400 and 889 AA residues for c-aconitase.[10,25] The m- and c-aconitases are now known to have 30% AA sequence identity, with all those residues conserved that are considered to be essential parts of the active site according to crystallography[26] and mutational studies.[27] The m- and c-enzymes also differ noticeably in their stability. The m-enzyme loses all activity on purification beyond >80%,[28] whereas the c-enzyme can be purified to >95% with retention of 70−90% of its activity.[25] This circumstance makes it likely that all reports on highly purified enzyme, predating 1951, before the necessity for reactivation with iron had been recognized, actually refer to the c-enzyme. There is also a great difference in the relative distribution of the two enzymes in various tissues and organs. Heart, e.g., contains little of the c-form, while this is abundant in liver.

In 1972, one of us discovered labile sulfide in highly purified aconitase at a ratio of 3:2 to iron.[29,30] Labile sulfide is an almost infallible sign for the presence of Fe-S clusters. However, the EPR spectrum was not seen at that time, because the spectra were recorded at liquid nitrogen temperature. Thus, only the signal typical of high spin iron in a rhombic environment ($g = 4.3$) was found,[31] which we now

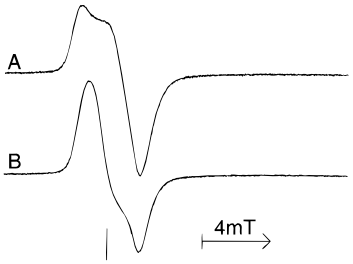

Figure 1. EPR spectra of c-aconitase (32 μM; spectrum A) and m-aconitase (25 μM; spectrum B) in 0.1 M Hepes buffer (pH 7.5). Conditions of spectroscopy: microwave power and frequency, 0.1 mW and 9.177 GHz; modulation amplitude and frequency, 0.5 mT and 100 kHz; time constant, 0.128 s; scanning time, 5 mT/min; temperature, 12 K. The marker is at $g = 2.018$. (Reprinted with permission from ref 25. Copyright 1992 National Academy of Sciences.)

know is a frequently occurring contaminant of proteins. It was taken as a suggestion for the presence of an isolated high-spin ferric iron site, which was, if anything, confusing. It was only in 1978, when an unidentified Fe-S protein in beef heart mitochondria, showing an unusual isotropic EPR signal at $g = 2.01$ in its oxidized form (Figure 1),[32] was identified as aconitase.[7] From this finding then, a link could be established to ongoing spectroscopic work on microbial ferredoxins, which rapidly furnished clues as to the properties of the iron and sulfide and the active site in m-aconitase.

III. Research Since 1978

A. Biochemical–Analytical Investigations

After it had been found that aconitase is an Fe-S protein and after its—at that time—unusual EPR signal had been discovered, there passed a period of about four years of biochemical−analytical explorations, which used enzyme activity, the EPR signal and light absorption spectroscopy in the visible region as monitors. This work raised more questions than it was able to answer. Those interested in details of this research and the uncertainties which confronted us in that period may want to consult the summary given in ref 3 or progress reports published in symposium volumes.[33,34] While it was generally accepted that iron is required for activation of aconitase, we observed that the active enzyme could be produced in up to 70−80% yield (100% being achieved with Fe and DTT) by simply adding a reducing agent, such as dithiothreitol (DTT), to the inactive form. Contamination with iron could not account for this activation, as we had used only reagents that we had analyzed for Fe. Thus, it appeared that Fe was involved in some phase of generating the active enzyme species, but that it was not necessarily a constituent of the active species. This, however was contradicted by experiments with radiolabeled Fe, which left no doubt that the added Fe was indeed incorporated into the protein and that on oxidation to the inactive form, the labeled Fe was specifically released.[28] In addition, having an iron chelator present during the activation period prevented formation of the active enzyme, whether Fe had been added or not.[28] The form of the enzyme that took up

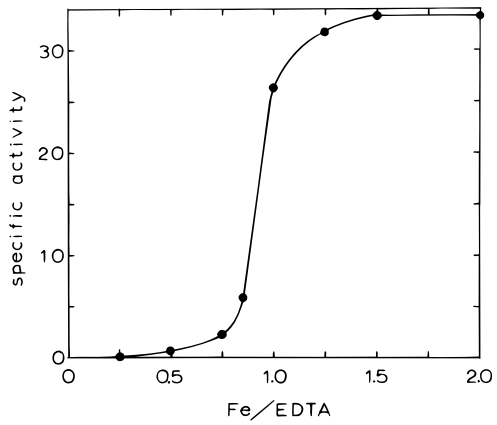

Figure 2. Effect of iron to EDTA ratio on the activation of aconitase. Aconitase (0.5 mg) was anaerobically activated in 80 mM Hepes (pH 7.5) containing 5 mM dithiothreitol, 100 mM EDTA, and varying iron concentrations. The samples were incubated for 30 min at room temperature before determining activity. (Reprinted with permission from ref 28. Copyright 1983 Am. Soc. Biochem. Mol. Biol., Inc.)

the Fe competed effectively with EDTA with a complex formation constant of 10^{10} vs 10^{14} for EDTA and ferrous iron (Figure 2).[28] It also became clear that a reductant was necessary to generate the active species from the inactive form obtained on purification, namely that showing the $g = 2.01$ signal. However, reduction per se in the absence of Fe, as monitored by the disappearance of the EPR signal and change of the absorption spectrum, was not sufficient to produce the active species; only a slow process following the rapidly occurring reduction led to optimal activity. Yet, after extensive reduction, e.g. by illumination in the presence of deazaflavin and oxalate, even an exposure to oxygen was required to reach maximal activity.

Seen from today's standpoint, there were several shortcomings in the information available to us and in our experimentation. According to cluster extrusion experiments,[35] the inactive enzyme, as obtained on purification, contained a [2Fe-2S] cluster. This seemed to be supported by medium-resolution X-ray data on FdI of *Azotobacter vinelandii*,[36] which showed the same EPR signal as inactive aconitase. Our results from chemical analyses for Fe and quantitative evaluation of the EPR signal were closer to 3Fe per molecule. The values for sulfide were more scattered, but often exceeded those for Fe.[7,32] From what was known at that time, the Fe and S^{2-} per protein stoichiometry could only be explained by assuming that we had a [4Fe-4S] cluster in the majority of the molecules mixed with some apoenzyme. On the other hand we did not have the precision in our assay for sulfide to be entirely sure whether we had a nonintegral Fe/S^{2-} stoichiometry. In addition, values between 66 and 90 kD had been reported for the molecular weight of aconitase as determined by different methods on different preparations, so that we were uncertain, whether we had used the correct one for determining the amounts of Fe and S^{2-} per molecule (in retrospect we know now that we happened to use the right value, but an incorrect molar absorptivity in the assay for protein). We were also only beginning to realize that we were

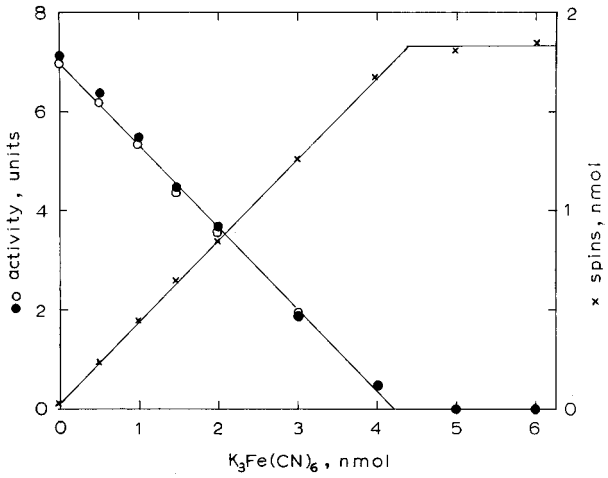

Figure 3. Oxidative titration of activated aconitase with potassium ferricyanide. Aliquots of an activated aconitase stock solution in 90 mM Hepes and 10 mM tricarballylate (pH 7.5) were placed in individual quartz EPR tubes in ice. To each tube was added a measured amount of potassium ferricyanide; the samples were incubated for 1 min, assayed (●), and quickly frozen in an isopentane bath at −140 °C. After determination of the number of spins by EPR at g = 2.01 (×), the samples were thawed and assayed again (○). All samples were reactivated and assayed to assure that the ferricyanide treatment did not destroy detectable amounts of Fe-S clusters. (Reprinted with permission from ref 37. Copyright 1983 Am. Soc. Biochem. Mol. Biol., Inc.)

dealing with more than two oxidation states in the system, so that the terms "oxidized" and "reduced" were ill defined.

The phenomenon of activation of aconitase in the "absence" of Fe, i.e., extraneous Fe, however, soon found an explanation. When the fully activated (Fe and DTT) enzyme was titrated with ferricyanide, as followed by monitoring the appearance of the g = 2.01 signal, disappearance of activity and loss of iron (Figure 3),[37] a strict correspondence between these quantities was observed. When the inactive enzyme was activated with DTT only, both maximal enzyme activity and EPR signal, after oxidation, were only about 75% of what we had found with activation by Fe and DTT. The explanation for these results is a reorganization within the population of Fe-S clusters: The Fe-S cluster in the oxidation state as it occurs in the active enzyme is unstable toward oxidants and is converted to the species giving the g = 2.01 signal by losing Fe, whereas, on reduction, the Fe-depleted species becomes less stable than the active species and is built up to the active form by recruiting Fe from decaying neighbors, a process which has occasionally been named cannibalization.

Subsequent experiments with MB in conjunction with EPR spectroscopy, to be discussed below, allowed us to formulate all these results in molecular terms as is shown in Scheme 3. More recent detailed kinetic studies showed that reduction of the 3Fe cluster precedes incorporation of Fe(II) to form active aconitase.[38] The same research group has also obtained evidence that other metal ions such as Co^{2+} and Mn^{2+} can be incorporated into aconitase when an excess of these ions is present.[39] The corresponding products have not been isolated. From our own work on substitution of the labile Fe, later referred to as Fe_a, with radioisotope-labeled Co^{2+}, Mn^{2+}, and

Scheme 3[a]

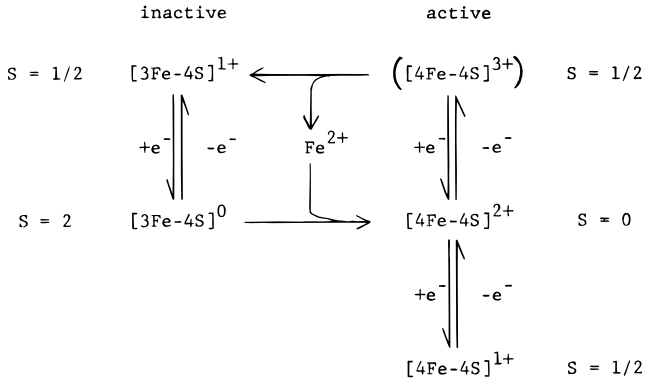

[a] This scheme shows the relationship between various cluster forms of aconitase excluding enzyme−substrate complexes and the linear form. For each cluster type the oxidation state (i.e. the charge balance of the cluster core) and the spin state are indicated. For $[3Fe\text{-}4S]^+$ the EPR signal is centered at g = 2.01 and for $[4Fe\text{-}4S]^+$ (substrate-free) the g values are 2.06, 1.93, 1.86; $[3Fe\text{-}4S]^0$ has a broad signal between 0 and 50 mT at 9.2 GHz similar to that found for other substances in the S = 2 state. The existence of a $[4Fe\text{-}4S]^{3+}$ cluster has not been demonstrated but there is evidence that oxidation precedes release of Fe. (Reprinted with permission from ref 37. Copyright 1983 Am. Soc. Biochem. Mol. Biol., Inc.)

Zn^{2+}, we have learned that there are secondary binding sites in the protein that can bind these metal ions, which may complicate the interpretation of results on substitution.

B. Spectroscopy (Exploratory Phase)

1. The 3Fe Cluster, EPR Spectroscopy

Answers to many of the above-mentioned questions came from the discovery that there exist Fe-S clusters other than [2Fe-2S] and [4Fe-4S]. As often in research, the missing clue emerged from seemingly unrelated work. By 1980 the field of Fe-S proteins had reached adolescence; however, our knowledge of the structural types of Fe-S clusters as well as of the range of their possible functions was still very limited to about the level found in the early classical books on Fe-S proteins published between 1973 and 1982.[40−42] The crucial event in establishing the cluster type in m-aconitase was the discovery by Münck and his colleagues of the 3Fe cluster in 1980.[43,44] As this discovery not only ushered in unexpected progress on a broad front over the whole field, but also stands as an example of the triumph of logical reasoning over conventional views—that initially even seemed to be supported by crystallographic data—we go into detail on this point.

At this time three Fds were intensively studied by various methods, FdI of *Azotobacter vinelandii* (FdI-Av), which was still thought to be the electron donor to nitrogenase, and FdI and II of *Desulfovibrio gigas* (FdIDg, FdII). The former contains two Fe-S clusters, which can, however, be studied separately to some extent by making use of their widely differing redox potentials, while the *D. gigas* Fds appeared to be oligomeric forms of the same protein, which differed, however, in the cluster to protein stoichiometry. We know now that some of the original assumptions concerning the *D. gigas* proteins are no longer valid;[45] however, FdII, the form with the lower

Fe/protein ratio, in its oxidized state, had a strong EPR signal at $g = 2.01$, as does aconitase. The EPR of FdI was as expected for [4Fe-4S] clusters, i.e., no signal in the oxidized state (except for a minor, but persistent admixture of FdII that showed the $g = 2.01$ signal), and the usual $g = 1.94$ signal from the reduced state of the [4Fe-4S] cluster. One of the Fe-S clusters of FdIAv behaved also like a typical [4Fe-4S] cluster, the other cluster showed the unexplained $g = 2.01$ signal.

2. The 3Fe Cluster, Mössbauer (MB) Spectroscopy

a. The Oxidized 3Fe Cluster. The MB spectra of the proteins that showed the EPR signal at $g = 2.01$ consisted of a single quadrupole doublet, when observed at a temperature where electronic relaxation is fast (77 K), but showed significant magnetic hyperfine structure at low temperature (4.2 K). The isomer shifts (δ) and quadrupole splittings (ΔE_Q) were characteristic of high spin ($S = {}^5/_2$) Fe(III) in a tetrahedral environment of sulfurs (e.g. $\delta = 0.27$ mm/s and $\Delta E_Q = 0.54$ mm/s for each site of FdII), as typified by oxidized rubredoxin (Rd), for which accurate measurements are available.[46] Because of uncertainties in M_r as well as in metal and sulfide analyses the Fe/protein stoichiometries for all these proteins had a sufficient error attached to them such that a 2Fe as well as a 4Fe per cluster stoichiometry was not entirely excluded. One of us (C.D.S.) concluded from a 4 Å resolution map of FdIAv that, while one cluster showed an electron density as expected for a 4Fe cluster, the other cluster did not have the electron density of a 4Fe cluster.[36] The MB spectra of FdIIox could not furnish a decisive answer on the stoichiometry.

b. The Reduced 3Fe Cluster; "Double Exchange". The MB spectrum of FdIIred, however, did provide an answer: There were two well-separated doublets (I, $\delta = 0.46$ mm/s, $\Delta E_Q = 1.47$ mm/s; II, $\delta = 0.30$ mm/s, $\Delta E_Q = 0.47$ mm/s) with a clear 2:1 intensity ratio. Obviously, there had to be three (or a multiple thereof) Fe atoms per site represented in this spectrum. Analogous data were obtained after reduction of aconitase and FdIAv.[44] This conclusion was not contradicted by the MB spectra of the oxidized forms. On the contrary, as the magnetic MB spectra of the oxidized forms showed clear signs of spin coupling between the iron atoms present, Münck et al. argued that the half integral spins of two ferric atoms could not be coupled to yield the observed $S = {}^1/_2$ cluster spin. Coupling of ferric ions to a radical, as has recently been proposed for intermediate X of ribonucleotide reductase,[47] was rejected when the whole MB data set was considered. Thus, the behavior of the oxidized forms also supported the proposal that there must be 3Fe clusters. Higher multiples of 3 were excluded, as they were incompatible with chemical analytical results.

On the basis of the MB data and the arguments just presented, Kent et al.[48] proposed a spin-coupling model for FdIIox. The model assumes isotropic exchange and different couplings between the iron sites. The intrinsic hyperfine interactions of the three sites are close to those of ferric Rd. The magnetic MB spectra, however, indicated that the individual hyperfine values A differed greatly in sign and magnitude: $A_1 = -38$ MHz, $A_2 = +20$ MHz, $A_3 = 3.5$ MHz. In the proposed spin−vector coupling model, the EPR and MB data are accounted for by the use of a Heisenberg−Dirac−vanVleck Hamiltonian with the differences of the observed interactions originating from the geometrical features of spin coupling.

Table 1. ^{57}Fe Isomer Shifts (δ) and Quadrupole Splittings (ΔE_Q) for the 3Fe Clusters in Proteins

	ΔE_Q (mm/s)	δ (mm/s)	
FdII, *D. gigas*			
ox.	0.54 ± 0.03	0.27 ± 0.03	
red.	1.47 ± 0.08	0.46 ± 0.02	I
	0.47 ± 0.02	0.30 ± 0.02	II
FdI, *A. vinelandii*			
ox.	0.63 ± 0.05	0.27 ± 0.04	
red.	1.45	0.47	I
	0.40	0.29	II
aconitase, beef heart			
ox.	0.71	0.27	
red.	1.34	0.45	I
	0.49	0.30	II

As MB can only give direct information on the iron atoms present and not on the number of ligands, it was originally assumed that the Fe/S^{2-} stoichiometry was 1 in keeping with what had been observed with 2Fe and 4Fe clusters. This was first also suggested from X-ray diffraction data on FdIAv, obtained at higher resolution.[49]

As mentioned above, the MB spectrum of FdIIred actually gave the most decisive clue leading to the discovery of a 3Fe cluster. A thorough study of the features of the MB spectra of FdIIred also initiated much progress in the development of concepts and views of the electronic and magnetic properties of the next largest cluster category, viz., the 4Fe clusters and eventually of clusters with metal nuclearity larger than four.[50] We know that in $[2Fe\text{-}2S]^{1+}$ clusters of $S = {}^1/_2$ the extra electron is essentially localized at one of the Fe atoms.[51] However, when one electron is added to a cluster of three Fe(III), the situation is obviously more complicated, and it turns out that a stable electronic structure can be formed by ferromagnetic coupling of two Fe atoms, which share the electron so that their charge becomes 2.5+, to a subspin of $S = {}^9/_2$; this "mixed valence" pair then is coupled antiferromagnetically to the remaining ferric Fe of $S = {}^5/_2$ to a total system spin of $S = {}^4/_2$. This is expressed in the MB spectrum in that one doublet (II) has δ and ΔE_Q typical of Fe(III), while the other doublet (I) has δ and ΔE_Q values intermediate between values typical for high spin ferric and ferrous Fe., i.e. of about $Fe^{2.5+}$ (Table 1, Figure 4).[52] The reduced 3Fe cluster is the smallest cluster that shows the phenomenon that has variously been called "double exchange",[53] "resonance splitting", "resonance delocalization",[54] or "spin-dependent electron delocalization",[55] of which the last expression seems to be the most descriptive. The basic ideas are not new,[56,57] but the encounter of the phenomenon in a simple biological system has been a great stimulus to the development of these and related concepts. The literature of the past few years on the subject will have to be consulted for detailed information.[55,58−62] What is important to keep in mind for our purposes

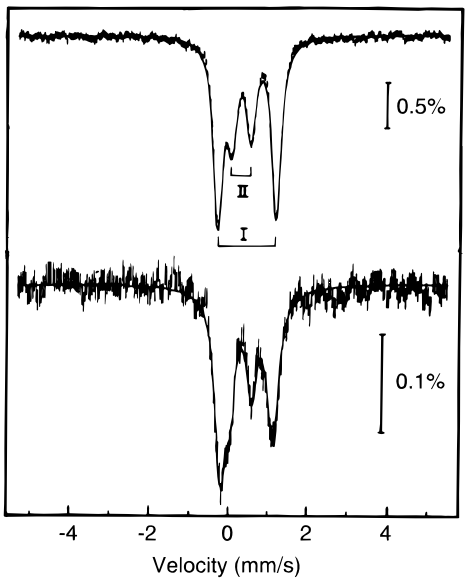

Figure 4. Zero-field Mössbauer spectra of reduced three-iron centers. (Top) Spectrum of *D. gigas* Fd II. The solid line is the result of fitting two doublets to the data. The least-squares fit yielded a concentration ratio of 2:1 for the two species. (Bottom) Spectrum of reduced aconitase isolated from beef heart mitochondria. The solid line is the result of least-squares fitting two doublets to the spectrum. The concentration ratio of the two species was held fixed at 2:1. (Reprinted with permission from ref 4. Copyright 1993 Fed. Am. Soc. Exptl. Biol.)

is that the extent of double exchange and its modulation by "vibronic coupling" (via geometrical constraints) are important determinants of the ground spin state in which a system is being encountered.[55,62]

c. FdII vs Aconitase. FdII was indeed an extraordinarily useful object for research, as a protein with M_r 6400 of reasonable stability with but a single cluster. Thus, well-resolved MB spectra could be obtained even at natural abundance (2.2%) of the MB isotope, ^{57}Fe. Its limitation was, however, that it was almost too stable, so that specific isotope incorporation was not straightforward and, above all, there is no simple test for a biological function. Here, aconitase, as an enzyme, offered superior opportunities and was clearly the object of choice for further studies. With the discovery of the 3Fe cluster and its properties as just described, it was now obvious to ask the questions: What is the relationship of the 3Fe to the 4Fe cluster, as they occur in FdII and FdIDg, respectively? And for aconitase, which is enzymatically inactive in the 3Fe form, the question was: What is then the active form of aconitase?

d. 3Fe → 4Fe Cluster Interconversion. We knew from chemical and enzymatic studies that the inactive 3Fe form, as obtained on purification, gained activity on reduction, somewhat dependent on the reductant used and the time of exposure.[28] A detailed study of reduced 3Fe aconitase by MB spectroscopy showed that in addition to the signal attributed to the reduced 3Fe form (Figure 5)[63] an additional minor signal was superimposed. This signal had properties typical of reduced 4Fe clusters and clearly represented a paramagnetic species. In confirmation of this, an EPR signal typical of reduced 4Fe clusters ([4Fe-4S]$^{1+}$) was observed for one such sample. As expected from the biochemical studies, it also had

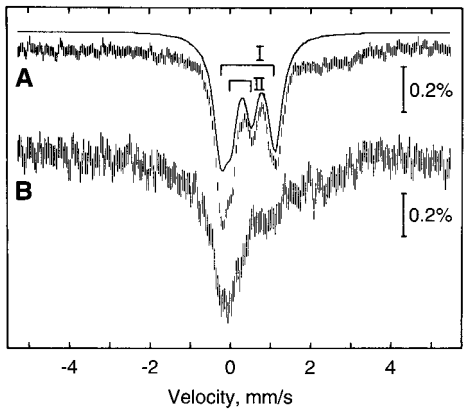

Figure 5. Mössbauer absorption spectra of dithionite-reduced beef heart aconitase (9mM Fe; ^{57}Fe, natural abundance) at 4.2 K. (A) Recorded in zero field (—), spectral contribution of the [3Fe-4S] cluster. (B) Recorded in a magnetic field of 60 mT applied parallel to the observed Mössbauer radiation. (Reprinted with permission from ref 64. Copyright 1985 Am. Soc. Biochem. Mol. Biol., Inc.)

Scheme 4

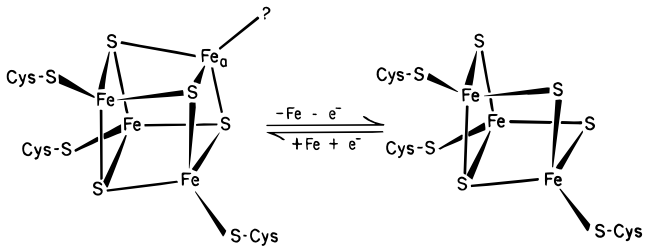

acquired respectable aconitase activity. The obvious conclusion from these experiments was that Fe is required for enzymatic activity, in order to build the 4Fe cluster of the active form (Scheme 4). Then, of course, interest turned to the oxidized 4Fe form ([4Fe-4S]$^{2+}$), which most likely was the naturally active species, as the 1+ state can only be reached anaerobically, by strong reductants and at elevated pH (>8). The 2+ form is diamagnetic and thus not suited for EPR or ENDOR experiments; it has, however, been studied by MB.[64] The findings just communicated readily suggested the path of research to be taken from here on, namely the use of isotopes, so as to be able to study individual iron sites and eventually, of course, enzyme-substrate interactions.

Before we proceed to that phase of the work, we must, at this point, describe related studies by analytical—chemical, physicochemical, and X-ray spectroscopic approaches, which did much to fill in important, but yet missing pieces of information about properties of aconitase. We will then describe, how, on the basis of this knowledge and that gathered by spectroscopy, we were able to produce the specifically labeled samples that were required in pursuing the isotope approach that we just projected.

C. Protein–Chemical Studies on Aconitase

1. Purity, Molecular Weight, Fe and S^{2-} Stoichiometries

It was shown by analyses on a large number of aconitase preparations of >95% purity that the inactive 3Fe enzyme in fact contained a [3Fe-4S] not a [3Fe-3S] cluster and EXAFS, first on FdII[65] and

then also on aconitase confirmed that the Fe−Fe and Fe−S distances in this cluster were the usual ones observed for other cubane Fe-S clusters and not the much longer ones calculated for the postulated [3Fe-3S] cluster.[66] In addition, determinations of the M_r of aconitase by amino acid analysis, SDS-PAGE and in the ultracentrifuge (by low-speed sedimentation equilibrium) gave us an accurate relationship of the M_r to the chemically determined protein concentration and confirmed the high purity of the protein with which we were working.[67]

2. Cysteinyl Peptides and Cluster Ligands of Aconitase

Before the X-ray sructure and the amino acid sequence of aconitase were known, Plank and Howard, in elegant studies, determined the sequence of eight cysteinyl peptides of the protein.[68] By selective radiolabeling studies, these authors were also able to predict which Cys residues, on the basis of their resistance to labeling, were the most likely ones to be the cluster ligands (Figure 6). They also observed that the number of of these protected ligands was the same for the 3Fe and the 4Fe form of the enzyme,

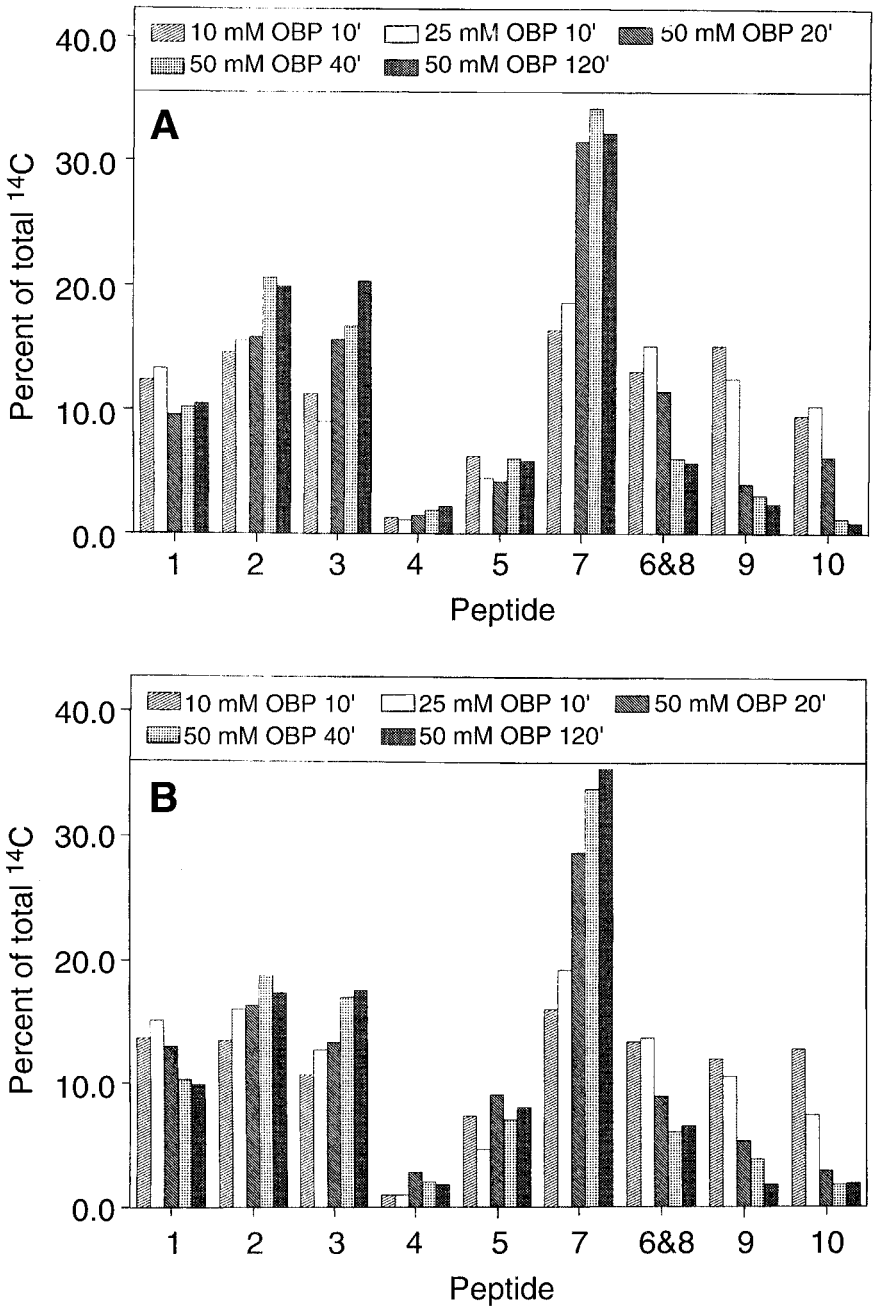

Figure 6. Distribution of radiolabel in aconitase cysteines which were protected from iodoacetamide reaction during iron chelation by 4,7-diphenyl-1,10-phenanthroline disulfonic acid (OBP): (A) 4Fe aconitase and (B) cubane 3Fe aconitase were incubated with OBP (at the concentrations indicated) in the presence of 5 mM iodoacetamide. The alkylation was stopped by adjusting the pH to 2 at the times indicated. The protein was fully reduced with dithiothreitol and carboxymethylated with iodo [2-^{14}C]acetic acid. Therefore, those cysteines incorporating the highest percentage of ^{14}C are the cysteines that are the most protected from iodoacetamide alkylation during iron chelation by OBP. The protein was digested with trypsin, and the cysteinyl peptides were separated and counted. Peptide 4, containing "the reactive cysteine", demonstrates that cysteines rapidly alklyated by iodoacetamide incorporate low amounts of radiolabel. (Reprinted with permission from ref 72. Copyright 1989 Am. Soc. Biochem. Mol. Biol., Inc.)

suggesting that the fourth iron (Fe_a) had no Cys ligand. This was consistent with sulfhydryl determinations, where, on conversion of the 3Fe to the 4Fe cluster, there was no evidence for freeing of a thiol group.[69] All these suggestions were soon verified by crystallography.

Aconitase had long been known to have a particularly reactive thiol, blockage of which inactivated the enzyme.[70] Plank and Howard determined the location of this cysteine, while Kennedy et al. showed that this Cys residue (Cys 565), contrary to previous suggestions, was not involved in the enzymatic reaction;[71] however, blockage of this Cys with a bulky residue, e.g., *N*-ethylmaleimide (NEM) obstructed access of the substrate to the cluster; EPR of this NEM-modified protein showed no shift of g values,[71] when substrate was added to the $[4Fe\text{-}4S]^{1+}$ form as is seen with the native protein (see below). The activity was barely influenced, when iodoactamide was attached to Cys 565. In subsequent studies and by approaches similar to those of ref 68, Plank et al.[72] determined which Cys residues were involved in the disulfides formed on elimination of the cluster by a chelator or by oxidation (see below) of the cluster. As close to two disulfide bonds were found on oxidation,[69] a Cys residue in addition to the cluster ligands had to be involved in disulfide formation. It was identified as Cys 383, and, according to the 3D structure, a considerable rearrangement of the structure is necessary for this Cys to join up with one of the cluster ligands. In the same paper and by analogous approaches, Plank et al. also determined the four ligands of the "linear" [3Fe-4S] cluster, which will be the subject of the following section.

3. The Linear 3Fe Cluster

The discovery of the "linear" 3Fe cluster was a byproduct of our studies on the properties of aconitase. It, however, deserves mentioning here because of its interest for protein chemistry, for protein−cluster interactions, cluster interconversions, and particularly also for synthetic model chemistry, where it has become a starting point for heterometal cluster synthesis.[73]

We had observed that on raising the pH of aconitase solutions beyond pH 9, as e.g., in electrofocusing, a purple color develops and enzyme activity is lost.[74] On spectroscopic examination of this material it became apparent that the typical EPR signal of the 3Fe cluster at $g = 2.01$ had disappeared and new signals at $g = 4.3$ and 9.6, such as frequently observed for the mononuclear $S = {}^5/_2$ Fe(III), appeared. MB studies, however, revealed that the $S = {}^5/_2$ spin did not belong to a single ferric ion, but rather originated from a system of three antiferromagnetically high spin Fe(III) sites, each residing in a tetrahedral environment of sulfur atoms. Analysis of the data within a spin-coupling model showed that $J_{13} \cong J_{23}$ and $2J_{12} < J_{13}$, indicating that site 3 is strongly coupled to both sites 1 and 2, whereas sites 1 and 2 are weakly coupled among each other. When we compared the UV/vis spectra of our purple protein to spectra shown by K. Hagen et al.[75] for a synthetic 3Fe cluster, which obviously had a linear structure (Scheme 5, Figure 7), it became clear that we were dealing with a similar species. That we had produced an identical structure from the cluster in aconitase was fully confirmed by comparison of their and our MB and EPR, and later also by MCD data.[76]

Scheme 5. Schematic Description of the Interconversions Involving the "Linear" 3Fe Cluster[a]

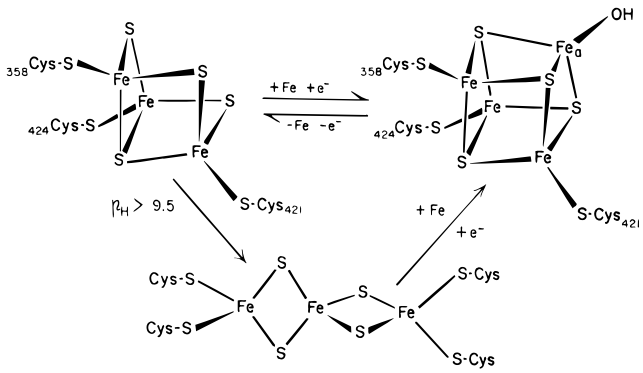

[a] Concerning the numbers identifying the Cys residues see the text. The Cys residues bound to the linear cluster are those at positions 250, 257, 421, and 424. Their precise disposition at the cluster is not known. (Reprinted with permission from ref 5. Copyright 1989 Fed. Eur. Biochem. Soc.)

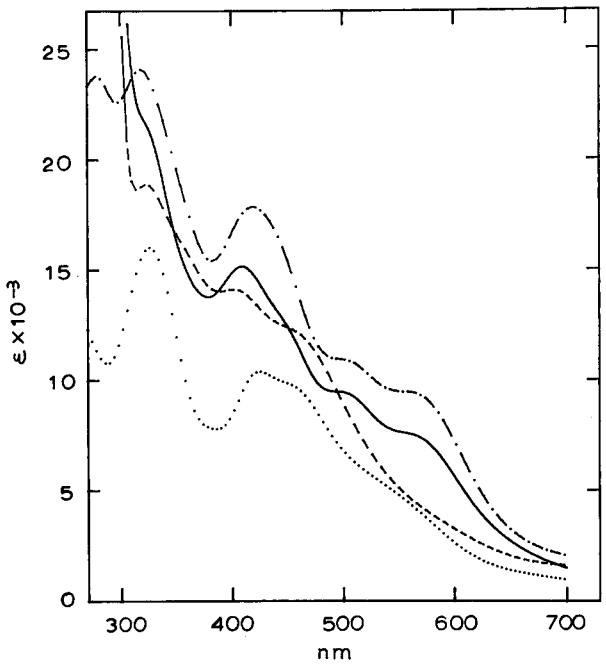

Figure 7. Electronic spectra of two 3Fe cluster forms of aconitase and of synthetic [3Fe-4S] and [2Fe-2S] model compounds: (- - -) aconitase, as isolated, diluted in 0.1 M HEPES buffer (pH 7.5); (—) purple aconitase in 0.1 M glycine buffer (pH 10.5). This spectrum was taken 40 min after aconitase (as isolated) was incubated in glycine buffer. In both cases, the enzyme was 25.2 mM in S^{2-}, 18.5 mM in Fe. The spectra were corrected for absorbance caused by the respective buffers and normalized to the molar extinction scale. (·—·) Replotted spectrum of $[Fe_3S_4(SEt)_4]^{3-}$; (···) replotted spectrum of $[Fe_2S_2(SEt)_4]^{2-}$. (Reprinted with permission from ref 74. Copyright 1984 Am. Soc. Biochem. Mol. Biol., Inc.)

Plank et al. could show by protein−chemical methods that, in contrast to the cubane-type 3Fe cluster, the linear cluster had four Cys ligands.[72] It had retained the two adjacent Cys residues (421 and 424), while releasing Cys 358. Instead, two Cys (250 and 257) from an adjacent helix had now become ligands.

According to the crystal structure of the protein with the cubane cluster, a considerable structural rearrangement is required to bring these new ligands in the proper position. By treating the purple protein with iron under reducing conditions it is possible to regain about 50% of the original enzyme activity. The purple form of aconitase can only be prepared from the 3Fe cubane form, not from the active enzyme. While the 3Fe cluster apparently has reached a more stable state in the linear form, the protein as a whole has become more labile. For instance, while there is one rapidly reacting thiol in the cubane form, there are 7−8 in the linear form. We have not been able to prepare a linear cluster from c-aconitase, which lacks the two newly recruited Cys residues of the linear cluster that are present in m-aconitase.

4. "Engineering" of Protein-Bound Fe-S Clusters

It was our good luck that the aconitase protein, like no other Fe-S protein, lent itelf to what we called "cluster engineering" in an earlier publication.[5] This is largely due to the lack of a fourth Cys ligand and thus the presence of an easily accessible and readily lost iron atom. It was, of course, easy to specifically label the Fe_a position, and we ascertained that under the conditions of protein concentration and pH (7−8.5) that we used and in the time span involved, e.g., for assay or preparation for freezing or spectroscopy, there was no exchange of added iron isotopes with irons of the clusters.[28] In order to introduce label specifically into the other sites (b_{1-3}), we needed to develop a clean and reliable method for the production of a viable apoenzyme. The methods generally used for this purpose with the smaller, more stable Fe-S proteins, such as the Fds, were acidification with trichloroacetic acid or exposure to mercurials.[77] These were not useful, as they led to largely heterogeneous and ill-defined products.

We found that we could determine the loss of the labile iron, Fe_a, by titration with ferricyanide, using the enzymatic assay as an indicator, and thus obtain almost stoichiometric amounts of the 3Fe form from the 4Fe enzyme.[37] When excess ferricyanide was added, we noted that the enzyme lost color, indicating the destruction of the Fe-S cluster. Eventually conditions for a method to obtain viable, air-stable apoenzyme were worked out by adding an excess of ferricyanide to the holoprotein in the presence of EDTA. The protein thus produced could be reconstituted with Fe and DTT with an overall yield of ~70%. This indicated, as had been found about 25 years ago by Petering et al.[78] in similar experiments with spinach Fd, that the apoprotein retained much of the original sulfide of the cluster as sulfane sulfur (S^0). It is important to note that on reconstitution, thiol should be added after iron, otherwise yields are low. Where necessary, excess reagents can be removed by gel filtration or membrane centrifugation. We are not aware that this procedure has ever been used for preparative purposes, although, more recently, this was suggested by Thomson in a review article.[79]

By this procedure we were then able to produce aconitase labeled in all iron atoms. By titration of Fe_a with ferricyanide, as mentioned above, we could make the fully labeled 3Fe enzyme (b_{1-3}) from this protein and then introduce ^{56}Fe (which is silent in MB) into the a position (Scheme 6). There was no way to differentiate the individual b positions by labeling, but as will be shown below, they could at least be segregated by spectroscopy into two groups with radically different behavior: b_1 vs b_2, b_3. As also shown below, we could readily identify Fe_a by X-ray crystallography, but not the individual b sites. Another cluster component lending itself readily to isotopic substitution is sulfide. It can be incorporated by exchange[80] which may be useful in work with radioisotopes, when monitoring the fate of sulfide in some procedure. However, for spectroscopy, such as EPR or ENDOR (^{33}S or ^{77}Se), resonance Raman (^{34}S) or MCD (^{77}Se), exchange is not suitable, as there is always some ^{32}S left, unless one were to use an iterative procedure, which not all the enzyme may survive intact. In this case again the route via the apoenzyme is the one to follow. There is one caveat, however, which applies to apoenzyme made by an oxidative procedure as the one described above: at least 75% of the originally present sulfide is trapped in di-, tri-, or tetrasulfides on oxidation and would substantially dilute the isotope introduced. Surprisingly, this polysulfide sulfur (S^0) can be selectively removed from the protein by the standard method for trapping S^0, namely treatment with cyanide, so that >90% of the S^0 can be eliminated and a suitable apoenzyme is obtained in good yield.[69]

Scheme 6. Scheme Describing Preparation of Specifically ^{57}Fe-Labeled Fe-S Cluster of Aconitase. (Reprinted with permission from ref 5. Copyright 1989 Fed. Eur. Biochem. Soc.)

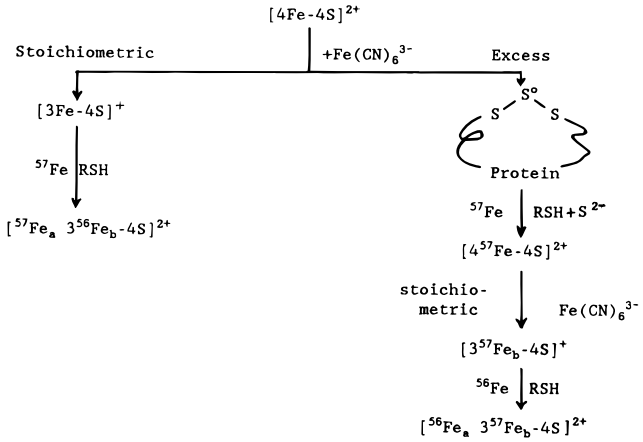

D. Spectroscopy on Specifically Isotope-Labeled Samples

1. MB of the $[4Fe-4S]^{2+}$ State

a. Without Substrate. The studies on Fe isotope ($^{55,56,57,59}Fe$) incorporation showed that the Fe added to the 3Fe species strictly entered only one discrete site of the aconitase cluster, from which it could also be released again on oxidation by ferricyanide, oxygen or persulfate.[28,37] The finding, mentioned above, that, in the inactive enzyme, we were actually dealing with a [3Fe-4S] cluster, i.e. an incomplete cubane cluster, made one actually expect this outcome of the MB experiments.

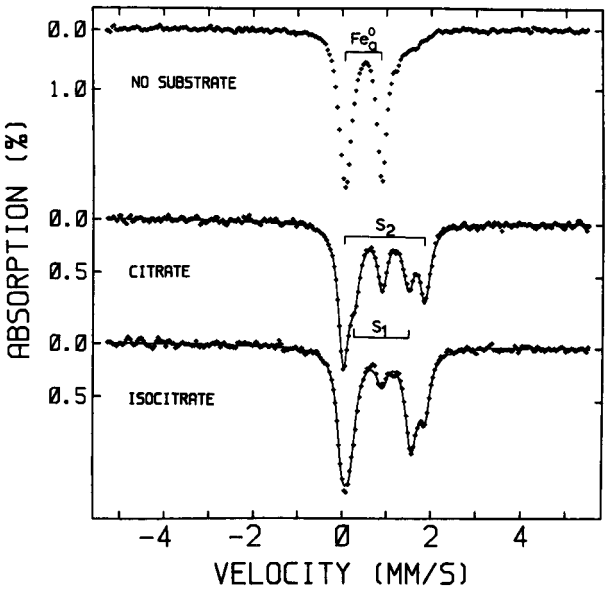

Figure 8. Mössbauer spectra of the $[4Fe\text{-}4S]^{2+}$ cluster of aconitase after rapid freezing 35 ms after mixing with 2.5 mM citrate or isocitrate at 0 °C. Only Fe_a was labeled with ^{57}Fe. It can be seen that the intensities of the newly appearing doublets (S_1 and S_2) initially have different proportions depending on the particular substrate added. (Reprinted with permission from ref 5. Copyright 1989 Fed. Eur. Biochem. Soc.)

The sites were clearly differentiated by MB, the a site (added Fe) showing ΔE_Q of 0.83 mm/s and δ of 0.44 mm/s, and the three b sites showing ΔE_Q of 1.30 mm/s and δ of 0.44 mm/s. In the 2+ form we could not differentiate between the individual b sites. While there have been a number of analogies between the behavior of the Fe-S clusters of aconitase and of FdII, the site specificity on conversion of FdII (3Fe) into FdIDg (4Fe) is not identical, and the newly acquired iron enters site b (see above; represented by doublet 2 in ref 81).

b. Effect of Substrate. The distribution of charge in the $[4Fe\text{-}4S]^{2+}$ cluster, however, changed drastically on addition of substrate, as now the a site acquired distinct ferrous character with ΔE_Q becoming 1.26 and 1.83 mm/s and $\delta = 0.84$ and 0.89 mm/s, respectively. While there was little change in the b sites, two doublets (designated S_1 and S_2) representing the a site appeared (Figure 8).[64,82] It was immediately tempting to speculate that the appearance of S_1 and S_2 may have something to do with the type of substrate bound to aconitase, or more precisely, whether binding was in the citrate or in the isocitrate mode (see below and Scheme 2). Evidence for the correctness of this assumption came from rapid freeze−quench experiments carried out at 4 °C, where distinct differences were seen in the relative intensities of the two doublets at 35 ms, when citrate or isocitrate was added. Independent support for this assumption came from X-ray crystallography, which showed that under the conditions used, aconitase crystallized with isocitrate bound.[83] These same crystals, labeled in Fe_a with ^{57}Fe, showed only one doublet by MB spectroscopy, with parameters closest to those observed a few milliseconds after isocitrate addition. The two doublets had δ and ΔE_Q values as shown in Table 2. These values are way out of the range of values found for Fe in a tetrahedral environment of sulfur ligands (Table 3),[84] they are even too large if one considers that a thiolate ligand is replaced by a non-sulfur ligand. The observed values, however, can be explained by assuming that the coordination around Fe_a has increased to five- or six-coordinate upon binding of substrate.[64,82] As we will see below, this assumption was verified by X-ray diffraction as well as ENDOR data. Despite the drastic differences in the properties of the different Fe sites of the clusters, according to the magnetic MB spectra, spin-coupling was maintained. It is of interest to anticipate here that, according to the X-ray data, the distance from Fe_a to the other Fe atoms is 0.2 Å longer than the other Fe−Fe distances (2.85 vs 2.65 Å).[83] While for lighter atoms this difference in distance is within the error of the measurements, for strong scatterers, such as Fe, it is significant.

In the MB experiments on the effects of substrate addition, we made an unexpected observation, for which we still do not have an entirely satisfactory explanation. As shown in Table 2 there always remained a certain amount of enzyme (<20%) in the original free state (Fe_a, $\delta = 0.44$ mm/s, $\Delta E_Q = 0.83$ mm/s). According to kinetic data,[85] titrations with substrate[37] and binding experiments with radiolabeled substrate,[86] the substrates have affinities such that with the concentrations used, all enzyme sites should have been occupied. Addition of more substrate had no effect. After these observations by MB we became aware that in many of our EPR experiments, which were carried out at about 1/10 the

Table 2. Mössbauer Parameters Observed after Reaction of Activated $[4Fe\text{-}4S]^{2+}$ Aconitase with Substrate

substrate, condition	none	citrate, rapid quench at 5 ms from 0 °C	citrate, equilibrated at 0 °C	isocitrate, rapid quench at 5 ms from 0 °C
		Fe_a		
ΔE_Q (mm/s)	0.81	0.81	0.81	0.81
δ (mm/s)	0.45	0.45	0.45	0.45
intensity[a] (%)	>92	62	17	18
		Doublet S_1		
ΔE_Q (mm/s)		1.21	1.23	1.43
δ (mm/s)		0.86	0.85	0.85
intensity[a] (%)		18	40	58
		Doublet S_2		
ΔE_2 (mm/s)		1.83	1.80	1.86
δ (mm/s)		0.96	0.90	0.91
intensity[a] (%)		17	40	23

[a] Percent of Fe_a originally present accounted for in signal observed.

Table 3. Mössbauer Parameters of Model Complexes and Fe-S Proteins at 77 K

compound	ΔE_Q (mm/s)	δ (mm/s)
$(Et_4N)_2[Fe_4S_4(SCH_2Ph)_4]$	1.26	0.34
$[Fe_4S_4(SCH_2Ph_4)]^{2-}$	1.15	0.34
$[Fe_4S_4(SCH_2Ph_4)]^{3-}$	1.15	0.46
Chromatium vinosum $HiPIP_{red}$	1.13	0.42
Clostridium pasteurianum Fd_{ox}	0.91	0.43
Clostridium pasteurianum Fd_{red}	1.25	0.57
Bacillus stearothermophilus Fd_{ox}	0.98	0.42
Bacillus stearothermophilus Fd_{red}	1.82[a]	0.60[a]
	1.18	0.5

[a] This doublet corresponds to that representing the a and b_1 sites in $[4Fe\text{-}4S]^{1+}$ aconitase.

protein concentration used for MB, we also had remaining unoccupied cluster sites. A possible explanation for the phenomenon might be that as we freeze the enzyme for spectroscopy, some sites are trapped just in the state when the substrate is disengaged for rearrangement within the site, so that, in a certain number of sites, Fe_a is not in the state, which is responsible for the typical "substrate" signals. This is, however, not entirely satisfactory, as it seems to make no difference, whether one freezes rapidly by quenching or slowly by hand. Nevertheless, what happens in viscous protein solutions near their freezing temperature, does not seem to be a well explored area. We have no evidence that any of the preparations used contained inactive enzyme.

2. The [4Fe-4S]$^{1+}$ State

a. EPR. In the native enzyme the Fe-S cluster is in the 2+ state and is diamagnetic. However, the [4Fe-4S]$^{1+}$ cluster of aconitase can be studied by EPR. Its behavior was first thoroughly explored by this technique and by biochemical approaches, which are much more economical and expedient than MB. We ascertained that this form of the enzyme-bound substrate, as indicated by the shifts in g values from $g_{1,2,3} = 2.06, 1.93, 1.86$ to 2.04, 1.85, 1.78 (Figure 9),[82] which were observed on addition of substrates or analogues; i.e., the rhombicity of the signal increases, which is in accord with the conclusions from MB spectroscopy (see above), namely that inequivalences arise between the cluster sites on addition of substrate.

An important point was also to establish, whether the 1+ form of the enzyme was still capable of catalysis. This was a difficult experiment to do because the high activity of the enzyme required that measurements before and after reduction be made in very dilute solution, where traces of oxygen adsorbed to glass can interfere by oxidizing the cluster to the 2+ state. To the best of our knowledge aconitase retains ~30% of its activity in the 1+ state.[37]

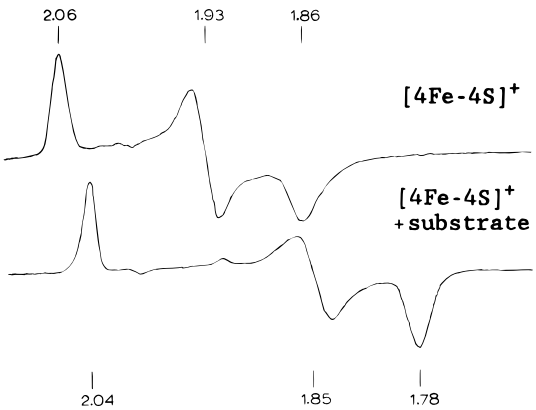

Figure 9. EPR spectra of the [4Fe-4S]$^{+}$ cluster of aconitase in the absence (top) and the presence (bottom) of substrate. Prominent features of the spectra are marked on a g value scale. Prior to freezing, the samples were photoreduced anaerobically in the presence of deazaflavin and oxalate. The spectra were recorded at a frequency of 9.24 GHz, 1 mW power, and 13 K. (Reprinted with permission from ref 5. Copyright 1989 Fed. Eur. Biochem. Soc.)

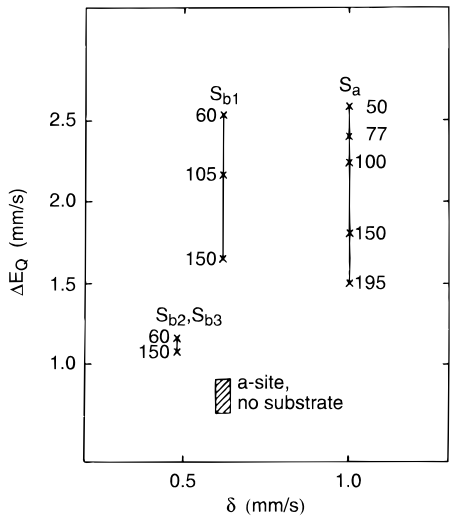

Figure 10. Graph of ΔE_Q versus δ for the reduced [4Fe-4S] cluster with bound substrate. All isomer shifts, δ, are referred to 4.2 K relative to Fe^{2+} metal at 298 K. The temperatures in K are given by the *numbers* next to the *data points*. Within the uncertainties, ΔE_Q is independent of temperatures for the two equivalent sites S_{b2} and S_{b3}. (Reprinted with permission from ref 64. Copyright 1985 Am. Soc. Biochem. Mol. Biol., Inc.)

EPR, unlike MB, also lends itself to probe for more specific interactions with substrate. We observed distinct line broadening in the EPR signals when we exposed the enzyme to substrate in the presence of $H_2{}^{17}O$. This may be attributed to exchange of the substrate hydroxyl with the medium or binding of $H_2{}^{17}O$ directly to the cluster at the a site. The fact that there was line broadening in $H_2{}^{17}O$ even when the inhibitor *trans*-aconitate had been added to aconitase,[82] clearly indicated that the substrate hydroxyl was not required for this effect. Looking at the mechanism as we visualize it now (Figure 26, a and b, below), we realize that during the reaction the components of water, whether OH^- or H_2O, are bound to Fe_a at some stage and should thus register in EPR. The logical extension of these observations was, of course, to study the enzyme−substrate interaction with ENDOR, as we will report shortly.

b. MB. A prelude to this was a study of the [4Fe-4S]$^{1+}$ cluster with bound substrate by MB spectroscopy.[64,82] Unfortunately, we ran into insurmountable difficulties in preparing the substrate-free [4Fe-4S]$^{1+}$ form in the desired purity, because MB requires such high protein concentrations. In order to have sufficient reductant present, concentrations of dithionite had to be added which destroyed a sizeable portion of the clusters in the time required for the reduction to proceed anywhere near to completion. In contrast, in the presence of substrate, a clean reaction product was obtained. We had samples available with ^{57}Fe either in Fe_a or in all three b sites.

In the reduced species with substrate bound, the site inequivalences observed on addition of substrate to the 2+ cluster are even more pronounced: the a site has clear ferrous character (Figure 10) and the b sites split into a pair of little affected sites (b_2, b_3) and b_1, which now also shows more ferrous character.[64] The a site in the 1+ form, however, shows a single quadrupole doublet, as opposed to the 2+ form with bound substrate. It is clear that we have here

a case of localized valence within a spin-coupled system.[64,82] Particularly at the a site electron density increases, while there is little change in two b sites (b_2, b_3). This suggests that electron density has been withdrawn from the bound substrate, as one would expect, if Fe_a acts as a Lewis acid. However, we must consider that the sulfurs of the cluster are also a reservoir of electron density, which we cannot monitor by MB spectroscopy. Formation of localized valence in a spin-coupled system to the extent found here, has never been observed before with a protein-bound Fe-S cluster. These observations by MB have been fully confirmed by ENDOR, as will be shown below, when the interaction of aconitase with substrate and inhibitors will be considered in more detail.

c. ENDOR. *i. ^{57}Fe ENDOR.* As our ENDOR studies with ^{57}Fe and ^{33}S labels in the cluster itself[87] complement the EPR and MB work, which we presented above, we will discuss this before proceeding to studies with labeled substrates and analogues. We have to remember that all ENDOR work had to be done with the less active $[4Fe\text{-}4S]^{1+}$ form, because the active $[4Fe\text{-}4S]^{2+}$ form is not paramagnetic. We also took advantage of high-frequency (35 GHz) ENDOR to observe ^{57}Fe and ^{33}S ENDOR signals, because under these conditions the intrinsic proton signals in the system are shifted toward higher frequencies and do not interfere.

The samples used for ENDOR as for EPR were frozen solutions and as such contained a random distribution of all protein orientations. However, ENDOR spectra taken with the magnetic fields set at the extreme edge of an EPR spectrum, near g_1 or g_3, give single-crystal-like ENDOR patterns from the subset of molecules, for which the magnetic field happens to be directed along a g tensor axis.[88,89] This will directly yield the desired A values. For intermediate orientations, points along the whole EPR envelope were scanned and analyzed by procedures to extract the desired A values.[89] In this fashion we were able to determine the complete hyperfine tensor in most instances.

We had available protein labeled either in the a site or in the b sites only. The inequivalence of the iron sites of the Fe-S cluster was manifest in the presence and absence of substrate and the dramatic effect of substrate addition on Fe_a observed by MB spectoscopy was clearly evident from ENDOR.[87] We also could confirm that the b_1 site had properties quite different from those of the a and b_2,b_3 sites. In the absence of substrate the A tensor of Fe_a is coaxial with the g tensor; however, when substrate is bound to the enzyme, the A tensor changes dramatically; each of the principal values is decreased by about one-third and A is no longer coaxial with g. These observations are summarized in Table 4 and Figure 11[85] together with MB data for the same state of the enzyme. From ENDOR we have been able to obtain complete sets of A values for Fe_a and $Fe_{b2,3}$, but could only observe two components for the b site. The values nicely complement the values calculated from MB; e.g., while MB is insensitive to the mutual orientation of the tensors, magnetic MB can furnish the sign of A, which is not provided by the ENDOR data. The reversal of the sign of A between the components of the cluster (Table 4) clearly indicates that we are dealing with a spin-coupled system. As indicated by MB, the $b_{2,3}$ sites are more ferric (charge ~2.5+), while the b_1 and the a sites clearly have ferrous character. On this basis we were able, by approximations,[90] to calculate the local intrinsic parameters of the individual iron sites. We were then able to apply this procedure to the sulfide sites (see below ii) and arrive at the geometrical relationship of the two pairs of iron sites (a and b_1 vs $b_{2,3}$) and the two pairs of sulfides of low and high hyper-

Table 4. ^{57}Fe Hyperfine Tensors for Fe_a, Fe_{b1}, Fe_{b2}, and Fe_{b3} Sites of the $[Fe\text{-}4S]^+$ Cluster of Aconitase, Substrate Free (E), and in the Enzyme-Substrate (ES) Complex

principal values and Euler angle[a]	E (ENDOR)	ES (ENDOR)	ES (Mössbauer)[b]
		Fe_a	
A_1 (MHz)	33	23	26
A_2 (MHz)	41	32	34
A_3 (MHz)	42	32	34
α (deg)	0	25	
		Fe_{b3}	
A_1 (MHz)	35	35	−32[c]
A_2 (MHz)	34	42	−39
A_3 (MHz)	42	43	−39
α (deg)	0	10	
		Fe_{b2}	
A_1 (MHz)	27	31	−32[c]
A_2 (MHz)	34	38	−39
A_3 (MHz)	37	39	−39
α (deg)	0	10	
		Fe_{b1}	
A_1 (MHz)			12
A_2 (MHz)	25[d] (18)	24[d] (17)	22
A_3 (MHz)	23[d] (15)	24[d] (17)	12

[a] If we begin with A and g coaxial, α refers to the rotation of the A tensor about its A_3 axis. [b] Reference 64. [c] Mössbauer does not distinguish the Fe_{b2} and Fe_{b3} sites. [d] There are two possible interpretations for the Fe_{b1} site; the less favored is placed in parentheses.

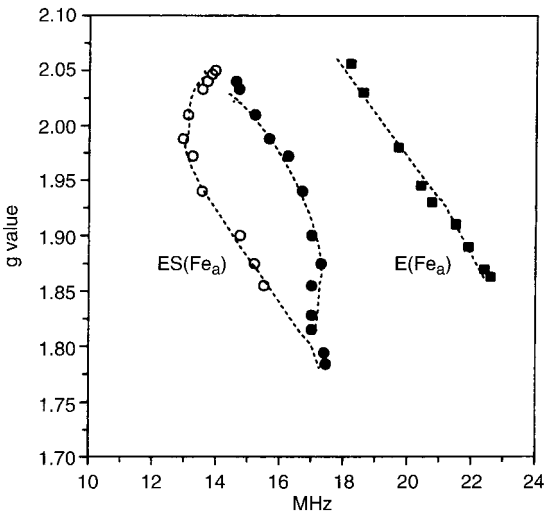

Figure 11. ^{57}Fe ENDOR peak position for the ν_+ feature(s) for Fe_a in the substrate-free enzyme (squares) and substrate-bound enzyme (circles) versus the observing g value. Theoretical values calculated by using parameters in Table 4 are indicated as dashed lines. (Reprinted with permission from ref 87. Copyright 1990 American Chemical Society.)

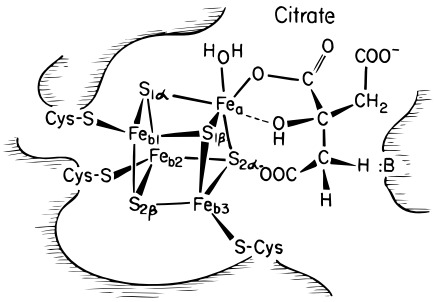

Figure 12. Representation of ENDOR-derived information about the [4Fe-4S]$^{+}$ cluster of the aconitase enzyme-substrate complex, showing the two pairs of sulfides, $S_{1\alpha}$, $S_{1\beta}$ and $S_{2\alpha}$, $S_{2\beta}$, in relationship to the four inequivalent iron sites, Fe_a, Fe_{b1}, Fe_{b2}, and Fe_{b3}, along with the bound substrate. (Reprinted with permission from ref 87. Copyright 1990 American Chemical Society.)

fine coupling, 0−1 and 6−12 MHz, respectively (Figure 12). We are not yet able to relate this geometrical information to the crystal structure of the enzyme.

ii. ^{33}S ENDOR. The interpretation of ^{33}S ENDOR data is considerably more complex than that for ^{57}Fe, because this isotope has a nuclear spin of $^{3}/_{2}$ and therewith a quadrupole moment. The four S^{2-} ions of the cluster together may, therefore, give rise to as many as 24 separate lines in a single-crystal-like spectrum. Nevertheless, the field dependence of the observed resonances suggests that there are two sulfides which show isotropic hyperfine couplings between 6−12 MHz and a pair with small hyperfine couplings of A <1 MHz. The relationship between the electronic state of the Fe ions of the cluster and that of the sulfides was discussed above.

iii. ^{14}N ENDOR. The reader of the original papers on this subject may wonder what happened to the ^{14}N signals that we detected and were somewhat at a loss to explain.[87] Since such signals were also seen in some other Fe-S proteins subjected to high-frequency ENDOR, we made a separate study of this phenomenon.[91] It became clear that those resonances in the range of 0−20 MHz are due to "distant" ^{13}C and ^{14}N nuclei, which have negligible coupling to the Fe-S cluster. This unexpected finding, which should be remembered by others using high-frequency ENDOR, opens up the possibility of observing weak interactions, as, e.g., expected from NH···S bonds to the cluster, a capability usually reserved for electron spin−echo (ESEEM) spectroscopy. Here, however, pulsed ENDOR will be superior to the continuous wave (CW) technique.

iv. ^{17}O ENDOR. As discussed above under EPR approaches, it became apparent from line-broadening in $H_2{}^{17}O$[82,92] that there is some kind of exchange with solvent which is sensed by the cluster. ^{17}O, ^{1}H, and ^{2}H ENDOR are the methods of choice for obtaining answers concerning cluster−solvent interactions. Again, high-frequency ENDOR was of great advantage. It was also of interest to determine, which groups of the substrate are bound to the cluster, as older models had proposed tridentate chelation by substrate (two carboxyls and one hydroxyl).[13,93] For approaching this problem, isotope exchange, as we had used it in the early kinetic studies, is no longer suitable, and stably labeled compounds have to be prepared.

Table 5. ENDOR Results on Aconitase with ^{17}O-Labeled Substrates[a] or Analogue

Added	^{17}O Labling (●)	Hyperfine coupling constant, A_y (MHz)
Citrate	HO, C●●, COO⁻, COO⁻	0
Citrate	HO, COO⁻, C●●, COO⁻	15
Isocitrate	HO, COO⁻, COO⁻, C●●	0
Nitroisocitrate	H●, C●●, NO_2, COO⁻	9,13
Nitroisocitrate	H●, COO⁻, NO_2, COO⁻	9

[a] Note that in the presence of active aconitase any substrate added is converted to an equilibrium mixture of the three substrates. (Reproduced with permission from ref 94. Copyright 1987 National Academy of Sciences.)

We have enumerated above some of the advantages of an enzyme over a Fd in the kind of studies that we are discussing here. In our case, these virtues were still enhanced by the fact that aconitase catalyses a reaction involving substrates that are metabolites central to a number of metabolic pathways. Thus, the substrates of aconitase are accessible via a number of routes and can therefore be specifically labeled with relative ease. We mentioned, at the beginning of this chapter, among the important steps in the development of our understanding of aconitase the introduction, by Alexander Ogston,[12] of the principle that bears his name, namely that compounds that appear symmetrical to us, such as citrate, may acquire chirality when binding to three sites of an asymmetric enzyme; in today's words, the concept of prochirality. Thus it is possible to distinguish the parts of the citrate molecule that are derived from oxaloacetate from those stemming from acetyl-CoA, when citrate is being acted upon by an enzyme. We could therefore introduce ^{17}O into the α-carboxyl by enzymatically synthesizing citrate with citrate synthase from acetyl-CoA, phosphoenolpyruvate and CO_2 in the presence of $H_2{}^{17}O$, bicarbonate, carbonic anhydrase, and phospoenolpyruvate carboxylase; into the β-carboxyl by again using carbonic anhydrase, etc. and running the oxidative decarboxylation of isocitrate to α-ketoglutarate by isocitrate dehydrogenase in reverse in the presence of aconitase; and into the γ-carboxyl by repeated alkaline hydrolysis of isocitrate lactone in $H_2{}^{17}O$ (Table 5).[94] We always based these syntheses on $H_2{}^{17}O$, as this compound could be obtained in the highest enrichment. Similar syntheses were done on the basis of $^{13}CO_2$. We similarly chemically labeled nitroisocitrate and *trans*-aconitic acid with ^{17}O and the latter also with ^{2}H.

The studies with selectively ^{17}O-labeled substrates in the three carboxyl groups clearly indicated that, at equilibrium, only the β-carboxyl is significantly

bound to Fe_a of the cluster.[94] As the enzyme converts any substrate to a mixture of the three substrates, this meant that either citrate is largely bound or *cis*-aconitate is bound in the citrate mode (Scheme 2, see also below). We favored the latter alternative, because we could not find any ENDOR signal from the hydroxyl group, whereas the analogous, but nonexchangeable hydroxyl group of nitroisocitrate (3-hydroxy-2-nitro-1,3-propanedicarboxylate) did give an ^{17}O ENDOR signal. In order to see, whether the α-carboxyl could also be bound, i.e., in the isocitrate mode, if the conversion to citrate was prevented, we added stably labeled [^{17}O]α-carboxyl- and [^{17}O]hydroxylnitroisocitrate to the enzyme. As expected, we did find ^{17}O ENDOR signals for both the carboxyl and the hydroxyl groups.

v. $^{1,2}H$ ENDOR. $H_2{}^{17}O$ ENDOR had also given us useful hints as to solvent interaction with the Fe−S cluster.[82,92] One of the most important pieces of information from this approach was the observation that whether substrate or an analogue was bound to the enzyme or not, ^{17}O ENDOR was found.[95] It is of interest to note here that neither MB nor EPR showed evidence for binding of a solvent species in the absence of substrate or analogue. The observation that in the presence of substrate a solvent species is bound, falls in line with the conclusions from MB spectoscopy, namely that Fe_a extends its coordination sphere on substrate binding.[64,82] Together with the just discussed ENDOR results these data indicate that, in addition to three sulfides, Fe_a now has three oxygens bound, one from solvent (H_xO), one from a substrate carboxyl, and one substrate hydroxyl or a species derived from it (see below). However, the finding of a solvent species bound to Fe_a in the absence of substrate demands another explanation. We attempted to further define this species, which we called H_xO.

We must digress here briefly to point out that, by this time, the crystal structure was not known to the extent that all the cluster ligands were identified. Our search by biochemical analytical methods for an SH group that might be liberated on making the 3Fe form of the enzyme from the 4Fe form was not successful.[69] Thus, the idea that the 4Fe cluster had only three Cys ligands and one non-sulfur ligand, presumably at Fe_a, entered our mind. It would have been the first such case observed with biological Fe-S clusters. Soon thereafter the X-ray data also indicated an oxygen ligand,[83] which obviously was the very H_xO that we had found to be a ligand of Fe_a at all times. From ^1H and ^2H ENDOR of samples studied in ^1H_2O or in ^2H_2O it became clear that in the presence of substrate and all analogues and inhibitors tested, this species was H_2O, whereas in the substrate-free enzyme only a single deuteron was detected indicating that ^2H_xO is -O^{2}H in this case (Figure 13).[95] Thus, the conclusion is that, during the aconitase reaction, substrate does in fact not replace one of the cluster ligands but is accommodated at Fe_a by changes in coordination with simultaneous protonation of the hydroxyl ligand originally present at Fe_a. This protonation can be expected, when one considers the charge balance at the Fe_a site.

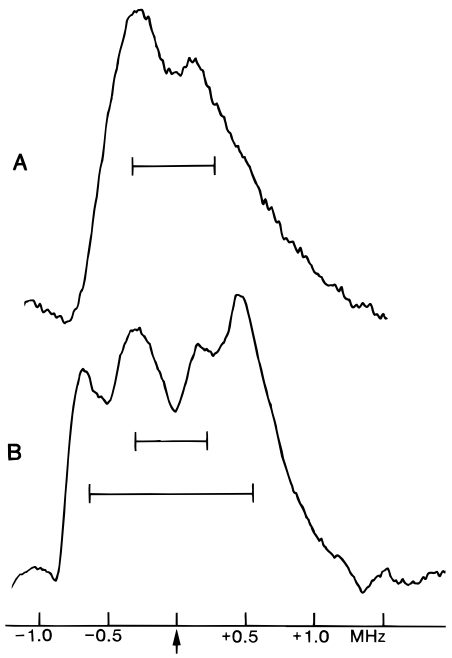

Figure 13. ^2H-ENDOR spectra of the [4Fe-4S]$^+$ cluster of aconitase in the absence (A) and presence (B) of substrate. The solvent was ^2H_2O; aconitase was photoreduced as for Figure 9. Microwave and modulation frequencies were 35.4 GHZ and 100 kHz, respectively. The modulation amplitude was 0.063 mT; rf scanning rate, 3 MHz/s; time constant, 0.03 s; H_0 for (A) and (B) were 1.356 T and 1.4188 T, respectively. (Reprinted with permission from ref 5. Copyright 1989 Fed. Eur. Biochem. Soc.)

3. Spectroscopy of Se Analogs

a. EPR and Mb. By reconstitution of the apoenzyme (see above) we were able to prepare a reasonably stable [4Fe-4Se] enzyme, which, curiously, showed higher activity with isocitrate as substrate than did the S enzyme. We were then able to convert this protein into the [3Fe-4Se] form by oxidation with ferricyanide (Figure 14). Thus EPR, MB,[96] and of the 3Fe species also MCD[97] spectra are available in different oxidation states, with and without substrate in some cases. As expected, there was much analogy to the properties observed with the corresponding sulfur-containing species; however, in comparison to the essentially isotropic g tensor of the [3Fe-4S]$^+$ cluster, that of the [3Fe-4Se]$^+$ cluster was substantially more anisotropic (g = 2.04, 1.985, 1.92 vs g = 2.204, 2.016, 2.004) (Figure 15). The spectra of the [3Fe-4Se]^0 cluster also showed the features typical of the S cluster; the slight inequivalence between the two members of the mixed valence pair was, if anything, more pronounced in the Se species, with one member being biased toward ferrous and the other toward ferric. It is also significant that the MB spectra of the [3Fe-4Se]^0 cluster showed no fully delocalized state over a broad temperature range, a state which had been observed with other Fe-S clusters of this structure.[98] With other Fe-S clusters so far no significant change in the isomer shifts had been observed on substitution of Se;[99,100] with aconitase, however, there consistently was a slight increase. Figure 15 shows the EPR spectra of the [4Fe-4Se]$^+$ cluster with and without substrate. The ^{77}Se isotope was used in these reconstitution experiments.

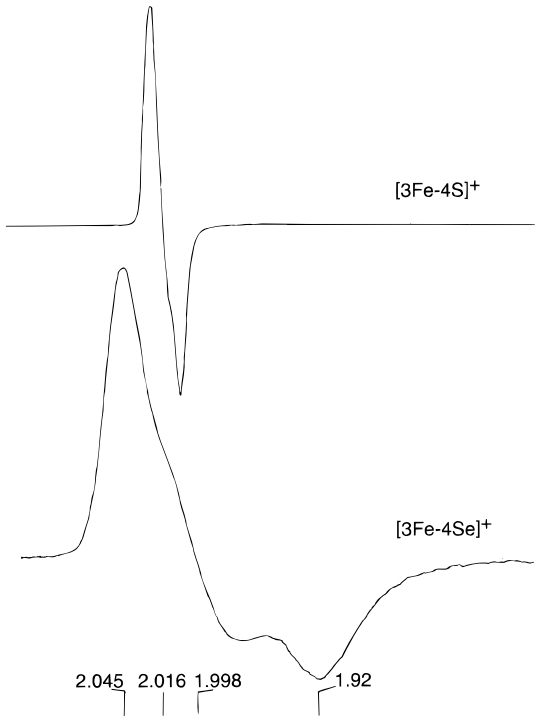

Figure 14. EPR spectra of the $[3Fe\text{-}4S]^+$ and $[3Fe\text{-}4Se]^+$ clusters. The conditions were those of Figure 9, except that a microwave power of 2 mW was used. The cluster concentration for the lower spectrum was about 20 times that for the upper one.

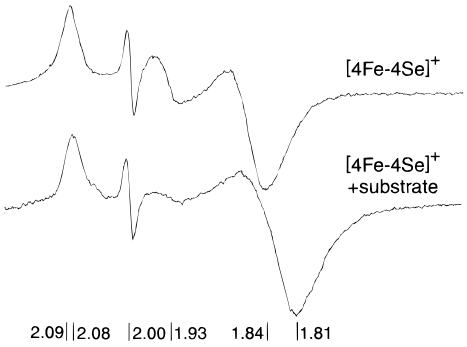

Figure 15. EPR spectra of the $[4Fe\text{-}4Se]^+$ cluster of aconitase in the absence (top) and the presence (bottom) of substrate. The conditions were essentially those used for Figure 9, except that the samples were in Taps buffer at pH 8.5 and were reduced by dithionite in the presence of methylviologen. The sharp signal at $g = 2$ is due to the methylviologen radical. (Kennedy and Beinert, unpublished.)

b. MCD. The availability of the Se-substituted 3Fe cluster of aconitase offered a rare opportunity to record the low-temperature MCD spectra of this species, from which, it was expected, the assignment of the charge transfer transitions to Cys ligands vs bridging chalcogenides could be achieved (Figures 16 and 17).[97] In keeping with previous experience, Se substitution had the general effect of decreasing charge transfer energies, so that the $Se^{2-} \rightarrow Fe$ transitions could be located from their bathochromic shift. The intensity of the MCD spectrum of the $[3Fe\text{-}4Se]^+$ cluster was at least twice that of its S counterpart; thus the effect of the 4-fold increase in the spin−orbit coupling brings about a doubling of the MCD intensity. The intensity of the $[3Fe\text{-}4Se]^0$ cluster was almost four times that of the corresponding S cluster.

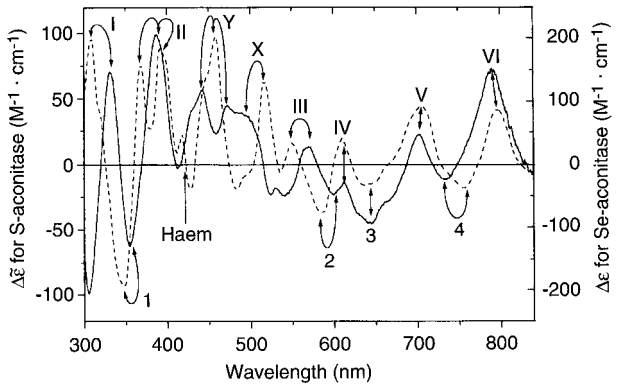

Figure 16. Comparison of the MCD spectra of $[3Fe\text{-}4Se]^{1+}$ seleno-aconitase (—) and $[3Fe\text{-}4S]^{1+}$ aconitase from bovine heart at pH 7.5 (- - -). The temperature was 4.2 K and the magnetic field 5 T. The Roman and Arabic numbers designate corresponding peaks or troughs, respectively, in different regions of the two spectra. (Reprinted with permission from ref 97. Copyright 1995 Biochem. Soc., London.)

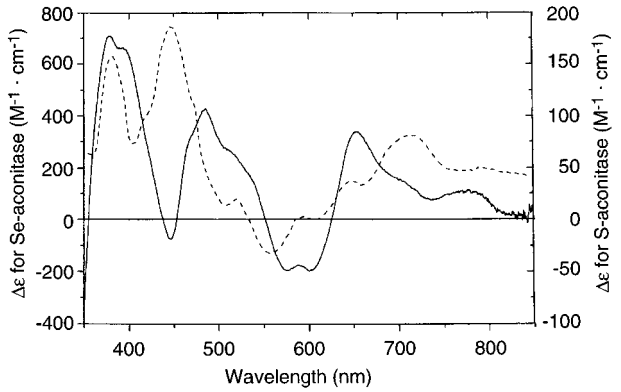

Figure 17. Comparison of the MCD spectra of $[3Fe\text{-}4Se]^0$ seleno-aconitase (—) and $[3Fe\text{-}4S]^0$ aconitase from bovine heart at pH 7.5 (- - -). The temperature was 4.2 K and the magnetic field 5 T. (Reprinted with permission from ref 97. Copyright 1995 Biochem. Soc., London.)

4. Resonance Raman (RR) Spectroscopy

a. Without Substrate. The description above, as to how our knowledge of the enzyme aconitase has developed, makes a convincing case for the mutual complementation of the three principal spectroscopic tools that we used, namely EPR, MB, and ENDOR, in furnishing decisive information about the Fe-S cluster, the active site, and enzyme−ligand interactions. Particularly ENDOR was able to provide valuable detail about the last topic, viz., the ligands to the iron (Fe_a) at the active site. Another spectroscopic technique, which is potentially capable of providing insights into subtle interactions between the cluster components and their immediate surroundings, is resonsance Raman (RR) spectroscopy. Although the resonance enhancement of the Fe→S charge transfer transitions of Fe-S clusters is known to be inferior to that given by most other biological chromophores, such as, e.g., heme,[101] it was nevertheless possible, from the results obtained, to extract interesting detail concerning hydroxide, substrate or analogue binding to Fe_a, about cysteine ligand con-

formational changes and hydrogen bonding to the cluster from protein donor groups.[102] Our efforts were greatly aided by comparisons of the experimental results with calculations of expected modes made on the basis of related and model structures and also on the basis of data from the various crystal structures available for aconitase and its substrate or analogue complexes.

We learned that the Fe−O stretching vibrations of bound hydroxide, substrates or inhibitors were not resonance enhanced. However, their influence could be detected in ^{18}O shifts of Fe-S modes of the cluster and in the large frequency elevation of one of the Fe-S(terminal) modes. Our results indicate that the substitution of a single thiolate by hydroxide does not alter the vibrational pattern of a [4Fe-4S] cluster significantly, at least not as far as the bridging modes are concerned. There are, however, a very few unique features, which we attribute to the replacement of one thiolate with a hydroxyl (for detail see ref 102). All Fe-S modes could be assigned by replacement of the inorganic sulfides by ^{34}S. Their frequencies and ^{34}S shifts could be reproduced by calculations of normal modes on a cluster model with ethyl thiolate ligands, provided that the Fe−S−C−C dihedral angles were adjusted to the values determined for the corresponding crystal structures. In addition, the differences of the force constants had to be taken into account that arise from the weakening of the bonds to the unique Fe_a, to which OH^- is attached, and from a stengthening of the bonds to the three other Fe atoms. The orientation of the thiolate ligands clearly determines to a significant extent the vibrational pattern observed in Fe-S proteins and their substrate or analogue complexes. The natural frequency for S−C−C bending is in the region of the Fe−S stretches and there is, therefore, potential for significant interaction between the two types of internal coordinates. This interaction is maximal when the dihedral angle about the S−C bond is 180° and minimal when the angle is 90°. According to the X-ray coordinates of substrate-free aconitase the three Cys ligands have dihedral angles of 127°, 94°, and 80°. With these angles the three terminal modes are spread out from 364−383 cm^{-1} and are separated by intervals of 13 and 6 cm^{-1}, features that could be satisfactorily reproduced by calculations. By following similar considerations, the frequencies and isotope shifts could also be reproduced for the inactive 3Fe form of the enzyme, if allowance was made for further strengthening of the bonds to the doubly bridging S atoms, when Fe_a is removed.

When a tight-binding inhibitor such as nitroisocitrate is added to the active enzyme, a dramatic change in the RR spectrum occurs. The strongest band in the spectrum of the substrate-free enzyme is the cluster breathing mode at 339 cm^{-1}, whereas now, with inhibitor bound, the dominant feature of protein is a new band at 356 cm^{-1} (Figure 18), which appears to replace the two terminal stretches at 352 and 360 cm^{-1}. However, when citrate is added to the enzyme, the RR spectrum is intermediate between the spectra of the enzyme with and without nitroisocitrate (Figure 18). It is striking that superposition of these two spectra produces a spectrum that resembles that of the enzyme after citrate addition quite well. We have made a similar observation with room temperature CD in the visible region, where the bands due to the cluster are found, namely that there is a dramatic effect of nitroisocitrate on the CD, while substrate addition leads to an intermediate position of bands. These observations lead us back to considerations which we have brought forth above, namely when we were searching for reasons why in MB and in many EPR spectra there was a significant amount of apparently "unoccupied" enzyme left after addition of a great excess of substrate. As pointed out, when any one of the substrates is added, the enzyme will instantly produce a mixture of species; the exact composition of which we do not know. What is known is the equilibrium of substrate species in the bulk solution but not what is bound to the enzyme. One might think, therefore, that in the process of the conformational change that has to occur during the interconversion of the substrates, there are always some species which are unoccupied by substrate, or merely appear to be "unoccupied" as far as our spectroscopic criteria are concerned. As now several spectroscopic approaches, MB, EPR, RR, and CD, independently point toward some so far not understood phenomenon, we feel, that we should put these observations on record.

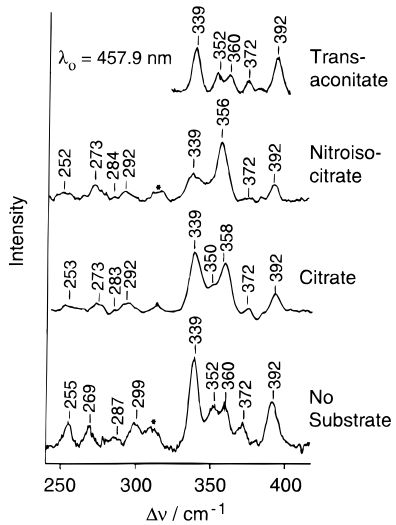

Figure 18. RR spectra (77 K) of aconitase, and after addition of citrate, nitroisocitrate, and *trans*-aconitate obtained with 457.9 nm excitation. The citrate and inhibitor concentrations were between 5 and 8 mM, and the enzyme concentration was between 1 and 2 mM. The asterisk (*) marks an ice band. (Reprinted with permission from ref 102. Copyright 1994 American Chemical Society.)

With RR, we also observed shifts of 2 cm^{-1} in the presence of ^2H_2O for a cluster mode of a bridging sulfur and for a terminal sulfur, when substrate was bound. This is consistent with the finding by crystallography of a hydrogen bond to both a bridging and a terminal sulfur.[83] In addition, we identified, by their ^2H_2O sensitivity, resonance enhancement for amide modes involving C=O stretching (amide I, 1655 cm^{-1})and C−C−N bending (466 cm^{-1}). The amide I band shifts to 1642 cm^{-1} when aconitase is dissolved in ^2H_2O, but to 1624 cm^{-1} when it is

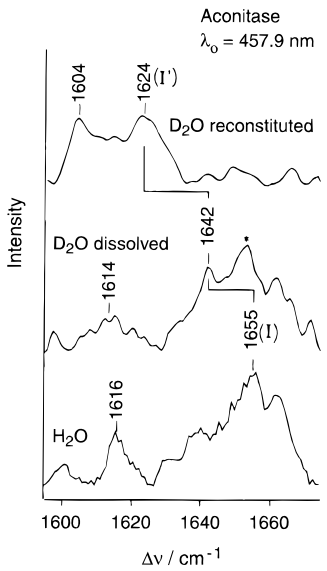

Figure 19. A 413.1 nm excited RR spectra (77 K) in the amide I region of aconitase. All spectra were collected using a triplemate/intensified diode array spectrometer system. (Reprinted with permission from ref 102. Copyright 1994 American Chemical Society.)

reconstituted from apoprotein in ^2H_2O (Figure 19). These shifts may be interpreted as resulting from $^1H/^2H$ exchange of one proton and, on reconstitution, of both protons on a primary amide. The finding of two exchangeable protons excludes the possibility that a backbone amide is involved. We suggest that these amide modes arise from one or both of the Asn side chains (Asn 258 and 446) involved in hydrogen bonds and that their resonance enhancement arises from electronic coupling with the resonant Fe→S charge transfer transition via the hydrogen bonds to the cluster.

IV. Crystal Structures

A. Crystallization

Experiments by one of us (M.C.K.) in O. Gawron's laboratory at Duquesne in Pittsburgh had established that an Fe-S cluster was very likely present in aconitase. A collaboration was initiated between O. Gawron and M. Sax's Biocrystallography Laboratory at the VA Medical Center in Pittsburgh. Crystals were obtained of porcine heart mitochondrial aconitase, but they were invariably twinned.[103] Sometime later, in conjunction with the discovery of 3Fe clusters and early work on the structure of *A. vinelandii* FdI,[43,44] efforts to obtain single crystals were resumed by A. H. Robbins. In one experiment excess (0.5 M) Tris·HCl, pH 7.8, was added to the crystallization solution to buffer an addition of $(NH_4)_2SO_4$, which, it was feared, would cause destruction of the Fe-S cluster because of the lowering of the pH. Transfer of twinned crystals from this solution to a protein solution in this buffer at pH 7.0 caused many single crystals to nucleate.[104] Subsequent experiments established that the excess chloride present in the original Tris·HCl buffer solution is essential for obtaining single crystals. Using macroseeding techniques it was possible to obtain large, single crystals which diffracted to 2.0 Å resolution. The crystals are orthorhombic, space group $P2_12_12$, and contain one 83 000 Dalton molecule per asymmetric unit.[104]

B. Structure Determination

The orthorhombic crystals were used for the initial structure determination of the [3Fe-4S] form of the porcine heart enzyme. The structure was solved by multiple isomorphous replacement in combination with anomalous scattering information from the Fe-S cluster and the 22 cysteine and methionine sulfurs in the protein.[9] In addition, colorless crystals of the apoprotein, formed by oxidation, were used to collect data to 3.0 Å resolution. The position of the Fe-S cluster was established by observing the differences in the data obtained for the apoprotein to that of the isomorphous, native [3Fe-4S] cluster containing protein. The cluster position was found to be consistent with anomalous scattering differences measured from the native data alone. The isomorphous difference data were then used to calculate approximate phases to deduce the sites of heavy atoms in two derivatives. The combined phase information from the derivatives and Fe-S cluster isomorphous and anomalous differences was used to compute a 3.0 Å resolution map for model building.

Initially the primary sequence of aconitase was unknown. Also, it was not possible to trace the entire 754 residue polypeptide chain in the experimental electron density map. Consequently, shorter segments of polyalanine models were fit to the density. The partial models were used to calculate phases, which in combination with the experimental phases led to increasingly clear electron density maps, permitting the polyalanine segments to be extended and linked in an iterative process. At a point where about two-thirds of the residues had been modeled, the primary sequence of seven unique cysteinyl tryptic peptides of bovine heart aconitase became available.[68] It was possible to align all of these (196 residues) with the polyalanine segments without change in chain direction or α-carbon register. The fit of these peptide sequences was confirmed by the overlap of each Cys and Met sulfur in the model with a significant peak in the anomalous difference Fourier map calculated with native data and experimental phases. Inclusion of these 196 residues further improved the partial structure model, and the resolution was increased by including more of the native data. At the stage where the model consisted of residues 1−294 and 305−754, and all data to 2.5 Å were being used, the complete sequence of porcine heart aconitase based on the cDNA sequence became available.[10] The complete amino acid sequence was then fit to the electron density. In the process all remaining Cys and Met sulfurs (22 in all) were found to overlap with significant peaks in the anomalous difference Fourier map. The Cys ligands to the [3Fe-4S] cluster were positively identified and the cluster was fit to the density and included in the model. The structure was then refined using simulated annealing methods using all the data to 2 Å resolution, and bound solvent molecules were included in the model.

C. Activated Aconitase and Enzyme Complexes

The orthorhombic crystals were used for anaerobic soaking experiments in which the [3Fe-4S] cluster was reduced and activated by addition of ferrous ammonium sulfate to form the $[4Fe\text{-}4S]^{2+}$ cluster state of the enzyme. This structure was studied by difference Fourier methods and refined to 2.5 Å resolution.[8] Subsequently, a series of crystallization experiments were carried out anaerobically using both porcine and bovine mitochondrial aconitase in the [4Fe-4S] form in the presence of substrates and inhibitors and seed crystals of both enzymes. These experiments yielded a related monoclinic crystal form, space group *B*2, which also diffracts to 2.0 Å resolution.[83] Crystals of porcine aconitase grown in the presence of *cis*-aconitate were used to obtain the structure in the new crystal form by molecular replacement. The structure was confirmed with a heavy atom derivative and anomalous scattering from the [4Fe-4S] cluster. This crystal form was then used to determine structures of five inhibitor complexes as well as the substrate free (sulfate bound) form of the enzyme in the monoclinic lattice. A summary of the crystal structures of aconitase which have been determined is given in Table 6.

1. Protein Fold

Mitochondrial aconitase folds into four domains (Figure 20a). The first three from the N-terminus are tightly associated and form a shallow depression where they adjoin near the center of the molecule. The Fe-S cluster is ligated to three cysteines of the third domain within this depression. The larger C-terminal fourth domain is tethered to the first three by an extended polypeptide chain segment termed the hinge-linker (Figure 20b). The shape of the fourth domain is complementary to the surface formed by the first three domains. However, the entire interface between the fourth domain and the first three is occupied with solvent molecules, or is

Table 6. Refined Crystal Structures of Mitrochondrial Aconitase

source	space group	[Fe-S] Cluster	bound species	resolution (Å)	*R* factor[a]	ref	PDB code
pig heart	$P2_12_12$	[3Fe-4S]	sulfate	2.1	0.209	9	5ACN
pig heart	$P2_12_12$	[4Fe-4S]·OH	sulfate	2.5	0.182	8	6ACN
pig heart	*B*2	[4Fe-4S]·OH_2	isocitrate	2.1	0.179	83	7ACN
beef heart	*B*2	[4Fe-4S]·OH_2	nitroisocitrate	2.1	0.161	83	8ACN
beef heart	*B*2	[4Fe-4S]·OH_2	nitrocitrate	2.05	0.172	105	1NIS[b]
beef heart	*B*2	[4Fe-4S]·OH_2	*trans*-aconitate	2.05	0.168	105	1ACO
beef heart	*B*2	[4Fe-4S]·OH_2	methylisocitrate	2.0	0.182	106	1AMI
beef heart	*B*2	[4Fe-4S]·OH	sulfate	2.0	0.168	106	1AMJ
beef heart	*B*2	[4Fe-4S]·OH_2	4-hydroxy-*trans*-aconitate	2.05	0.177	*c*	*c*

[a] $R = \sum|F_o| - |F_c|/\sum|F_o|$, where $[F_o]$ and $[F_c]$ are observed and calculated structure factor amplitudes for all observed reflections to the resolution limit indicated. [b] Minor occupancy sulfate bound form in this structure, PDB code 1NIT. [c] Reference 106a.

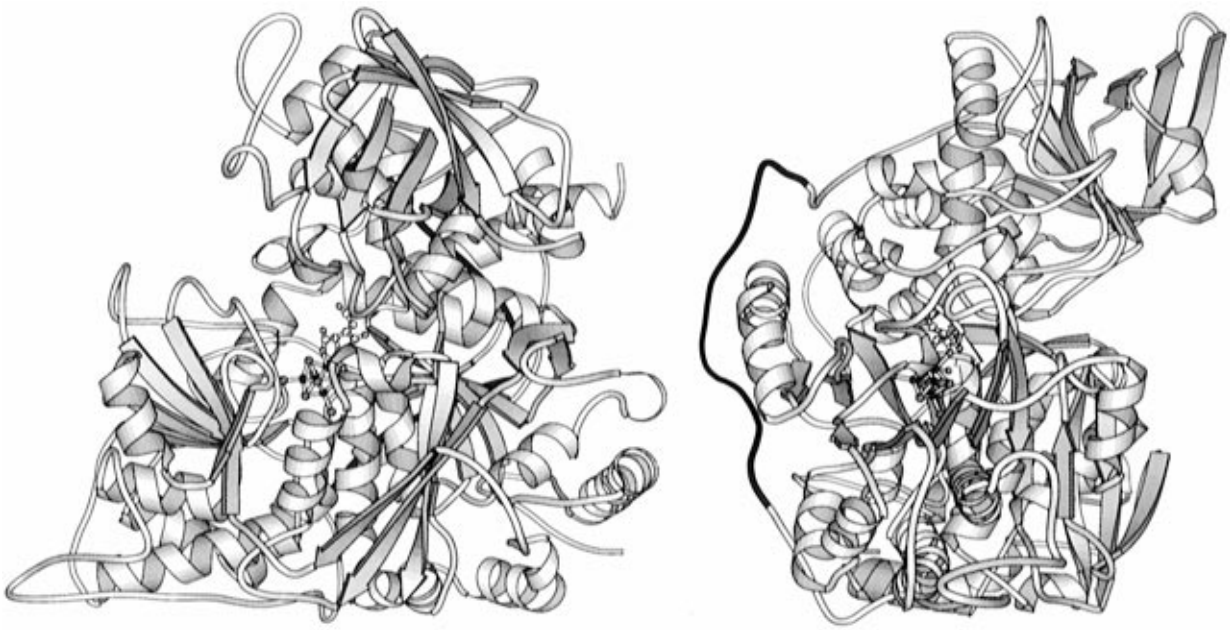

Figure 20. The three dimensional structure of porcine mitochondrial aconitase. α-helices and *β*-strands are represented as coils and twisted arrows, respectively. All atoms of the [4Fe-4S] cluster, cysteine ligand sulfurs, isocitrate and bound H_2O are shown. In a (left) the N-terminus is at the lower right and the C-terminus is at the upper right. The central *β*-sheets of the three N-terminal domains are visible from right to left in the lower part of the structure. The C-terminal fourth domain comprises the upper portion of the structure. In this view the cleft runs across the center of the molecule and opens to the left. The hinge-linker, connecting the third and fourth domains, is in back (darker connecting chain segment). In b (right) the structure is rotated 90° from its orientation in a so that the view is into the cleft toward the active site: i.e. the view is from the left side of the page in a. The fourth domain is at the top and the hinge-linker is indicated as a darker chain segment. These figures made using Molscript by P. Kraulis.

comprised of contacts between polar amino acids. Consequently, an extensive cleft is formed leading toward the Fe-S cluster from the surface of the protein from several directions. The side chains are more tightly packed within the cleft in the region adjacent to the hinge-linker, suggesting that the principal access to the Fe-S cluster is from the left in the view in Figure 20a. Together the hinge-linker and solvent-filled cleft suggest the possibility of hinge motion which would separate the fourth domain from the rest of the molecule and allow diffusion of substrates into and out of the active site.

The topology of the secondary structure elements of domains 1−3 contains a motif commonly observed in dehydrogenases and other enzymes termed a nucleotide binding domain.[107] The parallel β-sheets of this motif in domains 1−3 are comprised of five, four, and five strands, respectively, rather than six as in dehydrogenases. Additional antiparallel β-strands and α-helices in each domain contribute to the tight 3-fold association of these domains. The larger fourth domain is composed of a central five stranded parallel β-sheet extended at one edge by a three-stranded β-meander. The central β-sheet is flanked on one side by a four stranded antiparallel β-sheet and on the other by α-helices. The topology of this domain appears to be unique among known protein structures. The parallel β-sheets within domains 1 and 4 have the C-terminal ends of their strands oriented toward the active site, while those of domains 2 and 3 have the N-terminal ends of these strands oriented towards the cleft and not directly into the active site.

2. Active Site

The active site of aconitase is comprised of the Fe-S cluster and side chains of 21 AA from all four domains of the protein. These side chains surround a large, polar cavity within the cleft at the point where the fourth domain nestles into the shallow depression formed by the first three (Figure 21). Active site residues are considered as such if they ligate to, or are in contact with, the cluster, or if they are in contact with bound substrate,[83] or are involved in hydrogen bonding with residues directly in contact with substrate. Domain 1 provides seven residues to the active site: Gln72, Asp100, and His101 from loops connecting strands of the parallel β-sheet to α-helices; Asp165, Ser166, and His167 from the first turn of a three turn 3_{10}-helix; and His147 from an adjacent α-helix. Domain 2 provides only two active site residues, Glu262, on a central α-helix, and Asn258. Domain 3 provides the cluster ligands Cys358, Cys421, and Cys424. Cys358 resides on the central strand of the parallel β-sheet. A "crossover" loop connecting the two halves of this sheet provides the other two ligands (Cys421GlyProCysIle425). Another loop, connecting strands of the β-sheet provides Asn446, Arg447, and Arg452 to the active site. Domain 4 provides five active site side chains from the loops connecting the strands of the central β-sheet (Asp568, Ser642, Ser643, Arg644) and a flanking α-helix (Arg580).

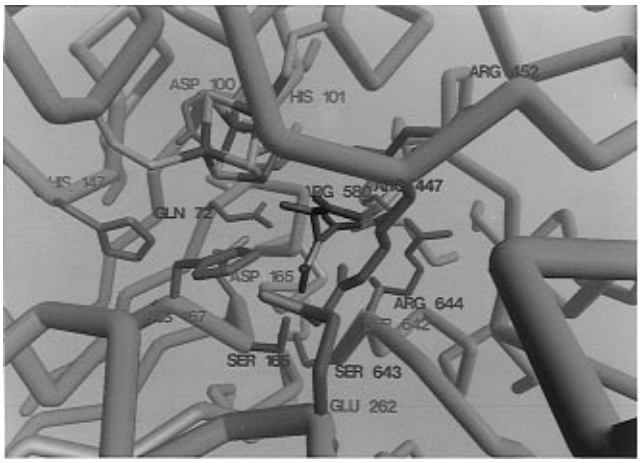

Figure 21. The active site region in mitochondrial aconitase. The side chains of 14 key active residues are shown with labels. Also shown are the [4Fe-4S] cluster, cysteine ligands and the bound isocitrate molecule (green and red). The main chain of the protein is depicted as a tube connecting Cα positions. (Reprinted with permission from ref 108. Copyright 1993 John Wiley and Sons.)

The active site residues can be grouped as follows: cluster cysteine ligands; asparagines which hydrogen bond to inorganic or cysteine sulfur (residues 446 and 258, respectively); Ile425, which has a significant hydrophobic contact with the cluster; three His·Asp/Glu pairs (Asp100·His101, Asp165·His147, Glu262·His167); four arginines in contact with substrate carboxyl groups (residues 447, 452, 580, and 644); residues hydrogen bonding to substrate (Gln72, Ser166, Ser643), and the catalytic base (Ser642). Asp568 is hydrogen bonded to both Arg452 and Arg644. Overall, the active site is a complex array of residues which form networks of hydrogen bonds with substrate, bound water molecules, the Fe-S cluster, and other residues. The involvement of 21 residues may in part be the reason why the enzyme is such a large protein. The active site also exhibits a net positive electrostatic field, as revealed by calculation,[108] because of the presence of four arginines and the fact that each of three histidines is paired with an aspartate or glutamate. This feature is clearly consistent with the requirement for binding anionic substrates.

3. Series of Structures

The available structures of aconitase (Table 6) can be arranged in a series, which is also chronological, in which each structure establishes an important feature of the active site or structural aspect of the chemical mechanism. These structures confirm, and are in complete accord with, the results from spectroscopic and kinetic experiments. They provide a structural context for understanding the role of the Fe-S cluster, protein side chains, and bound solvent molecules in the catalytic mechanism.

By comparison with the structure of aconitase containing a [3Fe-4S] cluster, the structure of activated enzyme established the structure and ligation for the [4Fe-4S] cluster.[8] The first structure with a substrate bound to aconitase, isocitrate, established the nature of the contacts within the active site and confirmed the mode of binding of isocitrate to the [4Fe-4S] cluster as deduced from spectroscopic experiments.[87] The structure of the enzyme with a

reaction intermediate analogue bound, nitroisocitrate, confirmed that the binding mode observed for isocitrate was a productive one. Subsequent enzyme structures with two other inhibitors bound, nitrocitrate and *trans*-aconitate, allowed information to be inferred about the binding modes of the substrates, citrate and *cis*-aconitate. The structure of aconitase with the inhibitor methylisocitrate bound confirmed stereochemical constraints on the catalytic mechanism deduced from kinetic experiments.[85] The structure of the substrate-free enzyme with sulfate bound in monoclinic crystals, when compared to the isocitrate complex, demonstrated that conformational changes of side chains, chain segments, and an entire domain are not artifacts of crystal packing, and may be important aspects of the catalytic mechanism. Finally, the structure of aconitase crystallized in the presence of fluorocitrate revealed electron density for 4-hydroxy-*trans*-aconitate as the bound species, as predicted from spectroscopic and chemical experiments[64] and in accord with the model for the catalytic mechanism (below).

a. Activated Aconitase. With ligands Cys358, Cys421, and Cys424 the [3Fe-4S] cluster has tetrahedral geometry at each Fe site, typical of other Fe-S clusters in proteins. The geometry of the [3Fe-4S] cluster resembles those in other proteins, being very similar to a [4Fe-4S] cluster cubane, only with one Fe missing. The open site faces into the active site cleft. However, there are no additional cysteine residues which could serve as a ligand to a fourth Fe. By soaking crystals anaerobically in a solution of synthetic mother liquor containing sodium dithionite and ferrous ammonium sulfate it was possible to collect data to 2.5 Å resolution on the [4Fe-4S] form of the enzyme in orthorhombic crystals. The structure of activated aconitase is isomorphous with the [3Fe-4S], inactive form, and comparison shows that the fourth Fe, termed Fe4 or Fe_a (for spectroscopy), is inserted into the empty corner of the [3Fe-4S] cluster with no significant change in the cluster geometry (Figure 22). The Fe4 site retains tetrahedral geometry and acquires a hydroxide ion as its fourth ligand. The electron density shows a distinct peak for a light atom (oxygen) within bonding distance (about 2 Å) from Fe4. Independent ENDOR experiments show that in the absence of substrate Fe4 is associated with a singly protonated solvent species, i.e. hydroxide.[95] The hydroxide ligand may be derived from a bound solvent molecule (water) in the [3Fe-4S] form which is about 0.5 Å further from the Fe4 site and hydrogen bonded to a histidine within the active site (Figure 22). Because Fe4 lacks a protein ligand and is positioned adjacent to the active site cleft it is ideally poised for interaction with both solvent molecules and substrates. Thus, the [3Fe-4S] cluster is the "ligand" for Fe4, conferring to this Fe unique electronic and bonding properties while avoiding the steric constraints which would arise if Fe4 were directly ligated by protein side chains.

b. Isocitrate and Nitroisocitrate. At equilibrium the ratio of aconitase substrates (Figure 23), citrate:*cis*-aconitate:isocitrate, is 0.88:0.04:0.08. In principle one could expect the crystal structure to reveal a mixture of bound substrates, or predominantly citrate, for crystals grown in the presence of any of the three substrates, since the time needed to reach equlibrium is much shorter than the crystallization time. It came as a surprise, therefore, that the electron density map at 2.0 Å resolution of pig heart aconitase, which had been crystallized in the presence of 75 mM *cis*-aconitate, could only be interpreted in terms of isocitrate as the bound species.[83] To confirm that the crystals did indeed contain isocitrate under these conditions, beef heart aconitase was activated with ^{57}Fe and crystallized in the presence of 75 mM citrate, and 5.5 mg of large single crystals where harvested, washed, and used to record the Mössbauer spectrum.[83] The spectrum showed only a single quadrupole doublet for one species of the bound form of the enzyme. The parameters of this form were the same as those for the form which is dominant in the first 35 ms after the rapid mixing of isocitrate with enzyme.[64] When assayed, the dissolved crystals gave the expected specific activity. Together these data supported the interpretation of the electron density. The result was further tested by using a crystal of pig heart aconitase grown in the presence of 75 mM citrate to collect data to 2.7 Å resolution. Again, the electron density for the bound species could only be interpreted in terms of isocitrate.[83] In other words, starting with either pig or beef heart aconitase in the presence of excess *cis*-aconitate or citrate, the crystals obtained contain only the form with isocitrate bound. The presence of a single substrate in the crystals is fortuitous and greatly simplifies the analysis. One explanation for this phenomenon is that only the form with isocitrate bound can be incorporated into

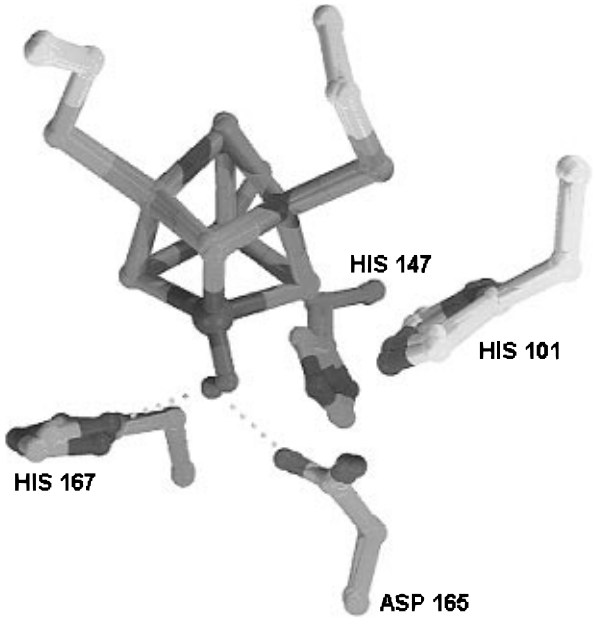

Figure 22. Activation of aconitase in the crystal. The structures of the [3Fe-4S] (inactive) and [4Fe-4S] (activated) forms of the enzyme are superposed to demonstrate how the fourth Fe site (Fe4/Fe_a, magenta) is inserted into the [3Fe-4S] cluster to form a [4Fe-4S] cubane structure. A H_2O molecule in the [3Fe-4S] form (light red), which is hydrogen bonded to both Asp165 and His167, becomes the fourth ligand to Fe4 as a hydroxyl group. Side chains in both structures are also depicted.

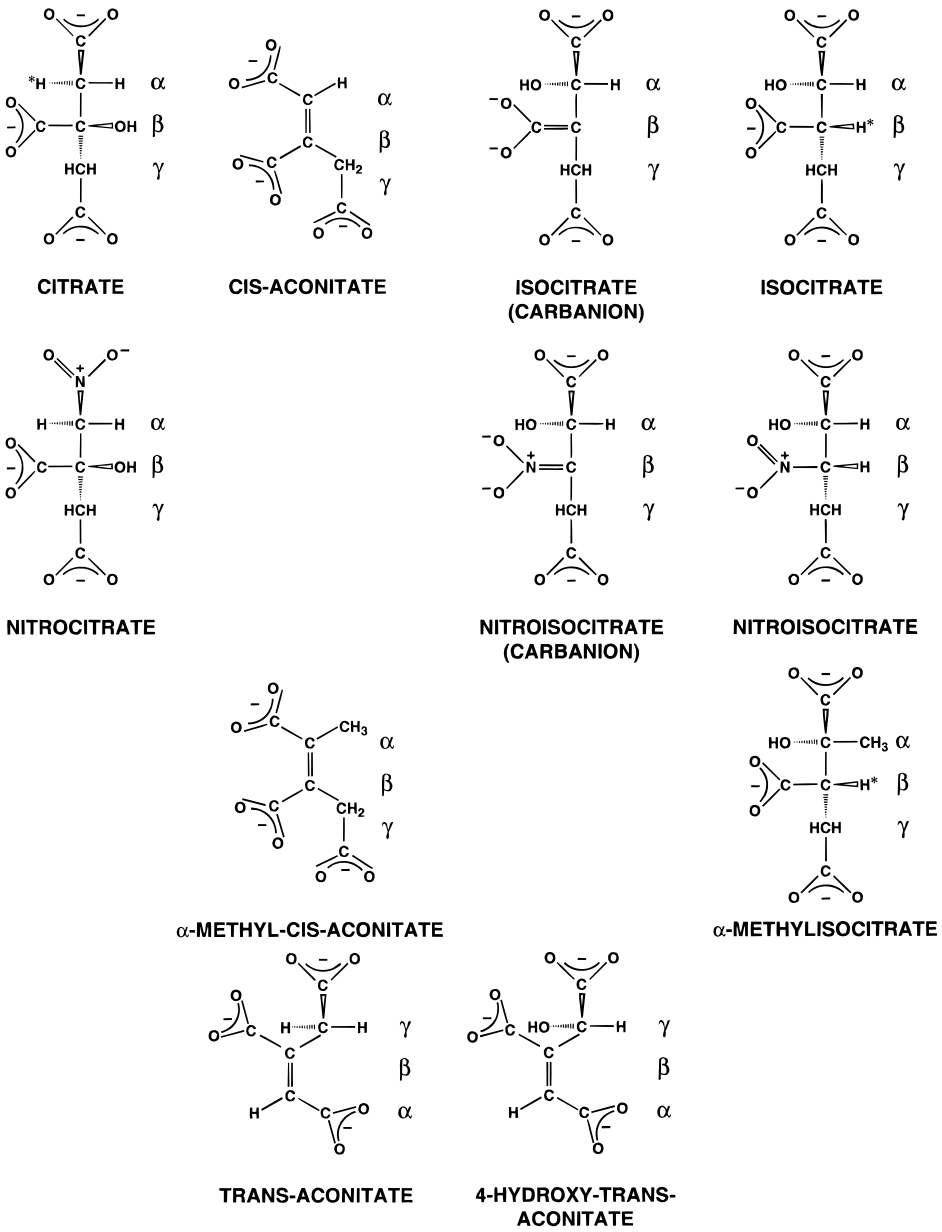

Figure 23. Chemical structures of aconitase substrates, inhibitors, and proposed transition state intermediates referred to in the text.

the monoclinic lattice and this shifts the equilibrium as the crystals grow. Alternatively, the equilibrium may be shifted in solution because of the high ionic strength (2.2 M $(NH_4)_2SO_4$) of the crystallization medium and competitive binding of sulfate in the active site (below).

The complex of isocitrate with the [4Fe-4S] cluster is shown in Figure 24a. Coordination to Fe4 is via one oxygen of the Cα carboxyl group and the hydroxyl group on Cα. A water molecule is also bound to Fe4, making this Fe site six-coordinate with three sulfur and three oxygen ligands. The structure is in agreement with the structure deduced from chemical labeling and spectroscopic experiments.[87] The identity of the bound solvent species as water vs hydroxyl in the presence of substrate is established by ENDOR experiments.[95] The geometry at Fe4 is slightly distorted from being ideally octahedral (90° angles) in that S−Fe−S angles are expanded (av 101°) toward the tetrahedral angles typical in Fe-S clusters (109°), while O−Fe−O angles are compressed (av 74°). Fe−O distances are in the range 2.20−2.33 Å. A distinct feature of the Fe4 site is that it is displaced about 0.2 Å away form the [3Fe-4S] moiety compared to the position it would occupy in a perfectly symmetrical [4Fe-4S] cluster.

In addition to two covalent bonds to Fe4, the isocitrate molecule makes 18 potential hydrogen bonds within the active site.[83] These contacts are part of three hydrogen-bonding networks surrounding three oxygen atom centers critically involved in the overall chemical transformations carried out by aconitase. Each oxygen atom center displays tetrahedral geometry of sigma and hydrogen bonds around it (Figure 24, parts a and b). One such site is the isocitrate hydroxyl group which is within hydrogen bonding distance to both Asp165 and His101 (which is paired with Asp100) (Figure 24a). A second such site is the hydroxyl group of the side chain of Ser642, which is the closest protein atom to the hydrogen on Cβ of isocitrate (Figure 24b). This is the hydrogen atom which is abstracted in the reaction and *trans*

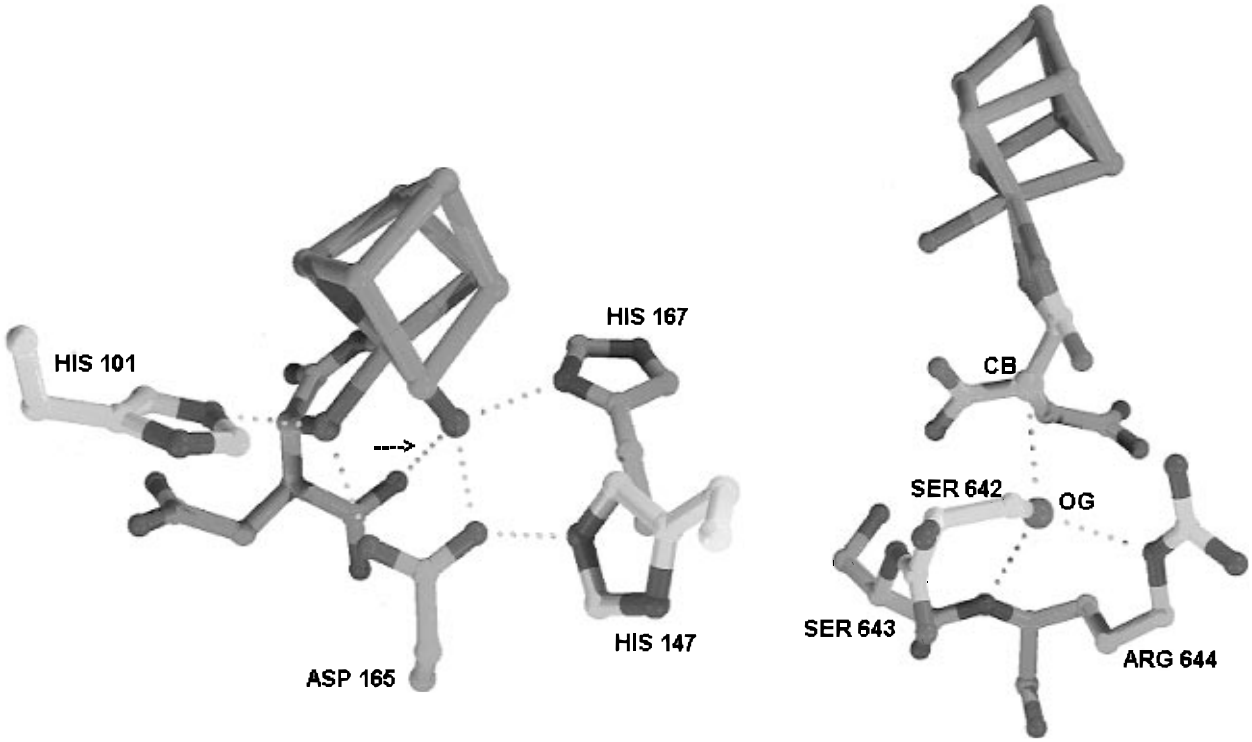

Figure 24. Three oxygen atoms in the aconitase active site which have tetrahedral geometry of σ and hydrogen bonds and which are proposed to be involved in proton transfers in the reaction mechanism. (a, left) One such atom is the hydroxyl oxygen of isocitrate which coordinates to Fe4 while accepting a hydrogen bond from His101 and donating a hydrogen bond to Asp165 (left side of figure). Proton transfer to this oxygen from His101 occurs concomitantly with cleavage of the carbon−oxygen bond. A second oxygen atom involved in a proton transfer is the H_2O molecule bound to Fe4 (right side of figure). Protonation of this oxygen atom as a hydroxyl ion bound to Fe4 in the substrate free state of the enzyme forms H_2O when substrate is also bound. The H_2O molecule is able to accept a hydrogen bond from His167 and donate hydrogen bonds to both Asp165 and the Cβ-carboxyl group of substrate. The latter hydrogen bond (arrow) is very short, <2.6 Å, in the structures of aconitase with nitroisocitrate and 4-hydroxy-*trans*-aconitate bound, and is proposed to be a low barrier hydrogen bond in the transition state. (b, right) A third oxygen atom directly involved in catalysis is the side chain Oγ atom of Ser642, the proposed base in the reaction mechanism. This oxygen accepts hydrogen bonds from both amide and guanidinium nitrogens of Arg644. This is expected to lower the pK_a of the side chain sufficiently that it is deprotonated when isocitrate or citrate bind. Proton transfer from Cβ of isocitrate to the alkoxide leads to formation of *cis*-aconitate. In this figure the Oγ and Cβ atoms are labeled as OG and CB, respectively.

to the isocitrate hydroxyl. The Ser642 hydroxyl resides in an "oxyanion hole" formed by short hydrogen bonds from the side chain and amide of Arg644. The third oxygen atom center is the water molecule bound to Fe4. It is in contact with His167 (which is paired with Glu262), Asp165 (which is paired with His147), and the Cβ carboxyl group of isocitrate (Figure 24a). In addition to these hydrogen bonding interactions and contacts, the three carboxyl groups of isocitrate are hydrogen bonded to the four active site arginines (residues 447, 452, 580, and 644), as well as to Gln72, Ser166, and Ser643.[83] Together these residues and interactions define a chiral binding pocket which specifically accommodates 2*R*,3*S* isocitrate.

Nitroisocitrate is a reaction intermediate analogue of the proposed carbanion intermediate in the transition state between *cis*-aconitate and isocitrate.[109] The carboxyl group on Cβ of isocitrate is replaced with a nitro group (Figure 23) making the proton on Cβ more acidic. In the deprotonated state the nitro group mimics the proposed carbanion (*aci*-acid) on the β-carboxyl so that nitroisocitrate becomes a very tight-binding inhibitor. The complex of nitroisocitrate and beef heart aconitase was prepared and crystallized by seeding in the monoclinic form. The structure is virtually identical to the isocitrate complex with respect to both the protein conformation and the mode of binding of the compound.[83] This establishes that the details of the active site interactions observed for isocitrate are relevant to a productive binding mode in solution. Further, the similarity of the structures demonstrates that the binding mode itself is not an artifact of crystallization because the nitroisocitrate complex was prepared prior to crystallization.

The refined structure of the nitroisocitrate complex also allowed a sequence to be derived for the remainder of the beef heart aconitase polypeptide not covered by the sequences of cysteinyl tryptic peptides.[68] Within these known peptide sequences (196 residues) only three positions differ between pig and beef heart aconitases. In the remaining 558 residues only three positions of the porcine sequence were clearly incompatible with the electron density for the bovine enzyme.[83] The six total substitutions all involve residues on the surface of the protein far from the active site. At the same time the electron density of all active site residues in the bovine aconitase structure is fully compatible with the pig heart sequence in cases where the sequence is not known from the peptide data.[83] Therefore, for purposes of analyzing inhibitor complexes (Table 6) the beef and pig heart enzymes are considered identical (Table 7).

Table 7. Primary Sequence Alignment of Six [Fe-S] Isomerases[a]

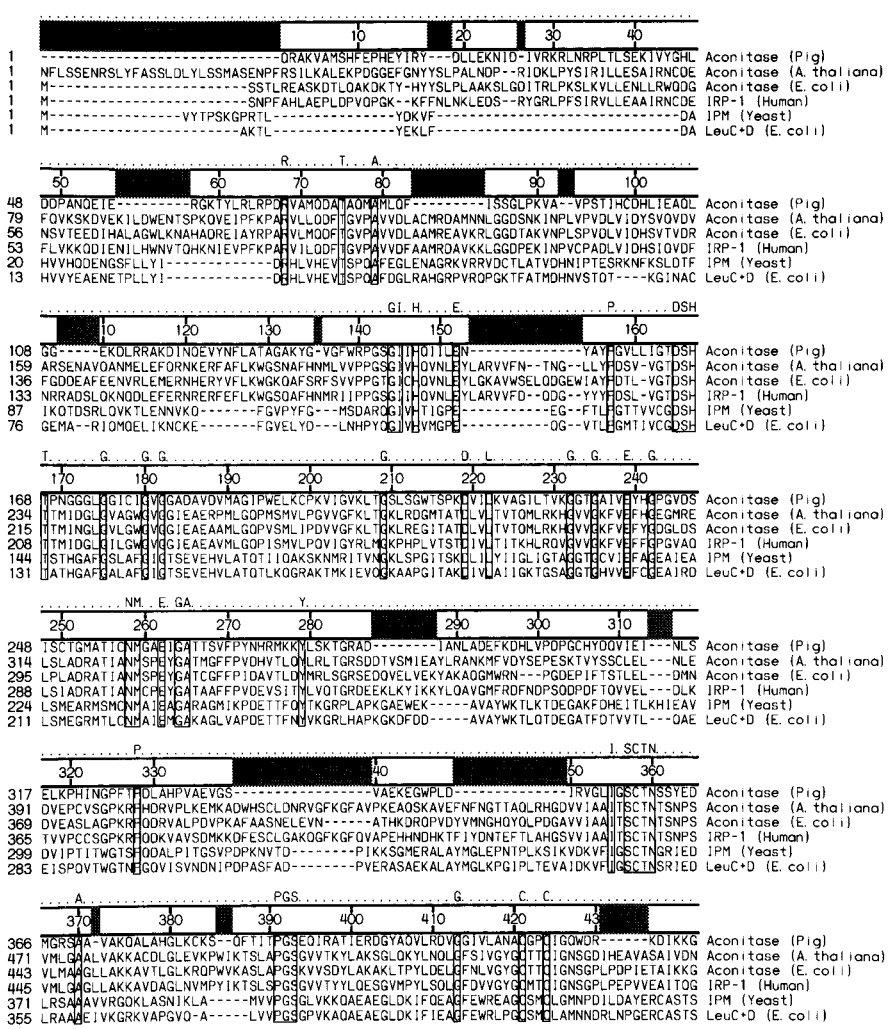

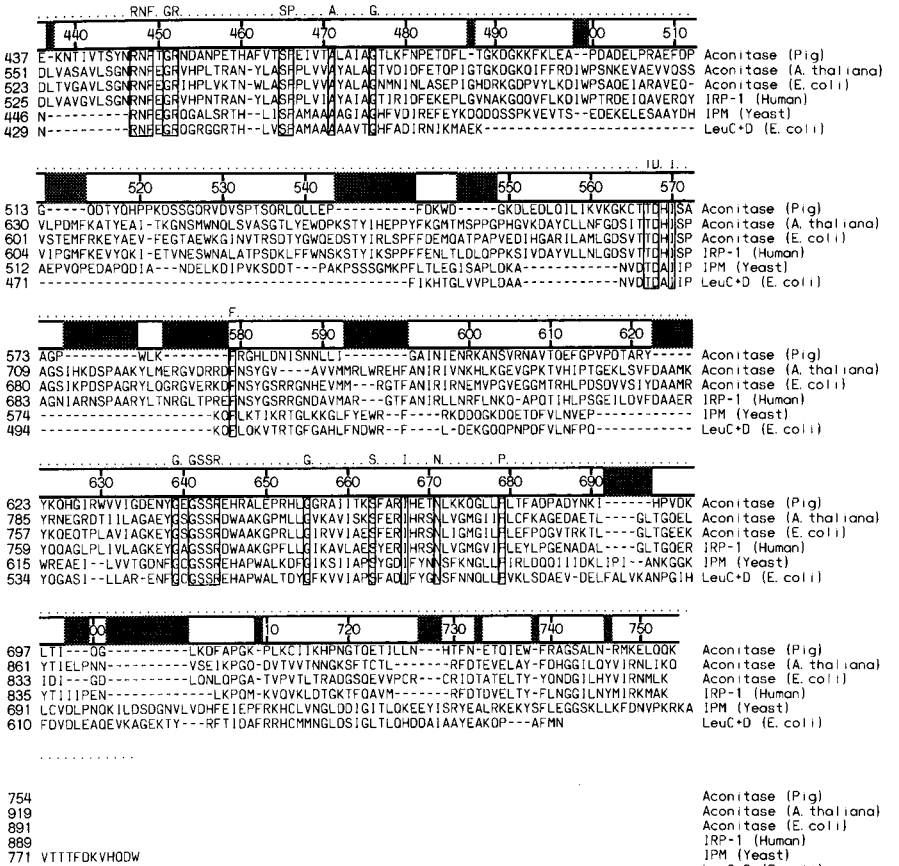

[a] The six sequences shown are porcine mitochondrial aconitase,[10] *A. thaliana* (plant) aconitase,[110] prokaryotic (*E. coli*) aconitase,[111] human iron-regulatory protein (isoform 1),[152] eukaryotic (*Saccharomyces cerevisiae*) isopropylmalate (IPM) isomerase,[112] and prokaryotic (*E. coli*) IPM isomerase.[113] The sequences are aligned with respect to the mature form of porcine aconitase. Residue numbers therefore correspond to the crystal structure. Residues identical in all six proteins are indicated in a consensus sequence on the top line. These residues include active site residues identified from the crystal structures as well as other structurally conserved amino acids. In five instances an active site residue in porcine aconitase is not conserved in all six sequences shown (Gln72, Asp100, His101, Ile425, and Arg580). The four domains and hinge-linker region of porcine aconitase correspond to the following residues: domain 1, 1−200; domain 2, 201−319; domain 3, 320−512; hinge-linker, 513−536; domain 4, 537−754. This table was kindly prepared by Dmitrij Frishman.

c. Nitrocitrate and *trans*-Aconitate. As discussed above we have not succeeded in crystallizing the wild-type enzyme such that the substrates citrate and *cis*-aconitate are bound. Therefore, the crystal structure of beef heart aconitase complexed with inhibitor analogues of these two substrates were analyzed (Table 6). Nitrocitrate is a reaction intermediate analogue of the transition state for the reaction of citrate to *cis*-aconitate in a manner analogous to nitroisocitrate (Figure 23).[109] The crystal structure of the complex shows that nitrocitrate binds to Fe4 via one oxygen of the Cβ carboxyl group, and via the hydroxyl group on Cβ.[105] The coordination geometry of these groups to Fe4 is essentially the same as for the corresponding Cα groups of isocitrate. This binding mode, with isosteric positions for carboxyl and hydroxyl moieties but with the Cα and Cβ positions inverted, confirms the model deduced from kinetic and spectroscopic labeling experiments.[3] In this model the binding modes of isocitrate and citrate are related by a 2-fold rotation about the Cα−Cβ bond. Other interactions within the active site are similar in the nitrocitrate and isocitrate complexes, including the presence of a water molecule bound to the sixth coordination site of Fe4.

Another inhibitor of aconitase is *trans*-aconitate. In the crystal structure of this complex the *trans*-aconitate molecule binds in such a way that it mimics all but one of the interactions made by isocitrate.[105] In so doing the entire propane backbone is inverted with respect to isocitrate (Figure 23) so that the Cγ carboxyl is coordinated to Fe4 and the Cβ−Cα double bond is one carbon removed from Fe4. Consequently, there is no proton to abstract from the central carbon (Cβ) and no double bond adjacent to Fe that can be hydrated. As in the other complexes, a water molecule is bound to Fe4 in the sixth coordination position. However, the Fe4 coordination site corresponding to the hydroxyl of isocitrate is vacant. While the Cγ atom of *trans*-aconitate does not have a hydroxyl group, steric clash with a hydrogen on Cγ may exclude a second water molecule from binding to Fe4.

The structure of the *trans*-aconitate complex provides a model for two aspects of *cis*-aconitate binding to aconitase. First, the Cβ carbon is trigonal and displaced 0.27 Å from Cβ of isocitrate, if these structures are superposed by least-squares fit of corresponding atoms. However, the distance from Cβ to the Oγ atom of Ser642, the proposed base in the reaction (below), remains constant at 3.1 Å. That this shift is accommodated in the binding of the two compounds is consistent with the requirement that *cis*-aconitate also bind. Second, the Fe4 site is five-coordinate, as would be expected following formation of *cis*-aconitate from isocitrate if the water molecule derived from the isocitrate hydroxyl were released first. In other words, the existence of a five-coordinate state in the absence of any other significant rearrangements is consistent with the formation of *cis*-aconitate in a productive binding mode.

d. Methyl Isocitrate. As deduced from kinetic and spectroscopic experiments, and demonstrated by the crystal structure of the isocitrate and nitrocitrate complexes of aconitase, citrate, and isocitrate bind to Fe4 to form isosteric, five-membered chelate rings involving groups on their α and β carbons. For isocitrate, the α-carbon is closest to Fe4; for (nitro)-citrate it is the β-carbon that is closest to Fe4. As described above, this requires that the Cγ acetate arm be positioned alternatively for the two substrates. Consequently, the intermediate dehydrated product in the reaction, *cis*-aconitate, must bind in two ways (see Scheme 2), termed citrate mode and isocitrate mode.[3] Further, the stereochemistry of the reactions, i.e. *trans* elimination/addition of H_2O across the double bond, requires two modes. The existence of two binding modes for *cis*-aconitate was demonstrated by experiments using α-methyl-*cis*-aconitate as a substrate (Figure 23), which is converted by the enzyme into α-methylisocitrate only, and not α-methylcitrate.[85]

This result is confirmed by the aconitase structure in crystals grown from solutions containing α-methyl-*cis*-aconitate (Table 6). Only α-methylisocitrate is observed bound to Fe4 in the active site.[106] As in all other structures of aconitase when a substrate or substrate analogue is bound, a H_2O molecule binds to the sixth coordination site of Fe4. The α-methylisocitrate molecule binds in a manner virtually identical to that of isocitrate. The methyl group is accommodated by a favorable van der Waals contact with Ile425. The presence of an isocitrate derivative in the active site is also consistent with the observation that crystallization selects for isocitrate bound molecules vs other enzyme−substrate complexes. Comparison to the structure of the nitrocitrate complex indicates that contact with Ile425 may be important for substrates bound in the citrate mode; in this case the methylene carbon of the Cγ acetate group makes a similar contact to Ile425 as the methyl group of α-methylisocitrate. The exclusion of methylcitrate as a possible product is explained by a steric clash that would occur between a methyl group on Cα of citrate and the side chain of Asp165. Thus, the structure of the methylisocitrate complex confirms previous results and highlights the role of Ile425, the only hydrophobic amino acid of 18 nonligand active site residues.

e. Sulfate vs Substrate Bound. In orthorhombic crystals of activated [4Fe-4S] and inactive [3Fe-4S] aconitase a sulfate ion is bound in the active site (Table 6). The inhibitor used in these crystallization experiments, tricarballylate, is weakly binding, while $(NH_4)_2SO_4$ is present at 2.2 M concentration. The sulfate ion binds to an electrostatically positive cavity about 9 Å from Fe4 formed by the side chains of Arg580 and Arg644. All four oxygens of the sulfate are involved in hydrogen bonds to these arginines and Gln72 and Ser643. It is not uncommon for sulfate to bind adventitiously to electropositive cavities in proteins.[114]

When the structure of the isocitrate complex of aconitase in monoclinic crystals was solved, with the use of coordinates from the orthorhombic form, it was necessary to adjust the conformation of a number of active site residues in order to fit the electron density. In addition, the Fe-S cluster and several chain segments, some far from the active site, were observed to shift position. There was also a small shift

of the entire fourth domain about the hinge-linker relative to the rest of the protein. Because the structures with sulfate vs isocitrate bound were observed in different crystal lattices, it was possible that these conformational changes were an artifact of crystal packing forces. Therefore, in order to make a direct comparison, monoclinic crystals were prepared in the absence of substrate or inhibitors, and the structure was solved and refined (Table 6). Essentially all of the conformational changes initially observed were again observed when the aconitase structures with sulfate bound vs isocitrate bound were compared.[106]

The form of aconitase with sulfate bound can also be treated as a substrate-free state of the enzyme. The [4Fe-4S] cluster is bound only to hydroxide, Fe4 is four coordinate, and the side chains of residues proximal to Fe4 are free of contacts to a substrate. The active site residues in contact with sulfate (Gln72, Arg580, Arg644) are those which contact only the Cγ-carboxyl of substrates. Therefore, the conformational changes observed can be viewed as relevant to the process of substrate binding and release during turnover.

Superposition and comparison of the structures of aconitase with isocitrate vs sulfate bound reveals a hierarchy of conformational changes which can be understood as originating in the active site and propagating to the surface of the protein. The side chain of Arg447, which is in contact with the isocitrate Cβ-carboxyl, undergoes complete rearrangement in order to form a new salt bridge with Glu640 in the cleft in the aconitase structure with sulfate bound. In order for this to occur, Glu640 also undergoes a large conformational change, breaking a salt bridge with Lys564 even farther from the active site at the entrance to the cleft. Because Glu640 resides on the fourth domain, the exchange of salt bridges may be related to opening and closing of the cleft, as would be required for isocitrate to gain access to the active site. At the same time the position of Arg447, when hydrogen bonded to Glu640 (sulfate bound), requires the side chain of Phe449 to rotate 90°. This in turn propagates a shift of residues in van der Waals contact (449−326−325−346). The last residue, Trp346, resides on an α-helix of residues 335−346 on the surface of the protein, also adjacent to the cleft. These changes may have an influence on the electrostatic field at the surface of the protein, which could also affect substrate binding and release.

In the absence of isocitrate binding there is also a significant shift (up to 1.3 Å) and reorientation of the [4Fe-4S] cluster. This is accommodated by a shift of the entire chain segment which carries the cluster ligand Cys358 (residues 355−365). This segment links a β-strand to an α-helix in the core of the third domain. In particular, Gly356 and Ser357 adopt different backbone torsion angles, and a hydrogen bond between Ser361 and Ser357 is broken. These conformational changes, being linked to the cluster ligand Cys358, cause the [4Fe-4S] cluster to be repositioned. However, the conformational change, which moves the cluster as a rigid body, is such that the hydroxide bound to Fe4 in the substrate free (sulfate bound) state virtually superposes on the water molecule bound to Fe4 in the substrate (isocitrate) bound state. In other words, the conformational change allows both the four- and six-coordinate states of Fe4 to exist without substantial change in the other residues which contact the bound hydroxide/water. This may be important in the mechanism of protonation of the bound hydroxide upon substrate binding (below). Of the other residues which contact isocitrate, in particular the His·Asp/Glu pairs, there is very little difference in conformation in the absence of isocitrate. This is due to three water molecules which bind in place of the isocitrate Cα-hydroxyl and Cα- and Cβ-carboxyl groups, preserving almost all of the hydrogen bonds which occur between these groups and the enzyme when isocitrate is bound.

In summary, conformational changes appear to arise directly as a result of two aspects of isocitrate binding. Interaction of the Cβ-carboxyl with Arg447 triggers an exchange of salt bridges within the cleft, repositioning of the fourth domain and reorienting a surface α-helix. At the same time, binding to the Fe-S cluster causes it to shift and reorient, accommodating a higher coordination number at Fe4 and inducing a shift of an entire chain segment carrying one of the cluster ligands. The fact that these changes involve chain segments and domains, and have effects distributed far from the active site (~30 Å), might imply that they are relevant to enzyme function. It seems unlikely that the complex architecture of the enzyme would otherwise undergo such concerted and long range conformational changes.

f. 4-Hydroxy-*trans*-aconitate. This compound is derived from the action of aconitase on (−)-*erythro*-2-fluorocitrate.[64] The details of this reaction are discussed below. The structure of the enzyme, crystallized following incubation with fluorocitrate, was determined at 2.05 Å resolution (Table 6). The unbiased electron density for the bound product is fully consistent with it being 4-hydroxy-*trans*-aconitate.[106a] The compound binds in a manner very similar to that of *trans*-aconitate, so that the enzyme can neither abstract a proton from the Cβ carbon nor hydrate the double bond. In addition, the hydroxyl group on the Cγ carbon coordinates to Fe4 so that all interactions present in the isocitrate complex are mimicked. Together, these features appear to account for the fact that 4-hydroxy-*trans*-aconitate is a very tight binding inhibitor. The complex also manifests four short (<2.7 Å) hydrogen bonds involving Asp165 and His167. In particular, the hydrogen bond between H_2O bound to Fe4 and the Cβ carboxyl group is short (2.58 Å) (see Figure 24a); in the nitroisocitrate complex the corresponding distance is also short (2.52 Å),[83] suggesting that 4-hydroxy-*trans*-aconitate acts as a reaction intermediate analogue as well (see below).

V. Enzyme Mechanism

Aconitase catalyzes four stereospecific reactions: the dehydration of citrate or isocitrate to *cis*-aconitate, and the rehydration of *cis*-aconitate to isocitrate or citrate. The body of information summarized above, derived from EPR, ENDOR, and Mössbauer

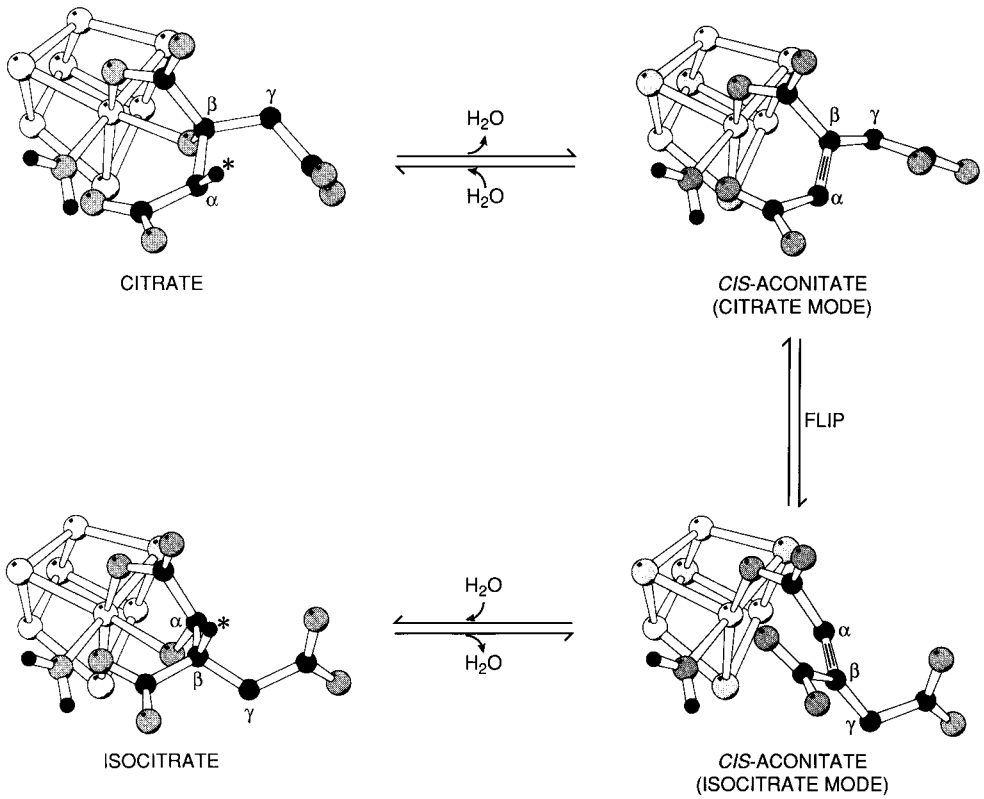

Figure 25. Summary of the steps in the overall reaction catalyzed by aconitase. The model for citrate is derived from the structure of the nitrocitrate complex. The models for *cis*-aconitate are derived from the structure of the *trans*-aconitate complex at Fe4 and from the structures of the nitrocitrate and isocitrate complexes for the corresponding binding modes. The Cα−Cβ double bond is modeled using the Cβ atom of *trans*-aconitate as a reference. The proton which is stereospecifically abstracted and replaced in the overall reaction is indicated by an asterisk. During turnover an additional H_2O molecule is expected to bind to Fe4 adjacent to the Cβ (citrate mode) and Cα (isocitrate mode) atoms of *cis*-aconitate (see also Figure 26b). The gray scale for atom types is H > C > O > S > Fe. (Reprinted with permission from ref 105. Copyright 1994 Academic Press Ltd.)

spectroscopic studies, isotopic labeling experiments, kinetic experiments, and a series of crystal structures of enzyme−substrate and enzyme−inhibitor complexes, has led to a model for these reactions in which the intermediate product, *cis*-aconitate must bind in two ways, a citrate-mode and an isocitrate-mode. The two binding modes are related by a rotation of 180° about the Cα−Cβ bond of the substrate. The overall three step process—dehydrate, flip, rehydrate—is depicted in Figure 25.[3] The crystal structures of aconitase complexes with isocitrate, nitrocitrate, and *trans*-aconitate provide a basis for the atomic models of the four discrete states in the overall reaction. With respect to chemical structure the details of the models are in accord with all available experimental data. The complexes shown for *cis*-aconitate depict Fe4 as five-coordinate, following release of, and prior to rebinding of a H_2O molecule derived from and incorporated into the substrate hydroxyl group. This H_2O molecule is readily exchanged with solvent. Overall, the model accounts for the stereospecificity of the reactions and the requirement for *trans* elimination/addition of a hydroxyl group and a proton at the first and third steps.

The "flip" step, in which bound *cis*-aconitate exchanges from citrate-mode to isocitrate-mode, is very likely not a single-step process. It would be unreasonable to assume that an individual molecule of *cis*-aconitate is released from Fe4, reorients within the active site, and then rebinds, given the favorable interactions observed for substrates and inhibitors in their bound states. More likely, one molecule of *cis*-aconitate is displaced by another and the displacement event can result in the second *cis*-aconitate molecule being oriented in the other binding mode. Displacement of *cis*-aconitate was originally inferred from kinetic data which show that release of product is rate-limiting.[85] Displacement also requires opening and closing of the active site cleft. This is in accord with observed conformational changes within the cleft and about the hinge-linker when the structures of aconitase with and without substrate are compared. Opening and closing of the cleft during turnover must occur because the cleft is occupied with side chains and bound water molecules which would otherwise prevent free diffusion of substrates into and out of the active site.[108] It should however be noted that at present there is no direct evidence precluding the possibility that the same *cis*-aconitate molecule formed by the dehydration of citrate can be rehydrated to form isocitrate.

The available crystal structures identify active site residues likely to be involved in the reactions catalyzed by aconitase. The mutational and kinetic analyses summarized below establish that these residues are critical to activity and imply specific functions for several of them. Together this information has led to specific mechanisms being proposed for the chemical transformations catalyzed by aconitase:[27,83] the binding of substrate which results in

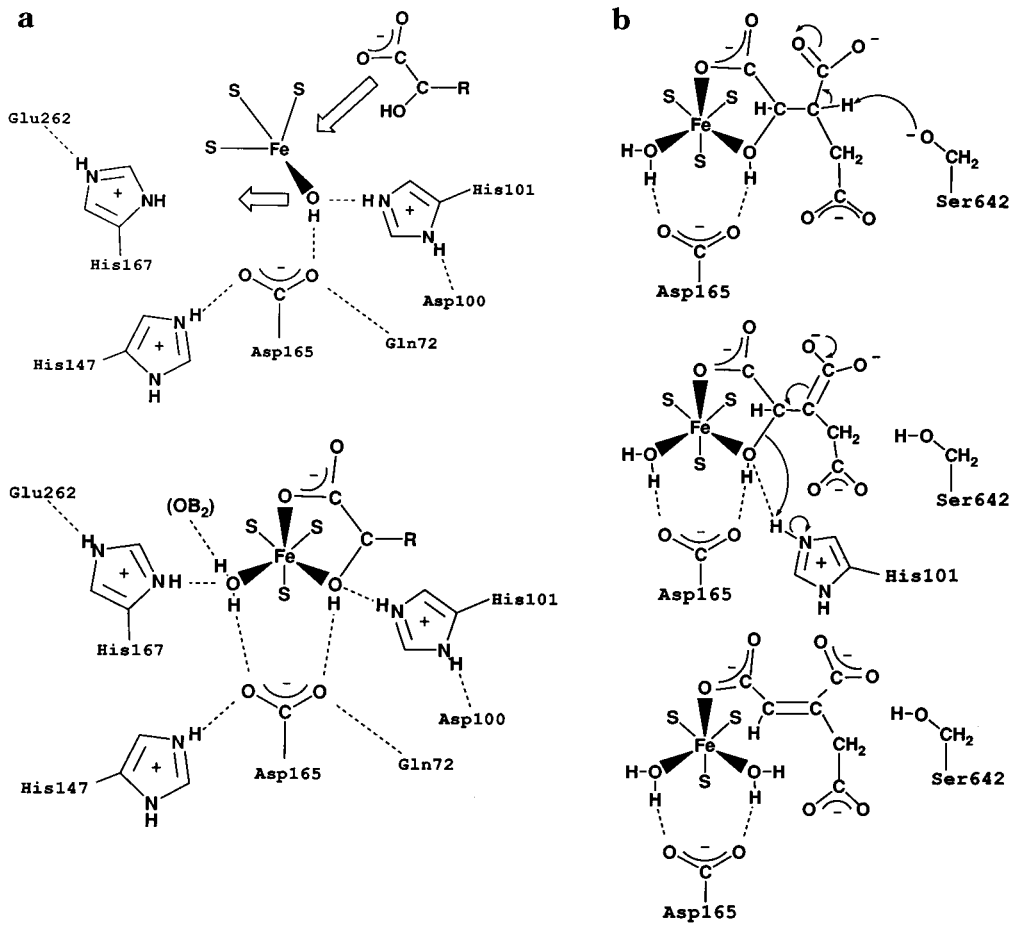

Figure 26. (a) Schematic representation of the transition from substrate-free aconitase to the substrate bound form. The proton added to Fe−OH to make Fe−OH_2 is formally equivalent to the proton derived from Ser642 to form an alkoxide. The contact of Fe−OH_2 to a Cβ carboxyl oxygen of isocitrate (OB_2) is shown separately for clarity. (b) Schematic representation of the reaction isocitrate to *cis*-aconitate assuming deprotonation of Ser642 when substrate binds and Fe−OH_2 is formed. Formation of an *aci*-acid intermediate and collapse of this intermediate forms the product. The *aci*-acid intermediate is proposed to be stabilized by a low barrier hydrogen bond between Fe-OH_2 and substrate Cβ carboxyl, as shown in a and in Figure 24a.

protonation of the hydroxyl group bound to Fe4; and the dehydration/rehydration reaction.

Substrate-free aconitase contains a $[4Fe\text{-}4S]^{2+}$ cluster with hydroxyl bound to Fe4. Upon binding of substrate the bound hydroxyl is protonated and the coordination number of Fe4 increases from four to six. This transformation is depicted in Figure 26a. A hydrogen bond from His101 to the isocitrate hydroxyl (Figure 24a) suggests that the proton donated to form H_2O is derived from this histidine. Alternatively, the proton could be donated by His167 as this histidine is hydrogen bonded to a H_2O molecule in the [3Fe-4S] form which is closest to the bound hydroxyl in the [4Fe-4S] form (Figure 22). His167 is also hydrogen bonded to the bound H_2O in the [4Fe-4S] from (Figure 24a). Both His101 and His167 are paired with carboxylates (Asp100 and Glu262, respectively) and are likely to be protonated. As noted, the conformational change associated with substrate binding which reorients the cluster also maintains the position of the hydroxyl/H_2O molecule on Fe4 with respect to the histidines.

The residue which abstracts a proton from Cβ of citrate and isocitrate is Ser642. Four pieces of information support the conclusion that this serine is the base in catalysis. First, the side chain Oγ atom is the closest protein atom to the hydrogen on Cβ of substrate which is abstracted (Figure 24b). Second, the environment of this Oγ atom in the active site suggests that its pK_a is lowered because it accepts hydrogen bonds from both the amide and side chain of Arg644, the latter being positively charged (Figure 24b). Third, as discussed below, the activity of the Ser642Ala mutant is reduced by 5 orders of magnitude.[27] Fourth, tritium exchange experiments show that the proton abstracted from substrate is retained on the enzyme during at least one turnover, i.e. it resides on a group with a relatively high pK_a.[18] A further consideration is that the geometry of σ and hydrogen bonds about the Oγ atom of Ser642 is tetrahedral, implying that a serine alkoxide would have a lone pair of electrons oriented toward the Cβ of isocitrate (Figure 24b). At the same time the hydrogen on Cβ of isocitrate, which must be *trans* to the hydroxyl group on Cα, is oriented directly toward the serine Oγ atom. The same is true for hydrogen on Cα of citrate (Figure 25). Binding of citrate and isocitrate to an alkoxide form of the enzyme is consistent with conservation of charge because the proton derived from Ser642 is formally equivalent to the proton added to the hydroxyl on Fe4 (Figure 26a).[3] (W. W. Cleland, personal communication.) In the protonated state Ser642 is expected to have a steric clash with the hydrogen on isocitrate or citrate

($C\beta\cdots O\gamma$ distance 3.1 Å, Figure 24b), but not with *cis*-aconitate, which in either binding mode has a trigonal carbon at this position. This suggests that no protonation/deprotonation of hydroxyl/H_2O bound to Fe4 need occur for *cis*-aconitate to be bound or released. This in turn facilitates the displacement step needed to accomplish the "flip" (Figure 25).

Upon abstraction of a proton from Cβ of isocitrate a carbanion intermediate is formed (Figure 26b). The possibility of this intermediate in the transition state is enhanced by the strong inhibition by nitro analogues of the substrates.[109] Collapse of this intermediate with concomitant protonation of the substrate hydroxyl by His101 cleaves the carbon−oxygen bond and yields the products, *cis*-aconitate and H_2O (Figure 26b). By comparison with the nitro analogues the carbanion intermediate can be depicted as an *aci*-acid (second step in Figure 26b). The excess negative charge on the Cβ carboxyl oxygens of the *aci*-acid may be stabilized by a "low-barrier" hydrogen bond with the water molecule bound to Fe4 (Figure 24a, arrow).[115] Low-barrier hydrogen bonds can occur when the distance between donor and acceptor atoms is very short and the pK_as of donor and acceptor are nearly equal. Under these circumstances the proton becomes equally shared between donor and acceptor atoms, resulting in a significant reduction in the overall free energy of the system.[115] In aconitase, the corresponding distance is <2.6 Å in the nitroisocitrate and 4-hydroxy-*trans*-aconitate complexes. It is plausible that the H_2O bound to Fe4 has a pK_a approaching that of the *aci*-acid because it is coordinated to a metal. Further, tetrahedral geometry suggests that the bound H_2O molecule accepts a hydrogen bond from His167 and donates a hydrogen bond to Asp165 (Figure 24a). Consequently, one of the hydrogens on the bound H_2O molecule is expected to be oriented toward the Cβ-carboxyl of isocitrate. All of the available data, therefore, are consistent with a serine alkoxide being the base and a low-energy barrier hydrogen bond stabilizing a carbanion intermediate in the transition state.

VI. Mutational Studies

Porcine heart aconitase was cloned by Zheng et al.[10] shortly after the crystal structures of the [3Fe-4S] and activated [4Fe-4S] forms of the enzyme without substrate were solved.[8,9] The enzyme as synthesized contains a mitochondrial targeting sequence of 27 amino acids and the blocked amino terminal of the mature protein was found to be a pyroglutamyl residue. By sequence comparison it was shown that 198 of 202 amino acids of eight cysteine-containing peptides for the bovine mitochondrial enzyme as determined by Plank and Howard[68] were identical to the porcine heart enzyme, establishing the homology of the two proteins. It soon became possible to over-express the mature protein in an *E. coli* system and to change by site-directed mutagenesis amino acids found to be in the proximity of the active site.[27]

Of particular interest at that time was to determine which residue functions as the catalytic base in the abstraction of the proton during the dehydration reaction. A possible candidate as determined by an initial inspection of the crystal stucture of the substrate-free protein[8,9] was Asp165. Mutation of this group to a Ser residue indeed resulted in an enzyme whose activity was 5 orders of magnitude less than that of the native protein.[27] However it was soon determined, when the crystal structure of the enzyme with bound substrate, isocitrate, became available (see above),[83] that Asp165 in fact was not the base. To the surprise of many, it was shown that a serine residue played this role. With this knowledge of the enzyme structure with bound substrate it became feasible to analyze systematically by site-directed mutagenesis those residues indicated in playing a role in substrate binding or catalysis.

Table 8. Summary of EPR, Tight Binding, and Kinetic Measurements on Aconitase Mutants (adapted from ref 27)

source or mutant	substrate EPR signal[a]	tight binding[b]	relative K_m (isocitrate)[c]	relative V_{max} $_D$s-isocitrate ⇀ aconitase[c]
beef heart	+	+	1.0	1.0
Asp100Ser	+	+	5−6	3.0×10^{-3}
His101Asn	−	−	3−4	1.3×10^{-3}
His147Asn	+	−	8−10	3.4×10^{-1}
Asp165Ser	−	+	3−4	$\sim 3 \times 10^{-5}$
Arg452Gln	±	−	1.0	2.1×10^{-3}
Arg580Lys	−	−	≥30	1.2×10^{-3}
Ser642Ala	+	+	2.3	2.6×10^{-5}

[a] (+) refers to a shift of *g* values from 2.06, 1.93, and 1.86 to 2.04, 1.85, and 1.78 upon the addition of substrate. [b] (+) indicates tight binding as described in text. [c] Ratio of values measured on mutant versus native enzyme under identical conditions.

Ten mutant enzymes were examined in detail, i.e. by EPR spectroscopy, by steady-state kinetics, and for their ability to form tight complexes with substrate as determined by quantitating the amount of radiolabeled substrate bound to protein after rapid passage through a gel filtration column. A summary of the more pertinent findings of these studies is given in Table 8. Since not all of the mutant proteins contained a full complement of the Fe-S cluster, the data obtained from binding assays and kinetic determinations were not related to protein concentrations. Rather, the results were related to cluster concentrations as determined from analyses of inorganic sulfide. The reasons for the variation in cluster concentrations (15−100%) of the various mutant proteins is not entirely clear. One possibility is decreased stability of the protein with subsequent loss of cluster during isolation. Despite this, all of the mutant proteins exhibited EPR signals for the $[3Fe\text{-}4S]^+$ and for the substrate-free $[4Fe\text{-}4S]^+$ clusters similar to those of the native enzyme. This would indicate that the mutations produced caused little or no gross perturbations in the environment of the Fe-S cluster. Upon the addition of excess substrate to the $[4Fe\text{-}4S]^+$ forms, the EPR changes in *g* values observed for wild-type protein were seen in four of the seven mutant proteins listed in Table 8 and for one of these, Ser642Ala, this change was not complete (80%). The K_D for binding of substrate to native enzyme, as determined by EPR is 1 μM.[37] Obviously, the binding of substrate and its interaction with the Fe-S cluster is very sensitive to changes within the active site. The Arg452Gln mutant, in addition, was the only protein that gave an EPR

signal different from that for the native enzyme. Upon addition of a large excess of substrate to the $[4Fe\text{-}4S]^+$ protein, a new signal at $g = 2.02$, 1.91, and 1.76 appeared. This would suggest that Arg452, which forms a bidentate ligand with the α-carboxyl of isocitrate in the native enzyme (Figure 21[83]) is important for the proper orienting of this carboxyl to Fe_a.

For most of the mutants, the results of experiments measuring tight binding correlated well with the changes in the EPR spectrum for the $[4Fe\text{-}4S]^+$ cluster upon addition of substrate, i.e. where there were changes in the EPR spectrum, tight binding was observed. There were, however, two exceptions. The Asp165Ser mutant exhibited tight binding of substrate while not showing any changes in the $[4Fe\text{-}4S]^+$ EPR signal. As shown in Figure 26, parts a and b, Asp165 is hydrogen-bonded to both the hydroxyl of substrate and to the water molecule of Fe_a. The 10 000-fold decrease in activity and the failure to observe changes in the $[4Fe\text{-}4S]^+$ EPR spectrum upon addition of substrate indicate that this residue is critical for the proper binding of substrate to Fe_a. The second exception was with the His147Asn protein where the opposite was true. There were changes in the EPR spectrum with substrate while substrate is not bound tightly. Although His147 is not in direct contact with substrate it is hydrogen bonded to Asp165 described above. This mutant is of particular interest in that in contrast to the wild-type enzyme, it is strongly inhibited by L$_S$-isocitrate, the enantiomer of the natural substrate. Thus His147 obviously plays an important role in the chiral selectivity of the enzyme.

Although an in-depth kinetic analysis was not performed on the mutants produced, the preliminary results obtained when related to the crystal structure, provide a number of insights or hints into the mechanism of the enzymatic reaction. It should be remembered that aconitase has a single substrate binding site and three natural substrates and furthermore that one of these substrates, *cis*-aconitate can bind in either a citrate or isocitrate mode. A thorough kinetic analysis would therefore have involved a study of the six different reactions involved. The results of experiments performed under V_{max} conditions were related to those obtained for the wild-type enzyme under identical circumstances. The mutant enzyme produced by the conservative change of the Ser642 catalytic residue to an Ala, while still binding substrate tightly, resulted in reductions of V_{max} of 5 orders of magnitude for both the citrate to aconitate and isocitrate to aconitate reactions. This was not true for the Arg580Lys mutant. This mutant protein does not bind substrate tightly and the reduction in V_{max} ranged between 3 and 5 orders of magnitude, depending on substrate.[27] This is understandable in that changing the catalytic Ser642 residue to an Ala should have little effect on the binding of individual substrates while affecting the catalytic rates of the individual reactions similarly. In contrast, Arg580 plays an important role in the binding of substrates through its interaction with the γ-carboxyl of each. Since the orientation of the γ-carboxyl is different for each of the substrates, changing this residue to a Lys, although retaining the positive charge, affects the binding of each differently. This is evidenced by a 30-fold increase in the K_M for isocitrate and a 10^{-3}-fold decrease in activity for the isocitrate to aconitate reaction. With citrate as substrate, V_{max} for the Arg580Lys mutant, when compared to wild type was decreased 10^{-4}-fold when measuring aconitate as product and 10^{-5}-fold for the formation of isocitrate. Thus a greater effect on the rate of reaction is observed for this mutant when citrate is substrate in comparison to isocitrate, reflecting the differences in the binding of the two substrates.

His101 and Asp100 form an ion pair (Figure 26a) with His101 within hydrogen-bonding distance to the hydroxyl of substrate. The mutant enzymes His101Asn and Asp100Ser both show a 100-fold decrease in activity and slight increases in their K_M values for isocitrate. They differ, however, in that His101Asn shows neither tight binding of substrate nor an EPR signal indicative of substrate bound to cluster. The opposite is true for Asp100Ser. These effects again illustrate the importance of those residues in close proximity to the cluster for the proper orienting of substrate for binding to Fe_a. Although each of the mutant proteins generated caused changes in one or more of the parameters measured,[27] it was not always possible to rationalize all of the observations made. The complexity of the innumerable contacts between enzyme and substrate, suggests that the interpretation of some of these changes will have to await a thorough kinetic analysis and the solution of the crystal structures of these mutant proteins.

VII. Inhibition of Aconitase by Fluorocitrate

The discovery of the potent inhibitory effect of fluorocitrate on aconitase has an interesting history.[116,117] Over 50 years ago[118] it was established that the active ingredient of the poisonous plant *Dichapetalum cymosum*, commonly known as *Gifbar*, was fluoroacetic acid. The sodium salt of this acid, compound 1080, has since found widespread use as a rodenticide. Early on it was shown by a variety of *in vivo* and *in vitro* experiments that flouroacetate itself could not account for all the effects seen for this compound.[118] In addition it was observed in animal studies that the administration of fluoroacetate causes the rapid accumulation of citrate in most body tissues.[119] Later, principally through the work of Sir Rudolf Peters and co-workers, it was determined that the actual inhibitory substance is fluorocitrate, formed metabolically by the condensation of fluoroacetate and oxaloacetate in the citrate synthase reaction of the tricarboxylic acid cycle.[120] Morrison and Peters presented convincing evidence regarding the site of inhibition when they demonstrated that partially purified aconitase preparations were similarly inhibited by fluorocitrate formed enzymatically or chemically synthesized.[121]

The synthesis and purification of the four different diastereoisomers of 2-fluorocitrate in the laboratories of Ernest Kun[122,123] and the identification of (−)-*erythro*-2-fluorocitrate, (2*R*,3*R*), as the inhibitory isomer by Glusker and co-workers[124,125] allowed for

more detailed studies with aconitase to be performed. The results from typical kinetic inhibition studies were seemingly in contradiction to the known toxic effects of the compound. A K_I of 22−45 μM for both cytosolic and mitochondrial aconitases could not account for the lethal effects of fluorocitrate[126] nor could it account for the accumulation of citrate if caused by inhibition of aconitase. It was then shown that although the compound initially acts as a competitive inhibitor, a time-dependent inactivation of the enzyme sets in.[127] In addition, during the reaction of (−)-*erythro*-2-fluorocitrate with aconitase fluoride ion is released[64,127,128] with a stoichiometry close to 1F$^-$/enzyme molecule,[64] indicating that fluorocitrate is acting as a substrate for the enzyme. Spectroscopic, kinetic and chemical studies have established that the product of the defluorination reaction is a very tight binding inhibitor of aconitase. This has now been confirmed by X-ray crystallography (see above). The spectroscopic evidence comes from Mössbauer studies where enzyme incubated with fluorocitrate was desalted to remove nonprotein-bound small molecules. The spectrum of the desalted enzyme showed that 90% of Fe_a was still bound to a species that could not be displaced by incubation with a 10−20-fold molar excess of citrate during a 75 min period. However, in an enzyme assay of the sample in a solution containing 10^6-fold excess of isocitrate, lag kinetics were observed, indicating that the inhibitor was not irreversibly bound to the enzyme. This was further substantiated when protein with bound inhibitor was precipitated and the supernatant solution was analysed by HPLC on a column used to separate organic acids. A compound with a retention time different from any of the natural substrates was isolated which when added back to active enzyme had all the characteristics of the inhibitory compound. Unfortunately it has not been possible to isolate sufficient quantities of the substance to carry out characterization studies. However, on the basis of the similarity of the Mössbauer results obtained for fluorocitrate and aconitase when compared to the nitro analogues of citrate and isocitrate as well as the wealth of information available from previous kinetic and stereochemical studies, it was suggested that a reasonable candidate for this product is 4-hydroxy-*trans*-aconitate.[64] X-ray crystallographic studies of crystals produced when aconitase is incubated with fluorocitrate has in fact shown that the electron density observed at 2 Å resolution is fully consistent with this conclusion.

The suggestion that the inhibitory product of the reaction of (−)-*erythro*-2-fluorocitrate with aconitase was 4-hydroxy-*trans*-aconitate was based on the proposed mechanism for the reaction. The reaction proposed (Scheme 7) calls for the conversion of fluorocitrate to fluoroaconitate which must then "flip" to bind in the alternate mode. Addition of OH$^-$ then results in the loss of fluoride with the formation of HTn. This compound, as demonstrated from the results of X-ray crystallography, is bound to the protein by a number of very short hydrogen bonds. Further evidence in support of this mechanism is the analysis of the product of the reaction of (+)-*erythro*-2-fluorocitrate, (2*S*,3*S*), with aconitase. Again, as

Scheme 7

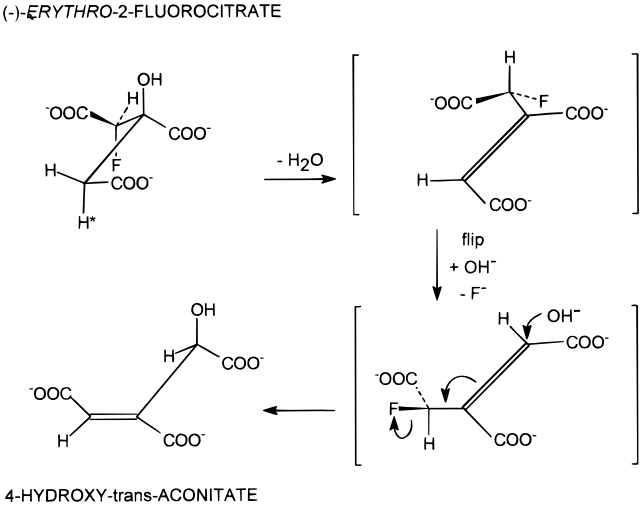

with the (−)-*erythro* compound it acts as a substrate. However, in this case the loss of fluoride is not stoichiometric with enzyme but is stoichiometric to the fluorocitrate added. Using HPLC as performed for the (−)-*erythro*-fluorocitrate reaction, a compound was isolated that coeluted with authentic oxalosuccinate. Furthermore, on treatment with acid and heat, this compound was converted to α-ketoglutarate which was identified by HPLC and, enzymatically, using glutamate dehydrogenase. The proposed mechanism for the formation of these products is shown in Scheme 8.

Scheme 8

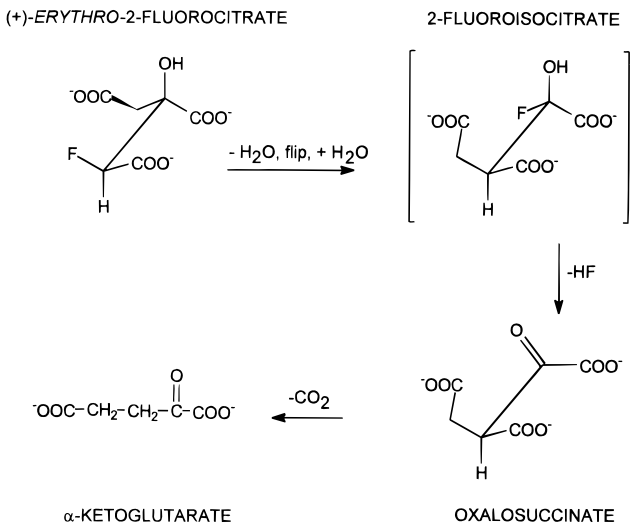

Whether or not the inhibition of aconitase by 4-hydroxy-*trans*-aconitate accounts for all of the toxic effects of (−)-*erythro*-2-fluorocitrate has yet to be determined, since all attempts to date to synthesize this compound have been unsuccessful.

VIII. The Relationship of Aconitase to the Iron-Regulatory Protein

When in the spring of 1991, two notes were published reporting that m-aconitase had 30% AA sequence identity with IRE-BP,[129,130] the iron-respon-

sive element binding protein (also called iron-regulatory factor, ferritin repressor protein, and most recently iron-regulatory protein, IRP), a new chapter in the history of aconitase was opened. We must digress at this point to fill in some background on iron metabolism.

A. Iron Homeostasis, Iron-Responsive Elements (IRE), and IRP

Iron is, with very few exceptions, an indispensable element for all living matter. Thus, the uptake, storage, and utilization of iron are important cellular functions. The problems arising from the poor solubility of Fe(III) and from the potential toxicity of iron have been solved by various organisms in different ways. At this time one of the mechanisms best understood in molecular terms is that involving IRP, to be correct IRP1. There is also an IRP2, which we will consider below. As one of the original names said, "IRE-binding protein" (=IRP) has the function of binding to iron-responsive elements, and thus control Fe uptake and storage at the translational level. IREs are stem-loops of ribonucleotides that are found in the untranslated regions of mRNAs (Figure 27); when placed at the 5′ end they can inhibit translation of the message and when at the 3′ end, they will protect the mRNA from degradation, when IRP is bound to them. A limited variability is tolerated in the sequence (Figure 27e). This has been thoroughly investigated,[131−134] as IREs have been found to regulate translation of several proteins.[135−139]

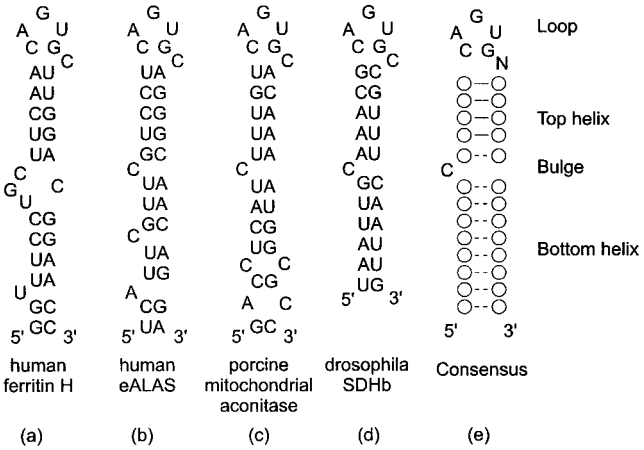

Figure 27. Single letter code for IRE mRNA sequences: (a) human ferritin H chain; (b) human erythroid 5-aminolevulinate synthase; (c) porcine mitochondrial aconitase; (d) *Drosophila* succinate dehydrogenase subunit b (iron-sulfur protein); and (e) consensus sequence where N is any nucleotide excepting G.

We are concerned here only with the biosynthesis of two key proteins of iron metabolism, ferritin, the storage protein, and the transferrin receptor, which is required for the transport of iron across the cell membrane. The mRNA for both the heavy and the light subunit of ferritin as well as the mRNA for the transferrin receptor contain IREs, the former a single one in the 5′ region and the latter five IREs in the 3′ region. On binding of IRP to these structures, the translation of ferritin is inhibited (Figure 28), and

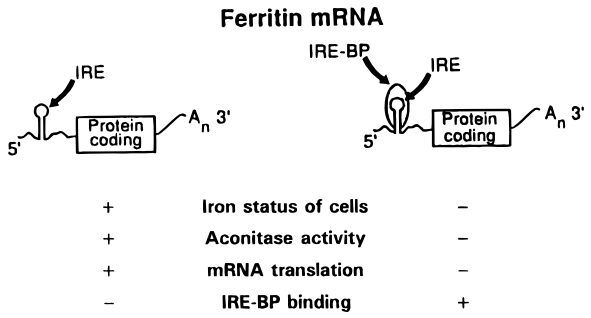

Figure 28. Schematic presentation of the function of an IRE and IRE-BP (IRP) in the regulation of ferritin biosynthesis. The synthesis of transferrin receptor is controlled in an analogous way, except that in this case five IREs are at the 3′ side of the coding region and the RNA is stabilized when IRE-BP is bound. (Reprinted with permission from ref 4. Copyright 1993 Fed. Am. Soc. Exptl. Biol.)

the mRNA for the transferrin receptor is protected from degradation. Thus, a single control protein, IRP, is able to exert the control in a coordinated fashion, when Fe uptake is required and storage is to be stopped. When, however, Fe is abundant and uptake becomes unnecessary and storage desirable, IRP has to be inactivated. Experiments with cultured cells indicated that this is accomplished, when so-called "chelatable" iron is readily available as occurs when cells are grown in the presence of iron salts.[140−143] On the other hand, in the presence of a permeable chelator, such as desferioxamine (Df), IRP is activated for RNA binding.

It was found that in this process IRP apparently was not degraded proteolytically, but was always present in some latent form, which could, in vitro, be activated again under reducing conditions in the presence of high, nonphysiological levels of thiol, such as 0.3 M 2-mercaptoethanol or 0.1 M DTT.[141,142,144,145] Inhibition of protein synthesis by cycloheximide had no influence on the regeneration of active IRP.[141,146−148] It was concluded at that point that some kind of oxidoreductive control was at play. In view of the effect of thiols and the observation that activation of latent IRP was prevented by treatment of cell extracts with NEM, the suspicion fell on a thiol−disulfide system, from which the idea of the "sulfhydryl switch" in IRP originated.[141,142,144] According to this model, a thiol form of IRP was typical for the active state, whereas a disulfide form was characteristic of inactive IRP. We will come back to a discussion related to this concept later.

B. Sequence Homology of IRP and m- or c-Aconitase

This was about the status of the problem at the time the sequence homology of IRP to aconitase was discovered.[129,130] The aconitase, however, to which the IRP sequence was found to be homologous is a mitochondrial protein, whereas IRP is a cytoplasmic one. Above, we have pointed out that there is indeed a cytoplasmic aconitase, which is coded for on a different chromosome than the mitochondrial aconitase.[149,150] However, at the time the sequence homology between the two aconitases was reported, c-aconitase was not well characterized. So the question was open, whether, what we know as c-aconitase,

might not be an alternative form of IRP. Measurements of aconitase activity in cell extracts indeed indicated that this may be the case, because, when cells were starved of Fe, e.g., by treating them with Df, aconitase activity was very low and RNA binding ability high, whereas when cells had been provided with iron, there was higher aconitase activity in the extracts, while RNA binding had decreased.[145,151] Enzyme activity could again be abolished by treatment with 0.3 M 2-mercaptoethanol (ME) and RNA binding of IRP restored.[145,151] The measurements of RNA binding were carried out in so-called gel-shift assays, in which a suitable RNA probe, labeled with ^{32}P, is added to the cellular extract or a purified fraction thereof, and complex formation with IRP is monitored by nondenaturing gel electrophoresis. These experiments suggested that the two activities of the protein IRP, namely binding to mRNA or enzymatic activity as aconitase, were mutually exclusive, i.e., an individual molecule cannot have both activities at the same time.

It was also possible to arrive at an approximate model for the structure of IRP starting from the known 3D structure of m-aconitase. It became apparent that IRP has all the residues that have been identified as being in contact with the active site (active site residues) including the three Cys residues that are cluster ligands.[129] With this information at hand, the problem now called for a decisive comparison of IRP with c-aconitase. For this purpose the quantities of purified IRP available from cellular studies were insufficient. On the other hand the enzyme c-aconitase is relatively abundant in tissues such as liver or placenta. The enzyme was prepared from beef liver in high purity on a scale such that physical, chemical−analytical, and protein−chemical methods could be applied.[25] The enzyme has an M_r of close to 100 000 and, on the whole, showed enzymatic activity and other properties very similar to those of m-aconitase. It also had some distinguishing features, such as a higher stability toward oxidation and, in the 3Fe form, a sufficiently different EPR signal, so that major cross-contamination between the two enzymes could readily be checked. A significant difference seems to be the presence in c-aconitase of one strong binding site for iron in addition to those used for ligation of the cluster. Neither the function nor properties of this additional iron are known at this time.

The protein resisted sequencing as it had a blocked N-terminal. We, therefore, resorted to hydrolysis with cyanogen bromide and were able to isolate in pure form seven peptides constituting 12% of the total sequence. For those portions of the protein that were sequenced, we found that only 3% of the residues differed from those in the corresponding peptides of IRP from human placenta; and these were almost all conservative substitutions. The IRPs from human, rat, and rabbit differ among each other by the same percentage.[152−155] Thus, the differences we found were almost certainly due to the usual minor differences between closely related species. We concluded from this comparison that the two proteins, IRP and c-aconitase, are identical, the only distinction being the Fe-S cluster, which is absent in IRP (IRP contains no Fe). We then subjected holo-c-aconitase, 3Fe c-aconitase, and apo-c-aconitase to gel-shift assays in the presence of low levels of thiol, with the result that the only form active in RNA binding was apo-aconitase, which, in our case, therefore, is beef liver IRP.[156] By using a baculovirus system it was possible to express milligram quantities of hIRP and purify and characterize it.[157] From the sulfide and protein concentrations it was calculated that there was between 1 and 8% of 3Fe plus 4Fe cluster present. From these preparations, up to 60% of active aconitase could be reconstituted in the presence of Fe, S^{2-}, and DTT. The EPR spectra of these preparations, after oxidation with ferricyanide, were identical to those shown in Figure 1, top. It was thus shown that active bovine aconitase can be converted to IRP and authentic IRP into aconitase.

Table 9. Comparison of the Properties of Purified Cytosolic Aconitase with Cellular Form of IRP

protein	aconitase activity	RNA binding in the presence of 2% 2-ME	
		−substrate	+substrate
pure aconitase			
apoprotein	−	+[a]	+
[3Fe-4S]	−	+	−
[4Fe-4S]	+	+	−
cytosol			
Df-treated cells	−	+[b]	+
Hemin-treated cells	+	+	+

[a] Only 0.02% 2-ME is required for RNA binding. [b] No reductant is required for RNA binding.

These findings and conclusions were confirmed, when the effect of aconitase substrates on the RNA binding activity of the various forms of c-aconitase was observed by gel-shift assays.[156] As mentioned above, c-aconitase can be converted to an active RNA-binding form on addition of 2% ME. Substrate effectively interfered with this conversion to the RNA binding form with the 3Fe and 4Fe proteins, which both bind substrate, but had no effect on RNA binding of the apo form (Table 9) which does not bind substrate. The experiments discussed in the last few paragraphs provided convincing proof for the identity of apo-c-aconitase with IRP, as it had been suggested from previous studies.[145]

C. Residues Involved in Aconitase- and RNA-Binding Functions

Above we have discussed in detail structural features of the active site for aconitase activity and the residues immediately involved in this function. Some of the pivotal residues appear to be the Cys ligands that bind the cluster to the protein and the arginines that bind the substrate. The experiments that led to the concept of the sulfhydryl switch (see above)[141] in IRP already had drawn attention to the involvement of Cys residues. By mutational studies it was observed that any one of the Cys ligands of the Fe-S cluster of aconitase could be replaced by serine without interfering with RNA binding, whereas aconitase activity was lost.[158,159] All mutations that prevent assembly of the Fe-S cluster produce a stably active RNA-binding protein. However, if NEM was bound to one of the Cys (437 in c-aconitase) or when

this Cys was involved in a disulfide bond, RNA could no longer bind.[158,160]

These two pieces of information together would indicate that Cys437 per se is not needed for RNA binding, but that the space around this residue has to be open. This then immediately places the RNA-binding site in the same area of the protein molecule as the enzymatically defined active site; at least, there must be some overlap of these sites, which would easily explain the mutual incompatibility of the alternative functions of IRP and aconitase. In addition, mutational studies showed that arginines 541 and 780 and, to a lesser degree Arg536, seem to be important for RNA binding.[158,159] Arginines have often been observed to be anchoring points for RNA on proteins.[161,162]

Although all four subunits of aconitase contribute essential AA residues to the active site for binding of substrate and of the cluster, the aconitase molecule shows a distinct cleft between domains 1−3 and domain 4 (Figure 21).[8,9,83] The covalent link between these two parts of the molecule is established by a loop, the hinge-linker. It is easy to visualize that this 25-residue loop that connects domains 1−3 with domain 4, by itself, is not able to hold the four subunits in as distinct a position, as when all the links provided by the cluster and the bound substrate are present; and one can expect that, in vivo, substrate is always available. When the cluster is removed by oxidative destruction or by excess thiol, the two parts of the molecule could easily open up around the cleft, so that RNA may be bound along the cleft (Figure 20). In an experimental attack on this problem by UV cross-linking,[163,164] coupled with proteolytic digestion of the cross-linked complex and in combination with RNA and protein sequencing, it could be shown that there were certain overlapping areas (between residues 121 and 130 of IRP) of the RNA binding site and the active site of aconitase.

D. Interconversion of IRP and c-Aconitase

A key feature of the proposed mechanism for the function of IREs and IRP and their control of iron homeostasis is the response to levels of iron via the assembly of the Fe-S cluster to form active aconitase at high iron levels, and its disassembly to IRP at low levels. This can be readily accomplished *in vitro* by using suitable chemicals. What happens *in vivo*, however, is not as obvious. The Fe-S cluster of c-aconitase, particularly in the presence of substrate, is fairly stable. On the other hand, in cellular systems, the interconversion of IRP and aconitase has been observed to proceed on a time scale of only hours.[147,165] One may, therefore, imagine that any adjuvant in this intracellular process, whether enzyme or low molecular weight compound, could easily tip the balance one way or another. Such agents may be H_2O_2, nitric oxide, or related compounds that are more reactive than molecular oxygen. In addition, citrate, which is a potential iron chelator as well as a substrate and protector of aconitase, may well play a role in these situations. We should consider here that *in vivo*—that is in excised tissues—there always has been found a mixture of the IRP and aconitase forms of the protein, with the latter in excess.[25,165] Thus, *in vivo*, it is probably rarely an all-or-none situation, as we are used to demand it in *in vitro* work. It has indeed been observed that *in vitro* NO leads to cluster disassembly[166] and O_2^- or H_2O_2 to the 3Fe form;[167−170] however, the quantitative aspects of the disassembly process and its reversal have not yet been worked out *in vitro*.

We will briefly summarize here the results we have obtained from *in vitro* experiments on the interaction of NO with pure m- and c-aconitases. (Kennedy, M. C.; Antholine, W. E.; Beinert, H., unpublished results.) The criteria for observing interactions were loss of enzyme activity and the appearance of EPR signals not shown by the original reactants. NO was added either as a saturated aqueous solution or in the form of compounds that release NO steadily in solution, such as NONOates (e.g. spermidine NONOate). Under anaerobic conditions, both m- and c-aconitases are inactivated by NO, initially at a faster rate, followed by a slower inactivation. According to EPR, the 3Fe cluster is not the main product of inactivation of the 4Fe species. The principal EPR signal observed is that of the dinitrosyl−iron−thiol complex, $Fe(NO)_2(Cys)_2$, $g = 2.04$, that is extensively described in the literature.[171] However, neither product can account for the percentage of enzyme inactivated; they may account for up to 40% of what has been lost. In addition other minor signals were observed that were due to nitrosyl−iron−His,[172] some unidentified signals and, only with c-aconitase and NO solutions, a thiyl radical ($g_{||} = 2.11$).

The products of the reaction of the inactive 3Fe enzyme with NO are not identical; however, as shown by EPR, the 3Fe form is also attacked by NO. Substrate does not prevent inactivation of the enzyme and also the pattern of inactivation and the appearance of the iron−thiol−nitrosyl signal is similar to the reaction in the absence of substrate. c-Aconitase is more stable toward NO than is m-aconitase. In the presence of oxygen the inactivation proceeds at a faster rate than anaerobically. Peroxynitrite inactivates the enzyme producing predominantly the 3Fe form of the protein. These results indicate that NO can cause disassembly of the cluster, even in the presence of substrate. The conversion of c-aconitase *in vivo* to IRP will certainly be a more complicated process.[148,173,174] *In vivo* there appear to be cross-connections between several control loops, which pertain to iron homeostasis, oxygen toxicity, NO production, energy metabolism[147,175−177] and probably other functions as well. This is likely to be a fruitful field for research by cell biologists in the near future; however, it will also be far more difficult to come to definitive conclusions as to mechanisms at the molecular level *in vivo*.

One aspect of the disassembly and assembly of Fe-S clusters must yet be considered—and this brings us back to what has been called the "sulfhydryl switch" (see above). We have seen that the interconversion of IRP and aconitase can be accomplished oxidatively (O_2 or ferricyanide) and reductively (high thiol levels at elevated pH). The apoenzmes, IRPs, produced by these procedures are not identical. The difference is found in the state of the original SH

ligands of the cluster that, of course, remain bound to the protein. On reductive disassembly the Cys residues will be in their SH forms and the protein is active as IRP. After oxidative disassembly, there will be disulfides formed and much of the original S^{2-} will be trapped as S^0 in the form of tri- or tetrasulfides. The apoprotein so obtained is not active as IRP and has to be reduced by low levels of thiol (~2 mM). On the other hand, oxidized IRP produced by, e.g. ferricyanide, can be converted in up to 70% yield to active aconitase simply by adding iron and thiol, as the original sulfide−sulfur is still present as S^0. After reductive conversion of aconitase to IRP, sulfide is required for reconstitution, in addition to iron and thiol. It was this Cys ligand chemistry in the active site of aconitase that produced the phenomena apparent as sulfhydryl switch.[141]

E. Synthesis of Other Proteins Controlled by IRP, Phosphorylation of IRP1, and IRP2

IREs are also found in the mRNAs for some iron-containing proteins, such as the iron protein subunit of succinate dehydrogenase[176,177] and, curiously, m-aconitase,[139] and also in erythroid 5-aminolevulinate synthase, a key enzyme in heme biosynthesis (Figure 27).[135,136] One may expect that other mRNAs with IRE-related structures will eventually be found. Thus, the control function of IRP extends to several metabolic functions. However, IRP itself is under the control of phosphorylation by protein kinase C and of cytokines and hormones. Two phosphorylation sites, Ser residues, have been identified on IRP.[178,179]

As IRP1 was purified in earlier work, a second, weaker band, which indicated complex formation with the RNA probe, was often observed in gel-shift assays. This protein was then purified from several mammalian sources and identified as a homologue of IRP1 with a somewhat larger M_r.[180−182] IRP2 contains a 73 AA insertion near the amino terminus.[182] While it originally seemed that IRP1 is much more abundant than IRP2, widely varying ratios of IRP1 to IRP2 have recently been found in some tissues.[147,183] IRP2 lacks the crucial serine residue that acts as the base in proton abstraction in the aconitase reaction. Thus one would not expect that it can be converted to an active aconitase. It has not been observed that IRP2 is able to assemble a stable Fe-S cluster, although it does contain the three Cys residues that are cluster ligands in aconitases. In addition, when IRP2 is exposed to thiol concentrations that convert the aconitase form of IRP1 into the RNA binding form, IRP2 loses some binding activity rather than being further activated. IRP2 is regulated in a way different from that of IRP1. As mentioned above, the function of IRP1 is not subject to proteolytic control; rather, IRP alternates between the active RNA binding form without Fe-S cluster, and the enzymatically active aconitase form containing the Fe-S cluster. IRP2, however, is degraded by proteolysis, when iron becomes abundant. It has been found that in the extra loop that IRP2 contains, there are five Cys residues in addition to those that occur in the sequence at positions corresponding to those, where the cluster ligands of IRP1 are found. This second set of Cys residues may sense iron, possibly via temporary Fe-S cluster formation, which could label the molecule for degradation by proteolysis. An example for such a function is suggested for the Fe-S cluster of glutamine phosphoribosyl-pyrophosphate amidotransferase.[184]

IX. Unanswered Questions and Outlook

Given the wealth and diversity of information derived about mitochondrial aconitase, do we now understand the role of the Fe-S cluster in enzyme activity? Although much remains to be learned about the details of the proposed chemical mechanism, one fundamental feature of the [4Fe-4S] cluster is important for activity: the Fe4 (Fea) site, being ligated to three sulfurs of the [3Fe-4S] moiety of the cluster, is uniquely free to interact with substrate and solvent molecules. The absence of direct protein ligands to Fe4 confers upon this site a maximal degree of steric freedom, in particular in forming chelates with carboxyl and hydroxyl groups on adjacent carbons of substrates. Concomitant with this degree of freedom is the ability of the Fe4 site to be four-, five-, or six-coordinate, binding to only hydroxyl, to water and substrate carboxyl, to water, substrate hydroxyl and carboxyl, or to two water molecules and substrate carboxyl. This malleability in coordination number, geometry and ligand type is essential to enzyme activity and apparently can only be conferred by a free Fe site within a [4Fe-4S] cluster.

What has been learned from aconitase (about the Fe_a site) has more recently benefited the complicated analysis of the MB spectra of carbon monoxide dehydrogenases. These enzymes have a Ni- and Fe-containing center, called the C-center, that is responsible for the oxidation of CO to CO_2. A recent MB study (E. Münck, personal communication) of enzymes from *Clostridium pasteurianum* and *Rhodospirillum rubrum* has shown that the C-center contains a [4Fe-4S] cluster with a specific, probably pentacoordinate, site-labeled FCII. The results suggest that the FCII site is coupled by a bridging ligand to a Ni^{2+} site. Cyanide, a potent inhibitor of CO dehydrogenases, binds to FCII, suggesting that this cluster site, like Fe_a of aconitase, has an open coordination position for interaction with substrates.

Established roles for metal ions in enzyme catalysis include delocalization of electron density in the transition state with the metal acting as a Lewis acid, and reduction of the pK_a of a water molecule bound to the metal. The Fe4 site in aconitase clearly can function in both of these roles. However, it is not clear whether the metal site need be embedded in an Fe-S cluster. In particular, the apparent occurrence of a low barrier hydrogen bond in the transition state implies that the potential role of the entire cluster in delocalizing excess electron density may be secondary. It should be noted that the water molecule bound to Fe4 is also the same group which participates in the putative short hydrogen bond. However, the same situation pertains for the water molecule bound to the Zn site in thermolysin and carboxypeptidase,[115] suggesting that this function for the metal is not strictly dependent on it being a component of an Fe-S cluster.

The unique chemical properties of incompletely ligated [4Fe-4S] clusters appear to be exploited in other dehydratase enzymes as well. Isopropylmalate (IPM) isomerase catalyzes a reversible dehydration/rehydration reaction in leucine biosynthesis and is expected to contain a [4Fe-4S] cluster based on strong sequence homology with aconitase (Table 7). In this case the chemistry is the same as for the citrate to isocitrate reaction except that the $-CH_2(\gamma)-COOH$ of citrate and isocitrate is replaced by an isopropyl group. In eukaryotes IPM isomerase is a single polypeptide, but in prokaryotes it is comprised of two subunits, the LeuC and LeuD gene products (Table 7). The LeuD protein corresponds to the fourth domain of aconitase, consistent with the expectation of conformation change about the hinge-linker. Another enzyme which catalyses a stereospecific, reversible hydration or dehydration reaction is *E. coli* fumarase A.[185] In this case the $-CH_2(\gamma)-COOH$ of citrate and isocitrate is replaced by a hydrogen. Fumarase A has been shown to contain a catalytically essential [4Fe-4S] cluster, which upon mild oxidation is converted to a [3Fe-4S] cluster with loss of activity. It is proposed that the fumarase A [4Fe-4S] cluster contains an Fe_a site which participates in catalysis exactly as the Fe_a site in aconitase.[185]

At least three enzymes have been shown to use Fe-S clusters (see D. H. Flint, this issue) in dehydration reactions analogous to the formation of *cis*-aconitate by aconitase. *E. coli* dihydroxyacid dehydratase (DHAD) contains a [4Fe-4S] cluster and catalyses the dehydration of a 2,3 dihydroxycarboxylic acid to the corresponding 2-keto acid in the biosynthesis of branched chain amino acids.[186] The reaction is expected to occur by coordination of the 3-hydroxyl group to one Fe of the cluster and abstraction of a proton on the 2-carbon *trans* to it, as in the aconitase mechanism. Tautomerization of the enol formed yields the 2-keto acid product. The distinctive feature with respect to aconitase is that the substrate chelate with the unique Fe must be either a five-membered ring with two hydroxyl ligands, or a six-membered ring with hydroxyl and carboxyl oxygen ligands.[186] DHAD in spinach catalyzes the same reaction as the *E. coli* enzyme, but employs a [2Fe-2S] cluster.[187] Novel spectroscopic features suggest that in this case the Fe involved in catalysis is either able to expand its coordination sphere, or one of its protein ligands is displaced, in order to accommodate the 3-hydroxyl group of substrate. L-Serine dehydratase catalyses the irreversible deamination of serine to pyruvate. One class of this enzyme in bacteria contains a [4Fe-4S] cluster with a Fe_a type of site which can coordinate to substrate hydroxyl and carboxyl to from a six-membered chelate ring.[188] Abstraction of a proton from the Cα-carbon of the amino acid leads to elimination of the hydroxyl group; the enamine formed tautomerizes and reacts with water to yield pyruvate. Together these examples illustrate the versatility of Fe-S clusters in catalyzing dehydration reactions with respect to substrate, coordination to the unique Fe, and even cluster type.

A surprising result to emerge from the studies of the aconitase structure and mechanism is that the base in the reaction is serine (Ser642). Normally, this amino acid with a pK_a of ~14 in free solution would not be expected to function as a base. However, all of the data available are consistent with Ser642 being the residue which abstracts a proton from citrate or isocitrate. It should be remembered that this reaction occurs in concert with delocalization of the negative charge of the carbanion intermediate by the Fe-S cluster, perhaps via a low barrier hydrogen bond which directly links the Fe4 site to the substrate (Figure 24a). However, in order for Ser642 to act as base it must first be deprotonated. In this regard, the structure implies that the serine pK_a is significantly reduced due to its electrostatic and hydrogen-bonding environment (Figure 24b). Examples in other enzymes show that it is not uncommon for serine to be deprotonated in active sites, as for instance, in the Asp·His·Ser catalytic triad of serine proteases.[189] In *E. coli* TEM1 β-lactamase a buried lysine is proposed to abstract a proton from serine which then acts as a nucleophile; in the subsequent step the tetrahedral intermediate of the substrate formed abstracts a proton from a second serine in the active site.[190] In penicillin acylase the amino group of a N-terminal serine abstracts a proton from its own side chain via a water molecule allowing the serine to act as a nucleophile.[191] And in UDP-N-acetylenolpyruvylglucosamine reductase an enol intermediate of the substrate abstracts a proton from serine to form the product.[192] In each of these cases an activated group is involved in the proton abstraction, whereas in aconitase no such group exists. This implies that the pK_a of Ser642 is in the range of 7 to 9, so that the alkoxide form is present in sufficient concentration for catalysis to occur. Nevertheless, it remains unclear why aconitase employs serine in this manner, and why it does so in conjunction with an Fe-S cluster.

Table 7 shows a sequence alignment of mitochondrial, plant, and bacterial aconitases with an iron-regulatory protein (IRP) and IPM isomerases from yeast and *E. coli*. These six sequences are taken from a total of 24 sequences of these proteins now available. Alignment of all 24 sequences reveals 36 residues which are absolutely conserved (41 if isoform 2 of IRP is excluded).[193] Analysis of these sequences provides insights into the aconitase fold which are not apparent from examination of the crystal structures of enzyme·substrate and enzyme·inhibitor complexes. No crystal structure of the other 23 proteins is yet available. Of the invariant residues, only 14 are active site residues as identified from the mitochonrial aconitase crystal structures. A number of the remaining 22 residues (27 without IRP2) reside in connecting regions between α-helices and β-strands, and frequently are glycines with nonstandard main chain torsion angles, implying that they are important for maintaining the three-dimensional structure. Two glycines (residues 180 and 182 in mitochondrial aconitase) have normal torsion angles but short contacts to other active site residues. Similarly, several of the invariant residues provide hydrogen bonds to the carbonyls of an active site residue. Overall, the primary sequence data indicate the versatility of the aconitase fold in carrying out a

variety of enzymatic and binding activities. Further, the data suggest that this class of proteins is likely to contain additional members with as yet undiscovered biological activities.

X. Acknowledgments

We acknowledge with appreciation the contributions of our colleagues, whose names appear on our joint papers and without whose contributions the work presented would not have been possible. Eckard Münck and Brian Hoffman kindly commented on early drafts of the manuscript. The work in our own laboratories was generously supported by research grants from the National Institutes of Health: GM12394 and GM34812 (H.B.), GM36325 and GM48495 (C.D.S.), and a Research Career Award to HB 5-K06 GM18442; and by the University of Wisconsin—Madison and the Medical College of Wisconsin, Milwaukee. We also acknowledge the use, since 1986, of the EPR facilities at the National Biomedical ESR Center at the Medical College of Wisconsin and the kind collaboration of William E. Antholine in this phase of the work.

XI. Abbreviations

AA, amino acids; c-, m-aconitase, cytoplasmic, mitochondrial; Df, desferrioxamine; DTT, dithiothreitol; DHAD, dihydroxyacid dehydratase; ESEEM, electron spin−echo envelope modulation; EXAFS, extended X-ray absorption fine structure; Fd, ferredoxin; Fe_a, labile Fe of aconitase (Fe4 for 3D structure); IRE, iron-responsive element (specific mRNA structures); IRP, iron-regulatory protein (formerly called IRE-BP or IRF); MB, Mössbauer; MCD, magnetic circular dichroism; ME, 2-mercaptoethanol; NEM, *N*-ethylmaleimide; Rd, rubredoxin; RR, resonance Raman.

References

(1) Martius, C. *Z. Physiol. Chem.* **1937**, *247*, 104.
(2) Breusch, F. L. *Z. Physiol. Chem.* **1937**, *250*, 262.
(3) Emptage, M. H. *Metal Clusters in Proteins*; ACS Symposium Series 372; American Chemical Society: Washington, DC, 1988; p 343.
(4) Beinert, H.; Kennedy, M. C. *FASEB J.* **1993**, *7*, 1442.
(5) Beinert, H.; Kennedy, M. C. *Eur. J. Biochem.* **1989**, *186*, 5.
(6) Kennedy, M. C.; Stout, C. D. *Adv. Inorg. Chem.* **1992**, *38*, 323.
(7) Ruzicka, F. J.; Beinert, H. *J. Biol. Chem.* **1978**, *253*, 2514.
(8) Robbins, A. H.; Stout, C. D. *Proc. Natl. Acad. Sci. U.S.A.* **1989**, *86*, 3639.
(9) Robbins, A. H.; Stout, C. D. *Proteins: Struct., Funct. Genet.* **1989**, *5*, 289.
(10) Zheng, L.; Andrews, P. C.; Hermodson, M. A.; Dixon, J. E.; Zalkin, H. *J. Biol. Chem.* **1990**, *265*, 2814.
(11) Potter, V. R.; Heidelberger, C. *Nature* **1948**, *164*, 180.
(12) Ogston, A. G. *Nature* **1948**, *162*, 963.
(13) Dickman, S. R.; Cloutier, A. A. *J. Biol. Chem.* **1951**, *188*, 379.
(14) Gawron, O.; Glaid, A. J., III; LoMonte, A.; Gary, S. *J. Am. Chem. Soc.* **1958**, *80*, 5856.
(15) Gawron, O.; Glaid, A. J., III; Fondy, T. P. *J. Am. Chem. Soc.* **1961**, *83*, 3634.
(16) Englard, S. *J. Biol. Chem.* **1960**, *235*, 1510.
(17) Gawron, O.; Mahajan, K. P. *Biochemistry* **1966**, *5*, 2343.
(18) Rose, I. A.; O'Connell, E. L. *J. Biol. Chem.* **1967**, *242*, 1870.
(19) Morrison, J. F. *Austr. J. Exp. Biol.* **1954**, *32*, 867.
(20) Thomson, J. F.; Nance, S. L.; Bush, K. J.; Szczepanik, P. A. *Arch. Biochem. Biophys.* **1966**, *117*, 65.
(21) Henson, C. P.; Cleland, W. W. *J. Biol. Chem.* **1967**, *242*, 3833.
(22) Dickman, S. R. *The Enzymes*; Academic Press: New York, 1961; p 495.
(23) Villafranca, J. J.; Mildvan, A. S. *J. Biol. Chem.* **1971**, *246*, 772.
(24) Eanes, R. Z.; Kun, E. *Biochim. Biophys. Acta* **1971**, *227*, 204.
(25) Kennedy, M. C.; Mende-Mueller, L.; Blondin, G. A.; Beinert, H. *Proc. Natl. Acad. Sci. U.S.A.* **1992**, *89*, 11730.
(26) Rouault, T. A.; Stout, C. D.; Kaptain, S.; Harford, J. B.; Klausner, R. D. *Cell* **1991**, *64*, 881.
(27) Zheng, L.; Kennedy, M. C.; Beinert, H.; Zalkin, H. *J. Biol. Chem.* **1992**, *267*, 7895.
(28) Kennedy, M. C.; Emptage, M. H.; Dreyer, J.-L.; Beinert, H. *J. Biol. Chem.* **1983**, *258*, 11098.
(29) Kennedy, M. C. Ph.D. Dissertation, Duquesne University, May 1972.
(30) Kennedy, C.; Rauner, R.; Gawron, O. *Biochem. Biophys. Res. Commun.* **1972**, *47*, 740.
(31) Gawron, O.; Kennedy, M. C.; Rauner, R. A. *Biochem. J.* **1974**, *143*, 717.
(32) Ruzicka, F. J.; Beinert, H. *Biochem. Biophys. Res. Commun.* **1974**, *58*, 556.
(33) Ruzicka, F. J.; Beinert, H. *Frontiers of Biological Energetics*; Academic Press: New York, 1978; p 985.
(34) Beinert, H.; Ruzicka, F. J.; Dreyer, J.-L. *Membrane Bioenergetics*, Addison-Wesley: Reading, MA, 1979; p 45.
(35) Kurtz, D. M.; Holm, R. H.; Ruzicka, F. J.; Beinert, H.; Coles, C. J.; Singer, T. P. *J. Biol. Chem.* **1979**, *254*, 4967.
(36) Stout, C. D. *Nature* **1979**, *279*, 83.
(37) Emptage, M. H.; Dreyer, J.-L.; Kennedy, M. C.; Beinert, H. *J. Biol. Chem.* **1983**, *258*, 11106.
(38) Zhuang, H.-Y.; Faridoon, K. Y.; Sykes, A. G. *Inorg. Chim. Acta* **1992**, *201*, 239.
(39) Faridoon, K. Y.; Zhuang, H.-Y.; Sykes, A. G. *Inorg. Chem.* **1994**, *33*, 2209.
(40) Lovenberg, W. *Iron-Sulfur Proteins*; Academic: New York, 1973; Vols. I and II.
(41) Lovenberg, W. *Iron-Sulfur Proteins*; Academic: New York, 1977; Vol. III.
(42) Spiro, T. G. *Iron-Sulfur Proteins*; Wiley-Interscience: New York, 1982.
(43) Kent, T. A.; Dreyer, J. L.; Emptage, M. H.; Moura, I.; Moura, J. J. G.; Huynh, B. H.; Xavier, A. V.; LeGall, J.; Beinert, H.; Orme-Johnson, W. H.; Münck, E. *Electron Transport and Oxygen Utilization*; Ho, C., Ed.; Elsevier: North Holland, 1982; p 371.
(44) Emptage, M. H.; Kent, T. A.; Huynh, B. H.; Rawlings, J.; Orme-Johnson, W. H.; Münck, E. *J. Biol. Chem.* **1980**, *255*, 1793.
(45) Kissinger, C. R.; Sieker, L. C.; Adman, E. T.; Jensen, L. H. *J. Mol. Biol.* **1991**, *219*, 693.
(46) Winkler, H.; Schultz, C.; Debrunner, P. D. *Phys. Lett.* **1979**, *69A*, 360.
(47) Ravi, N.; Bollinger, J. M., Jr.; Huynh, B. H.; Edmondson, D. E.; Stubbe, J. *J. Am. Chem. Soc.* **1994**, *116*, 8007.
(48) Kent, T. A.; Huynh, B. H.; Münck, E. *Proc. Natl. Acad. Sci. U.S.A.* **1980**, *77*, 6574.
(49) Stout, C. D.; Ghosh, D.; Patthabi, V.; Robbins, A. H. *J. Biol. Chem.* **1980**, *255*, 1797.
(50) Kim, J.; Rees, D. C. *Science* **1992**, *257*, 1677.
(51) Gibson, J. F.; Hall, D. O.; Thornley, J. H. M.; Whatley, F. R. *Proc. Natl. Acad. Sci. U.S.A.* **1966**, *56*, 987.
(52) Huynh, B. H.; Moura, J. J. G.; Moura, I.; Kent, T. A.; LeGall, J.; Xavier, A. V.; Münck, E. *J. Biol. Chem.* **1980**, *255*, 3242.
(53) Papaefthymiou, V.; Girerd, J. J.; Moura, I.; Moura, J. J. G.; Münck, E. *J. Am. Chem. Soc.* **1987**, *109*, 4703.
(54) Noodleman, L.; Baerends, E. J. *J. Am. Chem. Soc.* **1984**, *106*, 2316.
(55) Bominaar, E. L.; Hu, Z.; Münck, E.; Girerd, J.-J.; Borshch, S. A. *J. Am. Chem. Soc.* **1995**, *117*, 6976.
(56) Anderson, P. W.; Hasegawa, H. *Phys. Rev.* **1955**, *100*, 675.
(57) Zener, C. *Phys. Rev.* **1951**, *82*, 403.
(58) Noodleman, L.; Case, D. A. *Adv. Inorg. Chem.* **1992**, *38*, 423.
(59) Borshch, S. A.; Bominaar, E. L.; Blondin, B.; Girerd, J.-J. *J. Am. Chem. Soc.* **1993**, *115*, 5155.
(60) Kent, T. A.; Münck, E. *Hyperfine Intact.* **1986**, *27*, 161.
(61) Belinskii, M. I. *Chem. Phys.* **1993**, *172*, 189; 213.
(62) Bominaar, E. L.; Borshch, S. A.; Girerd, J.-J. *J. Am. Chem. Soc.* **1994**, *116*, 5362.
(63) Kent, T. A.; Dreyer, J.-L.; Kennedy, M. C.; Huynh, B. H.; Emptage, M. H.; Beinert, H.; Münck, E. *Proc. Natl. Acad. Sci. U.S.A.* **1982**, *79*, 1096.
(64) Kent, T. A.; Emptage, M. H.; Merkle, H.; Kennedy, M. C.; Beinert, H.; Münck, E. *J. Biol. Chem.* **1985**, *260*, 6871.
(65) Antonio, M. R.; Averill, B. A.; Moura, I.; Moura, J. J. G.; Orme-Johnson, W. H.; Teo, B.-K.; Xavier, A. V. *J. Biol. Chem.* **1982**, *257*, 6646.
(66) Beinert, H.; Emptage, M. H.; Dreyer, J.-L.; Scott, R. A.; Hahn, J. E.; Hodgson, K. O.; Thomson, A. J. *Proc. Natl. Acad. Sci. U.S.A.* **1983**, *80*, 393.
(67) Rydén, L.; Öfverstedt, L.-G.; Beinert, H.; Emptage, M. H.; Kennedy, M. C. *J. Biol. Chem.* **1984**, *259*, 3141.
(68) Plank, D. W.; Howard, J. B. *J. Biol. Chem.* **1988**, *263*, 8184.
(69) Kennedy, M. C.; Beinert, H. *J. Biol. Chem.* **1988**, *263*, 8194.
(70) Hahm, K.-S.; Gawron, O.; Piszkiewicz. *Biochim. Biophys. Acta* **1981**, *667*, 457.
(71) Kennedy, M. C.; Spoto, G.; Emptage, M. H.; Beinert, H. *J. Biol. Chem.* **1988**, *263*, 8190.

(72) Plank, D. W.; Kennedy, M. C.; Beinert, H.; Howard, J. B. *J. Biol. Chem.* **1989**, *264*, 20385.
(73) Holm, R. H. *Adv. Inorg. Chem.* **1992**, *38*, 1.
(74) Kennedy, M. C.; Kent, T. A.; Emptage, M.; Merkle, H.; Beinert, H.; Münck, E. *J. Biol. Chem.* **1984**, *259*, 14463.
(75) Hagen, K. S.; Watson, A. D.; Holm, R. H. *J. Am. Chem. Soc.* **1983**, *105*, 3905.
(76) Richards, A. J. M.; Thomson, A. J.; Holm, R. H.; Hagen, K. S. *Spectrochim. Acta* **1990**, *46A*, 987.
(77) Rabinowitz, J. C. *Methods Enzymol.* **1972**, *24*, 440.
(78) Petering, D.; Fee, J. A.; Palmer, G. *J. Biol. Chem.* **1971**, *246*, 643.
(79) Thomson, A. J. *Top. Mol. Struct. Biol.* **1985**, *6*, 79.
(80) Kennedy, M. C.; Emptage, M. H.; Beinert, H. *J. Biol. Chem.* **1984**, *259*, 3145.
(81) Moura, J. J. G.; Moura, I.; Kent, T. A.; Lipscomb, J. D.; Huynh, B. H.; LeGall, J.; Xavier, A. V.; Münck, E. *J. Biol. Chem.* **1982**, *257*, 6259.
(82) Emptage, M. H.; Kent, T. A.; Kennedy, M. C.; Beinert, H.; Münck, E. *Proc. Natl. Acad. Sci. U.S.A.* **1983**, *80*, 4674.
(83) Lauble, H.; Kennedy, M. C.; Beinert, H.; Stout, C. D. *Biochemistry* **1992**, *31*, 2735.
(84) Debrunner, P. G.; Münck, E.; Que, L.; Schulz, C. E. *Iron-Sulfur Proteins, III*; Academic Press: New York, 1977; p 381.
(85) Schloss, J. V.; Emptage, M. H.; Cleland, W. W. *Biochem. J.* **1984**, *23*, 4572.
(86) Zheng, L.; Kennedy, M. C.; Beinert, H.; Zalkin, H. *J. Biol. Chem.* **1992**, *267*, 7895.
(87) Werst, M. M.; Kennedy, M. C.; Houseman, A. L. P.; Beinert, H.; Hoffman, B. M. *Biochemistry* **1990**, *29*, 10533.
(88) Hoffman, B. M.; Martinsen, J.; Venters, R. A. *J. Magn. Reson.* **1985**, *62*, 537.
(89) Gurbiel, R. J.; Batie, C. J.; Sivaraja, M.; True, A. E.; Fee, J. A.; Hoffman, B. M.; Ballou, D. P. *Biochemistry* **1989**, *28*, 4861.
(90) Noodleman, L. *Inorg. Chem.* **1988**, *27*, 3677.
(91) Houseman, A. L. P.; Oh, B.-H.; Kennedy, M. C.; Fan, C.; Werst, M. M.; Beinert, H.; Markley, J. L.; Hoffman, B. M. *Biochemistry* **1992**, *31*, 2073.
(92) Telser, J.; Emptage, M. H.; Merkle, H.; Kennedy, M. C.; Beinert, H.; Hoffman, B. M. *J. Biol. Chem.* **1986**, *261*, 4840.
(93) Glusker, J. P. *J. Mol. Biol.* **1968**, *38*, 149.
(94) Kennedy, M. C.; Werst, M.; Telser, J.; Emptage, M. H.; Beinert, H.; Hoffman, B. M. *Proc. Natl. Acad. Sci. U.S.A.* **1987**, *84*, 8854.
(95) Werst, M. M.; Kennedy, M. C.; Beinert, H.; Hoffman, B. M. *Biochemistry* **1990**, *29*, 10526.
(96) Surerus, K. K.; Kennedy, M. C.; Beinert, H.; Münck, E. *Proc. Natl. Acad. Sci. U.S.A.* **1989**, *86*, 9846.
(97) Breton, J. L.; Farrar, J. A.; Kennedy, M. C.; Beinert, H.; Thomson, A. J. *Biochem. J.* **1995**, *311*, 197.
(98) Day, E. P.; Peterson, J.; Bonvoisin, J. J.; Moura, I.; Moura, J. J. G. *J. Biol. Chem.* **1988**, *263*, 3684.
(99) Münck, E.; Debrunner, P. G.; Gunsalus, I. C. *Biochemistry* **1972**, *11*, 855.
(100) Moulis, J.-M.; Auric, P.; Gaillard, J.; Meyer, J. *J. Biol. Chem.* **1984**, *259*, 11396.
(101) Czernuszewicz, R. S.; Macor, K. A.; Johnson, M. K.; Gewirth, A.; Spiro, T. G. *J. Am. Chem. Soc.* **1987**, *109*, 7178.
(102) Kilpatrick, L. K.; Kennedy, M. C.; Beinert, H.; Czernuszewicz, R. S.; Qui, D.; Spiro, T. G. *J. Am. Chem. Soc.* **1994**, *116*, 4053.
(103) Lee, J.; Chang, S. C.; Hahm, K.; Glaid, A. J.; Gawron, O.; Wang B. C.; Yoo, C. S.; Sax, M.; Glusker, J. *J. Mol. Biol.* **1977**, *112*, 531.
(104) Robbins, A. H.; Stout, C. D.; Piszkiewicz, D.; Gawron, O.; Yoo, C. S.; Wang, B. C.; Sax, M. *J. Biol. Chem.* **1982**, *257*, 9061.
(105) Lauble, H.; Kennedy, M. C.; Beinert, H.; Stout, C. D. *J. Mol. Biol.* **1994**, *237*, 437.
(106) Lauble, H.; Stout, C. D. *Proteins: Struct., Funct., Genet.* **1995**, *22*, 1. (a) Lauble, H.; Kennedy, M. C.; Emptage, M. H.; Beinert, H.; Stout, C. D. *Proc. Natl. Acad. Sci. U.S.A.*, in press.
(107) Richardson, J. S. *Adv. Protein Chem.* **1981**, *34*, 167.
(108) Goodsell, D. S.; Lauble, H.; Stout, C. D.; Olson, A. J. *Proteins: Struct., Funct., Genet.* **1993**, *17*, 1.
(109) Schloss, J. V.; Porter, D. J. T.; Bright, H. J.; Cleland, W. W. *Biochemistry* **1980**, *19*, 2358.
(110) Peyret, P.; Perez, P.; Alric, M. *J. Biol. Chem.* **1995**, *270*, 8131.
(111) Prodromou, C.; Artymiuk, P. J.; Guest, J. R. *Eur. J. Biochem.* **1992**, *204*, 599.
(112) Rubin, B. P.; Li, D.; Holloman, W. K. *Gene* **1994**, *140*, 131.
(113) Lau, P. C.; Forghani, F.; Labbe, D.; Bergeron, H.; Brousseau, R.; Holtke, H. J. *Mol. Gen. Genet.* **1994**, *243*, 24.
(114) Birktoft, J. J.; Banaszak, L. J. *J. Biol. Chem.* **1983**, *258*, 472.
(115) Cleland, W. W.; Kreevoy, M. M. *Science* **1994**, *264*, 1887.
(116) Peters, R. *Endeavour* **1954**, 147.
(117) Marais, J. S. C.; Onderstepoort, J. *Vet. Sci. Anim. Ind.* **1944**, *20*, 67.
(118) Buffa, P.; Peters, R. A. *J. Physiol.* **1949**, *110*, 488.
(119) Hodge, H. C.; Smith, F. A.; Chen, P. S. In *Fluorine Chemistry*; Simons, J. H., Ed.; Academic Press: New York, 1963; Vol. III, pp 1−25.
(120) Peters, R. A.; Wakelin, R. W.; Buffa, P.; Thomas, L. C. *Proc. R. Soc. B.* **1953**, *140*, 497.
(121) Morrison, J. F.; Peters, R. A. *Biochem. J.* **1954**, *56*, 473.
(122) Fanshier, D. W.; Gottwald, L. K.; Kun, E. *J. Biol. Chem.* **1964**, *239*, 425.
(123) Dummel, R.; Kun, E. *J. Biol. Chem.* **1969**, *244*, 2966.
(124) Carrel, H. L.; Glusker, J. P.; Villafranca, J. J.; Mildvan, A. S.; Dummel, R. J.; Kun, E. *Science* **1970**, *170*, 1412.
(125) Stallings, W. C.; Monti, C. T.; Belvedere, J. F.; Preston, R. K.; Glusker, J. P. *Arch. Biochem. Biophys.* **1980**, *203*, 65.
(126) Eanes, R. Z.; Kun, E. *Mol. Pharm.* **1974**, *10*, 130.
(127) Villafranca, J. J.; Platus, E. *Biochem. Biophys. Res. Commun.* **1973**, *55*, 1197.
(128) Tecle, B.; Casida, J. E. *Chem. Res. Toxicol.* **1989**, *2*, 429.
(129) Rouault, T. A.; Stout, C. D.; Kaptain, S.; Harford, J. B.; Klausner, R. D. *Cell* **1991**, *64*, 881.
(130) Hentze, M. W.; Argos, P. *Nucleic Acids Res.* **1991**, *19*, 1739.
(131) Theil, E. C. *Biochem. J.* **1994**, *304*, 1.
(132) Leibold, E. A.; Laudano, A.; Yu, Y. *Nucleic Acids Res.* **1990**, *18*, 1819.
(133) Jaffrey, S. R.; Haile, D. J.; Klausner, R. D.; Harford, J. B. *Nucleic Acids Res.* **1993**, *21*, 4627.
(134) Henderson, B. R.; Menotti, E.; Bonnard, C.; Kühn, L. C. *J. Biol. Chem.* **1994**, *269*, 17481.
(135) Cox, T. C.; Bawden, M. J.; Martin, A.; May, B. K. *EMBO J.* **1991**, *10*, 1891.
(136) Dandekar, T.; Stripecke, R.; Gray, N. K.; Goossen, B.; Constable, A.; Johansson, H. E.; Hentze, M. W. *EMBO J.* **1991**, *10*, 1903.
(137) Melefors, Ö.; Goossen, B.; Johansson, H. E.; Stripecke, R.; Gray, N. K.; Hentze, M. W. *J. Biol. Chem.* **1993**, *268*, 5974.
(138) Bhasker, C. R.; Burgiel, B.; Neupert, B.; Emery-Goodman, A.; Kühn, L. C.; May, B. K. *J. Biol. Chem.* **1993**, *263*, 12699.
(139) Zheng, L.; Kennedy, M. C.; Blondin, G. A.; Beinert, H.; Zalkin, H. *Arch. Biochem. Biophys.* **1992**, *299*, 356.
(140) Leibold, E. A.; Munro, H. N. *Proc. Natl. Acad. Sci. U.S.A.* **1988**, *85*, 2171.
(141) Hentze, M. W.; Rouault, T. A.; Harford, J. B.; Klausner, R. D. *Science* **1989**, *244*, 357.
(142) Haile, D. J.; Hentze, M. W.; Rouault, T. A.; Harford, J. B.; Klausner, R. D. *Mol. Cell Biol.* **1989**, *9*, 5055.
(143) Aziz, N.; Munro, H. N. *Proc. Natl. Acad. Sci. U.S.A.* **1987**, *84*, 8478.
(144) Barton, H. A.; Eisenstein, R. S.; Bomford, A. B.; Munro, H. N. *J. Biol. Chem.* **1990**, *265*, 7000.
(145) Haile, D. J.; Rouault, T. A.; Tang, C. K.; Chin, J.; Harford, J. B.; Klausner, R. D. *Proc. Natl. Acad. Sci. U.S.A.* **1992**, *89*, 7536.
(146) Tang, C. K.; Chin, J.; Harford, J. B.; Klausner, R. D.; Rouault, T. A. *J. Biol. Chem.* **1992**, *267*, 24466.
(147) Pantopolous, K.; Gray, N. K.; Hentze, M. W. *RNA* **1995**, *1*, 155.
(148) Pantopolous, K.; Hentze, M. W. *EMBO J.* **1995**, *14*, 2917.
(149) Shows, T. B.; Brown, J. A. *Cytogenet. Cell Genet.* **1977**, *19*, 26.
(150) Sparkes, R. S.; Mohandas, T.; Sparkes, M. C.; Shulkin, J. D. *Biochem. Genet.* **1978**, *16*, 751.
(151) Emery-Goodman, A.; Hirling, H.; Scarpellino, L.; Henderson, B. Kühn, L. C. *Nucleic Acids Res.* **1993**, *21*, 1457.
(152) Rouault, T. A.; Tang, C. K.; Kaptain, S.; Burgess, W. H.; Haile, D. J.; Samaniego, F.; McBride, O. W.; Harford, J. B.; Klausner, R. D. *Proc. Natl. Acad. Sci. U.S.A.* **1990**, *87*, 7958.
(153) Hirling, H. A.; Emery-Goodman, A.; Thompson, N.; Neupert, B.; Seiser, C. Kühn, L. C. *Nucleic Acids Res.* **1992**, *20*, 33.
(154) Patino, M. M.; Walden, W. E. *J. Biol. Chem.* **1992**, *267*, 19011.
(155) Yu, Y.; Radisky, E.; Leibold, E. A. *J. Biol. Chem.* **1992**, *267*, 19005.
(156) Haile, D. J.; Rouault, T. A.; Harford, J. B.; Kennedy, M. C.; Blondin, G. A.; Beinert, H.; Klausner, R. D. *Proc. Natl. Acad. Sci. U.S.A.* **1992**, *89*, 11735.
(157) Basilion, J.; Kennedy, M. C.; Beinert, H.; Massinople, C.; Klausner, R. D.; Rouault, T. A. *Arch. Biochem. Biophys.* **1994**, *311*, 517.
(158) Philpott, C. C.; Klausner, R. D.; Rouault, T. A. *Proc. Natl. Acad. Sci. U.S.A.* **1994**, *91*, 7321.
(159) Hirling, H.; Henderson, B. R.; Kühn, L. C. *EMBO J.* **1994**, *13*, 453.
(160) Philpott, C. C.; Haile, D. J.; Rouault, T. A.; Klausner, R. D. *J. Biol. Chem.* **1993**, *268*, 17655.
(161) Puglisi, J. D.; Tan, R.; Calnan, B. J.; Frankel, A. D.; Williamson, J. R. *Science* **1992**, *257*, 76.
(162) Harada, J.; Frankel, A. D. *EMBO J.* **1995**, *14*, 5798.
(163) Basilion, J. P.; Rouault, T. A.; Massinople, C. M.; Klausner, R. D.; Burgess, W. H. *Proc. Natl. Acad. Sci. U.S.A.* **1994**, *91*, 574.
(164) Swanson, G. R.; Walden, W. E. *Nucleic Acids Res.* **1994**, *22*, 2627.
(165) Müllner, E. W.; Rothenberger, S.; Müller, A. M.; Kühn, L. C. *Eur. J. Biochem.* **1992**, *208*, 597.
(166) Kennedy, M. C.; Beinert, H. J. *Inorg. Biochem.* **1994**, *56*, 48.
(167) Gardner, P. R.; Fridovich, I. *J. Biol. Chem.* **1991**, *266*, 19328.
(168) Gardner, P. R.; Raineri, I.; Epstein, L. B.; White, C. W. *J. Biol. Chem.* **1995**, *270*, 13399.
(169) Flint, D. H.; Tuminello, J. F.; Emptage, M. H. *J. Biol. Chem.* **1993**, *268*, 22369.

(170) Gardner, P. R.; Nguyen, D.-D. H.; White, C. W. *Proc. Natl. Acad. Sci. U.S.A.* **1994**, *91*, 12248.
(171) Vanin, A. F. *Biochemistry (Moscow)* **1995**, *60*, 225.
(172) Lee, M.; Arosio, P.: Cozzi, A.; Chasteen, N. D. *Biochemistry* **1994**, *33*, 3679.
(173) Drapier, J.-C.; Hirling, H.; Wietzerbin, J.; Kaldy, P.; Kühn, L. C. *EMBO J.* **1993**, *12*, 3643.
(174) Weiss, G.; Goossen, B.; Doppler, W.; Fuchs, D.; Pantopolous, K.; Werner-Felmayer, G.; Wachter, H.; Hentze, M. W. *EMBO J.* **1993**, *12*, 3651.
(175) Pantopolous, K.; Hentze, M. W. *Proc. Natl. Acad. Sci. U.S.A.* **1995**, *92*, 1267.
(176) Kohler, S. A.; Henderson, B. R.; Kühn, L. C. *J. Biol. Chem.* **1995**, *270*, 30781.
(177) Gray, N. K.; Pantopolous, K.; Dandekar, T.; Ackerell, B. A. C.; Hentze, M. W. *Proc. Natl. Acad. Sci. U.S.A.* **1996**, *93*, 4925.
(178) Eisenstein, R. S.; Tuazon, P. T.; Schalinske, K. L.; Anderson, S. A.; Traugh, J. A. *J. Biol. Chem.* **1993**, *268*, 27363.
(179) Schalinske, K. L.; Eisenstein, R. S. *J. Biol. Chem.* **1996**, *271*, 7168.
(180) Henderson, B. R.; Seiser, C.; Kühn, L. C. *J. Biol. Chem.* **1993**, *268*, 27327.
(181) Guo, B.; Yang, Y.; Leibold, E. A. *J. Biol. Chem.* **1994**, *269*, 24252.
(182) Iwai, K.; Klausner, R. D.; Rouault, T. A. *EMBO J.* **1995**, *14*, 5350.
(183) Cairo, G.; Pietrangelo, A. *J. Biol. Chem.* **1994**, *269*, 6405.
(184) Grandoni, J. A.; Switzer, R. L.; Makaroff, C. A.; Zalkin, H. *J. Biol. Chem.* **1989**, *264*, 6058.
(185) Flint, D. H.; Emptage, M. H.; Guest, J. R. *Biochemistry* **1992**, *31*, 10331.
(186) Flint, D. H.; Emptage, M. H.; Finnegan, M. G.; Fu, W.; Johnson, M. K. *J. Biol. Chem.***1993**, *268*, 14732.
(187) Flint, D. H.; Emptage, M. H. *J. Biol. Chem.* **1988**, *263*, 3558.
(188) Hofmeister, A. E. M.; Albracht, S. P. J.; Buckel, W. *FEBS Lett.* **1994**, *351*, 416.
(189) Frey, P. A.; Whitt, S. A.; Tobin, J. B. *Science* **1994**, *264*, 1927.
(190) Swaren, P.; Maveyraud, L.; Guillet, V.; Masson, J.-M.; Mourey, L.; Samama, J.-P. *Structure* **1995**, *3*, 603.
(191) Duggleby, H. J.; Tolley, S. P.; Hill, C. P.; Dodson, E. J.; Dodson, G.; Moody, P. C. E. *Nature* **1995**, *373*, 264.
(192) Benson, T. E.; Filman, D. J.; Walsh, C. T.; Hogle, J. M. *Nature, Struct. Biol.* **1995**, *2*, 644.
(193) Frishman, D.; Hentze, M. W. *Eur. J. Biochem.* **1996**, *239*, 197.

CR950040Z